ANALYTICAL INVESTIGATION OF MULTI-LAYER COMPOSITE TUBES SUBJECT TO PRESSURE

A THESIS SUBMITTED TO

THE GRADUATE SCHOOL OF NATURAL AND APPLIED SCIENCES

OF

ATILIM UNIVERSITY

BY

AHMET ATLI

IN PARTIAL FULFILLMENT OF THE REQUIREMENTS FOR THE DEGREE OF

MASTER OF SCIENCE

IN

THE DEPARTMENT OF CIVIL ENGINEERING

JANUARY 2010

Approval of the Graduate School of Natural and Applied Sciences, Atılım University.

_____

Prof. Dr. İbrahim Akman
Director

I certify that this thesis satisfies all the requirements as a thesis for the degree of Master of Science.

_____

Asst. Prof. Dr. Cumhur Aydın
Head of Department

This is to certify that we have read the thesis "Analytical Investigation of Multi-Layer Composite Tubes Subject to Pressure " submitted by Ahmet Atlı and that in our opinion it is fully adequate, in scope and quality, as a thesis for the degree of Master of Science.

_____

Asst. Prof. Dr. Tolga Akış
Supervisor

Examining Committee Members

Asst. Prof. Dr. Hakan Argeşo _____
Manuf. Eng. Dept., Atılım University

Asst. Prof. Dr. Tolga Akış _____
Civil Eng. Dept., Atılım University

Asst. Prof. Dr. Ayhan Gürbüz _____
Civil Eng. Dept., Atılım University

Date: January 21, 2010

I declare and guarantee that all data, knowledge and information in this document has been obtained, processed and presented in accordance with academic rules and ethical conduct. Based on these rules and conduct, I have fully cited and referenced all material and results that are not original to this work.

Name, Last name: Ahmet Atlı

Signature:

ABSTRACT

ANALYTICAL INVESTIGATION OF MULTI-LAYER COMPOSITE TUBES SUBJECT TO PRESSURE

Atlı, Ahmet

M.S., Civil Engineering Department

Supervisor: Asst. Prof. Dr. Tolga Akış

January 2010, 98 pages

The aim of this study is to present an analytical approach for the stress analysis of multi-layer composite tubes under internal and external pressure. The expressions of stresses and displacements for single, two and three-layer tubes are obtained and the critical cases of yielding are examined using Tresca's and von Mises yield criterion. The analytical solutions are checked numerically for different material sets and the stress and displacement distributions are obtained. It is found that yielding begins at the inner surface of the single layer tubes under internal or external pressure. For the two-layer tubes, yielding may begin at the inner surface of the inner or outer tubes or simultaneously at both locations. For the three-layer tubes different cases of yielding may occur depending on the material properties. In the study, the conditions for these various yielding cases are thoroughly examined.

Key words: Stress analysis; Composite tubes; Tresca's criterion; von Mises criterion

ÖZ

BASINÇ ALTINDAKİ ÇOK KATMANLI KOMPOZİT TÜPLERİN ANALİTİK OLARAK İNCELENMESİ

Atlı, Ahmet

Yüksek Lisans, İnşaat Mühendisliği Bölümü

Tez Danışmanı: Yrd. Doç. Dr. Tolga Akış

Ocak 2010, 98 sayfa

Bu çalışmanın amacı iç ve dış basınç altındaki çok katmanlı kompozit tüplerin gerilme analizi için analitik bir yaklaşım sunmaktır. Tek, iki ve üç katmanlı tüpler için gerilme ve yer değiştirme ifadeleri elde edilmiş ve kritik akma koşulları von Mises ve Tresca akma kriterleri kullanılarak incelenmiştir. Bulunan analitik çözümler çeşitli malzeme setleri için uygulanmış, gerilme ve yer değiştirme dağılımları bulunmuştur. İç veya dış basınç altındaki tek katmanlı tüplerde akmanın iç yüzeyden başladığı bulunmuştur. İki katmanlı tüplerde akma iç veya dış tüplerin iç yüzeyinden veya aynı anda bu iki yerden başlayabilir. Üç katmanlı tüplerde ise malzeme özelliklerine göre farklı akma durumları oluşabilir. Çalışmada bu farklı akma durumlarını oluşturan koşullar etraflıca incelenmiştir.

Anahtar Kelimeler: Gerilme analizi; Kompozit tüpler; Tresca kriteri; von Mises kriteri

To My Wife Nesrinnur and Our Son Fahri Furkan

ACKNOWLEDGEMENTS

First of all, I would like to thank to my supervisor Asst. Prof. Dr. Tolga Akış for his guidance during this study. To my wife, Nesrinnur, I offer sincere thanks for her continuous encouragement and patience during this period. I also want to thank to my father, who has persuaded and encouraged me to study master's degree at Atılım University. Lastly, I want to thank to my baby boy, Fahri Furkan, despite the fact that his yelling sometimes has interrupted my study; just his presence has been enough for me.

TABLE OF CONTENTS

LIST OF TABLES

TABLES

LIST OF FIGURES

FIGURES

LIST OF SYMBOLS

r , θ , z	cylindrical polar coordinates
a , b	inner and outer radii of the tube assembly
r_1 , r_2	inner and outer interface radii
$\bar{a}$, $\bar{b}$	dimensionless form of inner and outer radii
$\bar{r}_1$, $\bar{r}_2$	dimensionless form of inner and outer interface radii
C_i	integration constants
E	modulus of elastcity
ν	Poisson's ratio
u	radial displacement
$\bar{u}$	dimensionless radial displacement
ε_i	strain components
ϕ	non-dimensional stress variable
σ_i	stress components
$\bar{\sigma}_i$	dimensionless stress components
σ_0	yield stress

CHAPTER 1

INTRODUCTION

The analysis of cylindrical structural members (shafts, pipes, tubes, etc.) is quite important especially in engineering design. These members are widely used in different areas of engineering practice. Among them, the pressurized thick-walled tube is a classical problem in mechanics. In this work, this problem is extended to the yielding of multi-layer tubes (with two and three layers) under pressure. In the literature, there are several studies investigating the stresses and deformations of these assemblies under different loading and boundary conditions in elastic, plastic or elastoplastic stress states. In this chapter, a summary about these studies is given first, and then the aim of the study is presented.

Tightly-fitted two-layer concentric tubes with fixed ends subjected to internal or external pressure are studied by Akış and Eraslan [1]. In that study, Tresca's yield criterion and associated flow rule are used to investigate the elastic-plastic stress distribution in the assembly. Elastic and elastic-plastic solutions are obtained and some numerical results are presented using brass and copper materials. A similar study using von Mises yield criterion is made by the same authors [2] in elastic stress state and the numerical results of a steel-aluminum tube is presented.

Three layer tubes under internal pressure are studied by You et al. [3]. The aim of their study was to analyze a three layer system which consists of a functionally graded layer in the middle of two homogeneous layers. According to the paper, the tube with the combination of metal-functionally graded material-ceramic could be used for withstanding the high temperatures. The paper also examines the thick-

walled spherical pressure vessels consisting of the functionally graded material only and compares it to the assembly explained above.

The effect of temperature on the behaviour of the pressure tubes are also an interesting subject and several studies were performed on it. In the study of Liew et al. [4], the analysis of the thermal stress behaviour of the functionally graded hollow cylinders is presented. Similar subject is studied in a different paper by Shao [5], but the problem is the cylinder with finite length under thermal and mechanical loads. The material combination used to monitor the stresses and the displacements are mullet and molybdenum. A comprehensive study is made by Tarn [6] on the thermo mechanical states in a series of functionally graded cylinders subjected to extension, torsion, shearing, pressuring and temperature changes. Besides, thermo elastic equations of rotating cylinders are obtained.

The thermal and mechanical properties of a thick hollow sphere made of functionally graded material subjected to the internal pressure is studied by Eslami et al. [7] in which the radial stress and temperature distribution is obtained by using the solution of the Navier equation. Another study on the analytical solution of nonlinear strain hardening pressure pipe having a temperature difference at the inner and the outer surfaces is made by Eraslan and Apatay [8]. The main objective of their study was to investigate an internally pressurized tube with a negative temperature change of the order of 20 ºC. Elastic, partially plastic, fully plastic stress states are investigated where Tresca's yield criterion with its associated flow rule is used. Their study demonstrates that elastic and plastic limit pressures are significantly affected by the existence of a small temperature changes within the tube.

Another interesting subject on the functionally graded pressure vessels is studied by Dai et al. [9]. In their paper, the exact solutions are obtained for the magneto elastic behaviour of the functionally graded vessel located in a uniform magnetic field and subjected to internal pressure. The main objectives of their study are to design the optimum functionally graded cylindrical and spherical vessels and to understand the effect of the volumetric ratio of constituents and porosity on magneto elastic stresses and perturbation of magnetic field vector.

In the study of Zhifei et al. [10], a comparison between elastic hollow cylinders, multi-layer cylinders and elastic cylinders with continuously graded properties is made. The solution for both cases is based on Lamé's [11] solution. At the end of the paper, an example problem showing the differences between these two cases is given. One of the findings of the study is the fact that under external or internal pressure, the absolute value of the displacement in the radial direction in the n-layered tube decreases with the increase in the number of layers. It is also found that, with the increase of the number of layers, the discontinuity for the circumferential stress (σ_θ) can significantly be reduced.

The problem of the elastic and elastic-plastic behaviour of functionally graded spherical pressure vessels is studied by Akis [12] using Tresca's yield criterion. It is found in this study that, different from a homogeneous spherical pressure vessel, different modes of plasticization may take place due to the radial variation of the functionally grading parameters.

Similar to the problem summarized above, elastic, partially plastic and plastic stress states of the plain strain functionally graded tube problem is studied by Eraslan and Akis [13]. The analytical plastic model is based on Tresca's yield criterion. What makes this study interesting is the fact that the elastoplastic behaviour of functionally graded tube may be different from a homogenous tube.

Functionally graded isotropic spheres subjected to internal pressure is investigated by Güven and Baykara [14]. The objective of the study is to understand the acceptable stress distributions in a hollow sphere under internal pressure for ductile and brittle material behaviours. It is stated that in a functionally graded isotropic hollow sphere designed according to the maximum shear stress failure theory, the material usage can be improved efficiently.

In the study of Tutuncu and Özturk [15] closed-form solutions for functionally graded cylindrical and spherical vessels under internal pressure is presented. The study defines an inhomogeneity constant β and by using this constant, the stresses for the functionally graded tubes are obtained.

As seen from the studies presented above, there is still a wide research area on the subject of the behaviour of the cylindrical tubes under pressure. Therefore, the main objectives of this study are to obtain the analytical solutions for the problem of the multi-layer tubes under internal and external pressure and to investigate the yielding behavior of these assemblies. In the study, single layer, two-layer and three-layer tube assemblies are taken into consideration.

For the single, two and three layer tubes, *a* stands for the inner radius and *b* stands for the outer radius of the tube. For the two-layer tubes, r_1 is the interface coordinate between the two tube layers. For the three layer tubes, r_1 and r_2 are the location of the inner and outer interfaces, respectively. The geometries of these assemblies are shown in Figs. 1.1, 1.2 and 1.3.

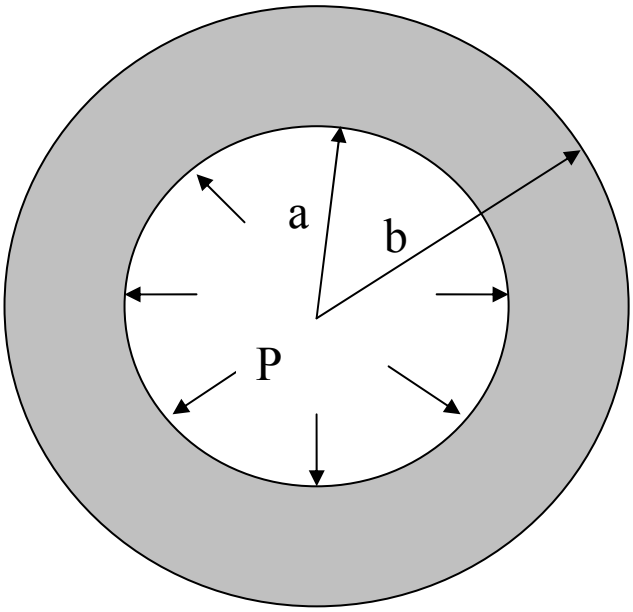

Figure 1.1 The section of a single-layer tube under internal pressure

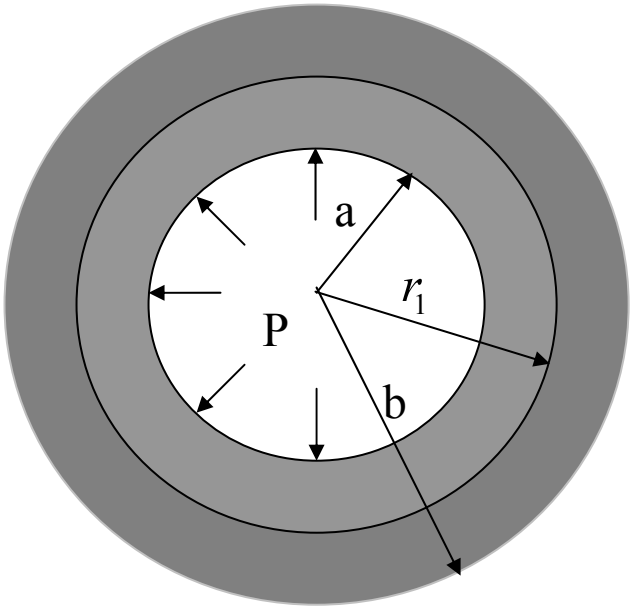

Figure 1.2 The section of a two-layer tube under internal pressure

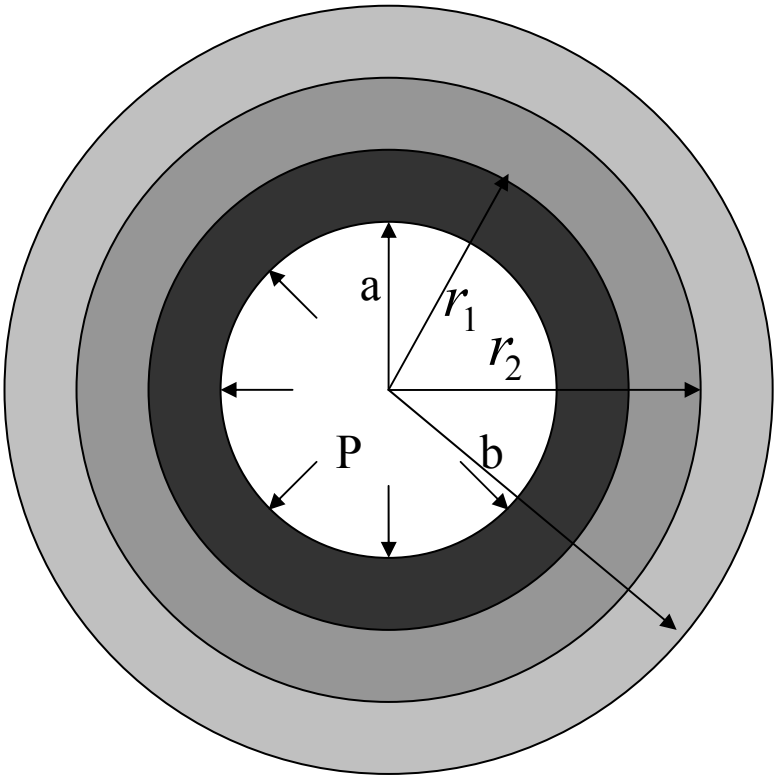

Figure 1.3 The section of a three-layer tube under internal pressure

In the second chapter, the formulation for the stresses and displacement are derived starting with the single layer tube. Afterwards, the studies are carried on with two and three-layer tubes. After obtaining the basic expressions, the elastic limit pressures and the corresponding critical interface radii values are obtained in Chapter Three by using the two common yield criteria, Tresca's and von Mises criterion.

In Chapter Four, using real-engineering materials, some numerical results about the yielding behavior of the multi-layer tubes are presented graphically. It is shown that the determination of the yielding behaviour is not as simple as the yielding of the single layer tube, since there may be more than one possible yielding location. Finally, in the last chapter, a brief summary of the study is made and some important findings are highlighted.

CHAPTER 2

FORMULATION

2.1 General

Throughout this study, cylindrical polar coordinates (r , θ and z) are used in all derivations (Fig. 2.1). First, the governing differential equations and stress and displacement relations for the single layer tubes are derived. Afterwards, the expressions for the two and three-layer tubes are presented. In the derivations, a state of plane strain and infinitesimal deformations are presumed.

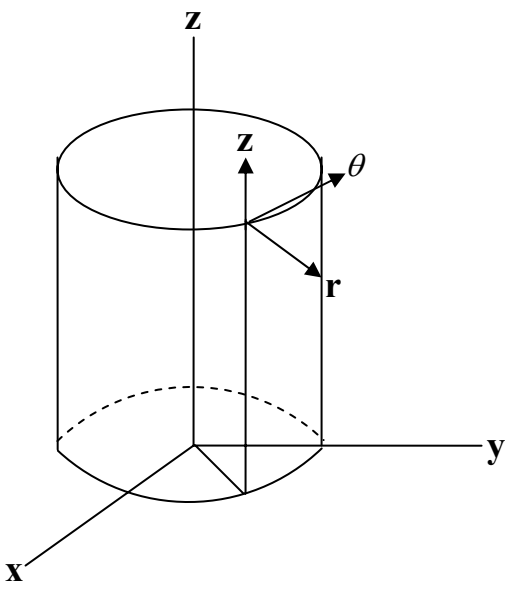

Figure 2.1 The cylindrical polar coordinates used in the derivations

2.2 Single Tube Under Pressure

The generalized Hooke's Law in cylindrical coordinates can be written as

$$\varepsilon_r = \frac{1}{E}\left[\sigma_r - \nu(\sigma_\theta + \sigma_z)\right], \tag{1}$$

$$\varepsilon_\theta = \frac{1}{E}\left[\sigma_\theta - \nu(\sigma_r + \sigma_z)\right], \tag{2}$$

$$\varepsilon_z = \frac{1}{E}\left[\sigma_z - \nu(\sigma_r + \sigma_\theta)\right], \tag{3}$$

For the tube with fixed ends $\varepsilon_z = 0$ and the stress in axial direction can be written as

$$\sigma_z = \nu(\sigma_r + \sigma_\theta)\,. \tag{4}$$

Inserting Eq. (4) into Eqs. (1) and (2) and using the strain-displacement relations

$$\varepsilon_r = \frac{du}{dr}, \tag{5}$$

$$\varepsilon_\theta = \frac{u}{r}\ , \tag{6}$$

the stress expressions in terms of displacements can be obtained. Putting these expressions into the equation of equilibrium in radial direction, which is

$$\frac{d\sigma_r}{dr} + \frac{\sigma_r - \sigma_\theta}{r} = 0\,, \tag{7}$$

the governing differential equation is obtained as

$$r^2 \frac{d^2u}{dr^2} + r\frac{du}{dr} - u = 0\,. \tag{8}$$

The solution of this differential equation for *u(r)* is

$$u(r) = \frac{C_1}{r} + C_2 r\,. \tag{9}$$

Putting u*(r)* into the stress-displacement relations give

$$\sigma_r(r) = \frac{E}{1+\nu}\left[-\frac{C_1}{r^2} + \frac{C_2}{1-2\nu}\right], \tag{10}$$

$$\sigma_\theta(r) = \frac{E}{1+\nu}\left[\frac{C_1}{r^2} + \frac{C_2}{1-2\nu}\right], \tag{11}$$

The stress in axial direction can be obtained by putting the above expressions into Eq. (4) which yields

$$\sigma_z(r) = \frac{2\nu E C_2}{(1+\nu)(1-2\nu)}\,. \tag{12}$$

In order to complete the solution, the integration constants C_1 and C_2 should be determined. For this purpose, the corresponding boundary conditions are used. For the tube under internal pressure $\sigma_r(a) = -P$ and $\sigma_r(b) = 0$, and the integration constants are obtained as

$$C_1 = \frac{a^2 b^2 P(1+\nu)}{(b^2 - a^2)E}\,, \tag{13}$$

$$C_2 = \frac{a^2 P(1+\nu)(1-2\nu)}{(b^2 - a^2)E}. \tag{14}$$

For the tube under external pressure, the boundary conditions become $\sigma_r(a) = 0$, $\sigma_r(b) = -P$. The corresponding integration constants are obtained as

$$C_1 = \frac{a^2 b^2 P(1+\nu)}{(a^2 - b^2)E}, \tag{15}$$

$$C_2 = \frac{b^2 P(1-2\nu)(1+\nu)}{(a^2 - b^2)E}. \tag{16}$$

2.3 Two-Layer Composite Tube Under Pressure

The generalized Hooke's Law for the two-layered tubes can be written as

$$\varepsilon_{r1} = \frac{1}{E_1}\left[\sigma_{r1} - \nu_1(\sigma_{\theta 1} + \sigma_{z1})\right], \tag{17}$$

$$\varepsilon_{r2} = \frac{1}{E_2}\left[\sigma_{r2} - \nu_2(\sigma_{\theta 2} + \sigma_{z2})\right], \tag{18}$$

$$\varepsilon_{\theta 1} = \frac{1}{E_1}\left[\sigma_{\theta 1} - \nu_1(\sigma_{r1} + \sigma_{z1})\right], \tag{19}$$

$$\varepsilon_{\theta 2} = \frac{1}{E_2}\left[\sigma_{\theta 2} - \nu_2(\sigma_{r2} + \sigma_{z2})\right], \tag{20}$$

$$\varepsilon_{z1} = \frac{1}{E_1}\left[\sigma_{z1} - \nu_1(\sigma_{r1} + \sigma_{\theta 1})\right], \tag{21}$$

$$\varepsilon_{z2} = \frac{1}{E_2}\left[\sigma_{z2} - \nu_2(\sigma_{r2} + \sigma_{\theta 2})\right]. \tag{22}$$

Here E_1 and E_2 are the modulus of elasticity of the inner and outer tubes, respectively. Similarly ν_1 and ν_2 are the Poisson's ratio of the two tube layers.

The corresponding stresses and displacements can be written as

$$\sigma_{r1} = \frac{E_1}{1+\nu_1}\left[-\frac{C_1}{r^2} + \frac{C_2}{1-2\nu_1}\right], \tag{23}$$

$$\sigma_{r2} = \frac{E_2}{1+\nu_2}\left[-\frac{C_3}{r^2} + \frac{C_4}{1-2\nu_2}\right], \tag{24}$$

$$\sigma_{\theta 1} = \frac{E_1}{1+\nu_1}\left[\frac{C_1}{r^2} + \frac{C_2}{1-2\nu_1}\right], \tag{25}$$

$$\sigma_{\theta 2} = \frac{E_2}{1+\nu_2}\left[\frac{C_3}{r^2} + \frac{C_4}{1-2\nu_2}\right], \tag{26}$$

$$\sigma_{z1} = \frac{2\nu_1 E_1 C_2}{(1+\nu_1)(1-2\nu_1)}, \tag{27}$$

$$\sigma_{z2} = \frac{2\nu_2 E_2 C_4}{(1+\nu_2)(1-2\nu_2)}, \tag{28}$$

$$u_1(r) = \frac{C_1}{r} + C_2 r, \tag{29}$$

$$u_2(r) = \frac{C_3}{r} + C_4 r. \tag{30}$$

In the above equations, C_1 and C_2 are the integration constants of the inner tube and C_3 and C_4 are the integration constants of the outer tube.

For the two-layer composite tubes under internal pressure, the boundary conditions are $\sigma_{r1}(a) = -P$ and $\sigma_{r2}(b) = 0$. In addition, two interface conditions can be written as: $\sigma_{r1}(r_1) = \sigma_{r2}(r_1)$, $u_1(r_1) = u_2(r_1)$. Using these boundary and interface conditions, the corresponding integration constants are obtained as

$$C_1 = \frac{a^2 M_1 r_1^{\,2} P(b^2 M_7 + M_5 r_1^{\,2})}{E_1[r_1^{\,2}(b^2 M_7 + M_5 r_1^{\,2}) - a^2(b^2 M_6 + M_8 r_1^{\,2})]}, \tag{31}$$

$$C_2 = \frac{a^2 M_1 M_3 P(b^2 M_6 + M_8 r_1^{\,2})}{E_1[r_1^{\,2}(b^2 M_7 + M_5 r_1^{\,2}) - a^2(b^2 M_6 + M_8 r_1^{\,2})]}, \tag{32}$$

$$C_3 = \frac{2a^2 b^2 M_2 r_1^{\,2} P(1-\nu_1^{\,2})}{[r_1^{\,2}(b^2 M_7 + M_5 r_1^{\,2}) - a^2(b^2 M_6 + M_8 r_1^{\,2})]}, \tag{33}$$

$$C_4 = \frac{2a^2 M_2 M_4 r_1^{\,2} P(1-\nu_1^{\,2})}{[r_1^{\,2}(b^2 M_7 + M_5 r_1^{\,2}) - a^2(b^2 M_6 + M_8 r_1^{\,2})]}, \tag{34}$$

where

$$M_1 = 1 + \nu_1, \tag{35}$$

$$M_2 = 1 + \nu_2, \tag{36}$$

$$M_3 = 1 - 2\nu_1, \tag{37}$$

$$M_4 = 1 - 2\nu_2, \tag{38}$$

$$M_5 = M_2 M_4 E_1 - M_1 M_3 E_2, \tag{39}$$

$$M_6 = M_2E_1 - M_1E_2\,, \tag{40}$$

$$M_7 = M_2E_1 + M_1M_3E_2\,, \tag{41}$$

$$M_8 = M_2M_4E_1 + M_1E_2\,. \tag{42}$$

For the two-layer composite tubes under external pressure, the stress and displacement expressions are the same with the internal pressure case. The only difference is on the boundary conditions. For the external pressure case, the boundary conditions become $\sigma_{r1}(a) = 0$ and $\sigma_{r2}(b) = -P$. On the other hand, the interface conditions remain the same.

Using these boundary and interface conditions, the corresponding integration constants are obtained as

$$C_1 = -\frac{2a^2b^2M_1{r_1}^2P(1-{\nu_2}^2)}{[{r_1}^2(b^2M_7 + M_5{r_1}^2) - a^2(b^2M_6 + M_8{r_1}^2)]}, \tag{43}$$

$$C_2 = -\frac{2b^2M_1M_3{r_1}^2P(1-{\nu_2}^2)}{[{r_1}^2(b^2M_7 + M_5{r_1}^2) - a^2(b^2M_6 + M_8{r_1}^2)]}, \tag{44}$$

$$C_3 = \frac{b^2M_2{r_1}^2P(a^2M_8 - M_5{r_1}^2)}{E_2[{r_1}^2(b^2M_7 + M_5{r_1}^2) - a^2(b^2M_6 + M_8{r_1}^2)]}, \tag{45}$$

$$C_4 = -\frac{b^2M_2M_4P({r_1}^2M_7 - a^2M_6)}{E_2[{r_1}^2(b^2M_7 + M_5{r_1}^2) - a^2(b^2M_6 + M_8{r_1}^2)]}. \tag{46}$$

2.4 Three-Layer Composite Tube Under Pressure

The generalized Hooke's Law for the three layer composite tubes can be written as

$$\varepsilon_{r1} = \frac{1}{E_1}\left[\sigma_{r1} - \nu_1(\sigma_{\theta 1} + \sigma_{z1})\right], \tag{47}$$

$$\varepsilon_{r2} = \frac{1}{E_2}\left[\sigma_{r2} - \nu_2(\sigma_{\theta 2} + \sigma_{z2})\right], \tag{48}$$

$$\varepsilon_{r3} = \frac{1}{E_3}\left[\sigma_{r3} - \nu_3(\sigma_{\theta 3} + \sigma_{z3})\right], \tag{49}$$

$$\varepsilon_{\theta 1} = \frac{1}{E_1}\left[\sigma_{\theta 1} - \nu_1(\sigma_{r1} + \sigma_{z1})\right], \tag{50}$$

$$\varepsilon_{\theta 2} = \frac{1}{E_2}\left[\sigma_{\theta 2} - \nu_2(\sigma_{r2} + \sigma_{z2})\right], \tag{51}$$

$$\varepsilon_{\theta 3} = \frac{1}{E_3}\left[\sigma_{\theta 3} - \nu_3(\sigma_{r3} + \sigma_{z3})\right], \tag{52}$$

$$\varepsilon_{z1} = \frac{1}{E_1}\left[\sigma_{z1} - \nu_1(\sigma_{r1} + \sigma_{\theta 1})\right], \tag{53}$$

$$\varepsilon_{z2} = \frac{1}{E_2}\left[\sigma_{z2} - \nu_2(\sigma_{r2} + \sigma_{\theta 2})\right], \tag{54}$$

$$\varepsilon_{z3} = \frac{1}{E_3}\left[\sigma_{z3} - \nu_3(\sigma_{r3} + \sigma_{\theta 3})\right], \tag{55}$$

Here E_1, E_2 and E_3 are the modulus of elasticity of the inner, middle and outer tubes, respectively. Similarly, ν_1 ν_2 and ν_3 are the Poisson's ratio of the tube layers. The corresponding stresses for each layer can be written as

$$\sigma_{r1} = \frac{E_1}{1+\nu_1}\left[-\frac{C_1}{r^2} + \frac{C_2}{1-2\nu_1}\right], \tag{56}$$

$$\sigma_{r2} = \frac{E_2}{1+\nu_2}\left[-\frac{C_3}{r^2} + \frac{C_4}{1-2\nu_2}\right], \tag{57}$$

$$\sigma_{r3} = \frac{E_3}{1+\nu_3}\left[-\frac{C_5}{r^2} + \frac{C_6}{1-2\nu_3}\right], \tag{58}$$

$$\sigma_{\theta 1} = \frac{E_1}{1+\nu_1}\left[\frac{C_1}{r^2} + \frac{C_2}{1-2\nu_1}\right], \tag{59}$$

$$\sigma_{\theta 2} = \frac{E_2}{1+\nu_2}\left[\frac{C_3}{r^2} + \frac{C_4}{1-2\nu_2}\right], \tag{60}$$

$$\sigma_{\theta 3} = \frac{E_3}{1+\nu_3}\left[\frac{C_5}{r^2} + \frac{C_6}{1-2\nu_3}\right], \tag{61}$$

$$\sigma_{z1} = \frac{2\nu_1 E_1 C_2}{(1+\nu_1)(1-2\nu_1)}, \tag{62}$$

$$\sigma_{z2} = \frac{2\nu_2 E_2 C_4}{(1+\nu_2)(1-2\nu_2)}, \tag{63}$$

$$\sigma_{z3} = \frac{2\nu_3 E_3 C_6}{(1+\nu_3)(1-2\nu_3)}. \tag{64}$$

In addition, the displacements for each layer become

$$u_1(r) = \frac{C_1}{r} + C_2 r, \tag{65}$$

$$u_2(r) = \frac{C_3}{r} + C_4 r, \tag{66}$$

$$u_3(r) = \frac{C_5}{r} + C_6 r \,. \tag{67}$$

Here, C_1 and C_2 are the integration constants of the inner tube, C_3 and C_4 are the integration constants of the middle tube, and C_5 and C_6 are the integration constants of the outer tube. For the internally pressurized three–layer composite tubes, the boundary conditions become $\sigma_{r1}(a) = -P$ and $\sigma_{r3}(b) = 0$. In addition, four different interface conditions can be written: $\sigma_{r1}(r_1) = \sigma_{r2}(r_1)$, $u_1(r_1) = u_2(r_1)$, $\sigma_{r2}(r_2) = \sigma_{r3}(r_2)$ and $u_2(r_2) = u_3(r_2)$. Using these conditions, the corresponding integration constants can be obtained as

$$C_1 = \frac{a^2 D_1 r_1^{\,2} P(b^2 D_{14} + r_2^{\,2} D_{15})}{E_1[r_1^{\,2}(b^2 D_{14} + r_2^{\,2} D_{15}) - a^2(b^2 D_{17} + r_2^{\,2} D_{16})]}, \tag{68}$$

$$C_2 = \frac{a^2 D_1 D_4 P(b^2 D_{17} + r_2^{\,2} D_{16})}{E_1[r_1^{\,2}(b^2 D_{14} + r_2^{\,2} D_{15}) - a^2(b^2 D_{17} + r_2^{\,2} D_{16})]}, \tag{69}$$

$$C_3 = \frac{2a^2 D_2 r_1^{\,2} r_2^{\,2} P(b^2 D_{19} + D_{18} r_2^{\,2})(1-\nu_1^{\,2})}{[r_1^{\,2}(b^2 D_{14} + r_2^{\,2} D_{15}) - a^2(b^2 D_{17} + r_2^{\,2} D_{16})]}, \tag{70}$$

$$C_4 = \frac{2a^2 D_2 D_5 r_1^{\,2} P(b^2 D_{20} + D_{21} r_2^{\,2})(1-\nu_1^{\,2})}{[r_1^{\,2}(b^2 D_{14} + r_2^{\,2} D_{15}) - a^2(b^2 D_{17} + r_2^{\,2} D_{16})]}, \tag{71}$$

$$C_5 = \frac{4a^2 b^2 D_3 E_2 r_1^{\,2} r_2^{\,2} P(1-\nu_2^{\,2})(1-\nu_1^{\,2})}{[r_1^{\,2}(b^2 D_{14} + r_2^{\,2} D_{15}) - a^2(b^2 D_{17} + r_2^{\,2} D_{16})]}, \tag{72}$$

$$C_6 = \frac{4a^2 D_3 D_6 E_2 r_1^{\,2} r_2^{\,2} P(1-\nu_2^{\,2})(1-\nu_1^{\,2})}{[r_1^{\,2}(b^2 D_{14} + r_2^{\,2} D_{15}) - a^2(b^2 D_{17} + r_2^{\,2} D_{16})]}, \tag{73}$$

where

$$D_1 = 1 + \nu_1 , \tag{74}$$

$$D_2 = 1 + \nu_2 , \tag{75}$$

$$D_3 = 1 + \nu_3 , \tag{76}$$

$$D_4 = 1 - 2\nu_1 , \tag{77}$$

$$D_5 = 1 - 2\nu_2 , \tag{78}$$

$$D_6 = 1 - 2\nu_3 , \tag{79}$$

$$D_7 = r_1^{\,2} - r_2^{\,2} , \tag{80}$$

$$D_8 = D_5 r_1^{\,2} + r_2^{\,2} , \tag{81}$$

$$D_9 = r_1^{\,2} + D_5 r_2^{\,2} , \tag{82}$$

$$D_{10} = D_3 D_6 D_8 E_2 + D_2 D_5 D_7 E_3 , \tag{83}$$

$$D_{11} = D_3 D_7 E_2 - D_2 D_9 E_3 , \tag{84}$$

$$D_{12} = D_3 D_6 D_8 E_2 + D_2 D_5 D_7 E_3 , \tag{85}$$

$$D_{13} = D_3 D_6 D_7 E_2 + D_2 D_9 D E_3 , \tag{86}$$

$$D_{14} = D_{12} D_2 E_1 - D_1 D_4 D_{11} E_2 , \tag{87}$$

$$D_{15} = D_{10} D_2 E_1 - D_1 D_{13} D_4 E_2 , \tag{88}$$

$$D_{16} = D_{10}D_2E_1 + D_1D_{13}E_2\,, \tag{89}$$

$$D_{17} = D_{12}D_2E_1 + D_1D_{11}E_2\,, \tag{90}$$

$$D_{18} = D_3D_6E_2 - D_2D_5E_3\,, \tag{91}$$

$$D_{19} = D_3E_2 + D_2D_5E_3\,, \tag{92}$$

$$D_{20} = D_3E_2 - D_2E_3\,, \tag{93}$$

$$D_{21} = D_2E_3 + D_3D_6E_2\,. \tag{94}$$

For the external pressure case, the boundary conditions are $\sigma_{r1}(a) = 0$ and $\sigma_{r3}(b) = -P$, and the interface conditions remain the same. Using these, the corresponding integration constants are obtained as

$$C_1 = -\frac{4a^2b^2D_1E_2r_1^{\,2}r_2^{\,2}P(1-\nu_2^{\,2})(1-\nu_3^{\,2})}{[r_1^{\,2}(b^2D_{14}+r_2^{\,2}D_{15}) - a^2(b^2D_{17}+r_2^{\,2}D_{16})]}\,, \tag{95}$$

$$C_2 = -\frac{4b^2D_1D_4E_2r_1^{\,2}r_2^{\,2}P(1-\nu_2^{\,2})(1-\nu_3^{\,2})}{[r_1^{\,2}(b^2D_{14}+r_2^{\,2}D_{15}) - a^2(b^2D_{17}+r_2^{\,2}D_{16})]}\,, \tag{96}$$

$$C_3 = -\frac{2b^2D_2r_1^{\,2}r_2^{\,2}P(a^2D_{22}-D_{23}r_1^{\,2})(1-\nu_3^{\,2})}{[r_1^{\,2}(b^2D_{14}+r_2^{\,2}D_{15}) - a^2(b^2D_{17}+r_2^{\,2}D_{16})]}\,, \tag{97}$$

$$C_4 = -\frac{2b^2D_2D_5r_2^{\,2}P(r_1^{\,2}D_{25}-D_{24}a^2)(1-\nu_3^{\,2})}{[r_1^{\,2}(b^2D_{14}+r_2^{\,2}D_{15}) - a^2(b^2D_{17}+r_2^{\,2}D_{16})]}\,, \tag{98}$$

$$C_5 = -\frac{b^2D_3r_2^{\,2}P(a^2D_{16}-D_{15}r_1^{\,2})}{E_3[r_1^{\,2}(b^2D_{14}+r_2^{\,2}D_{15}) - a^2(b^2D_{17}+r_2^{\,2}D_{16})]}\,, \tag{99}$$

$$C_6 = -\frac{b^2 D_3 D_6 P(r_1^{\,2} D_{14} - D_{17} a^2)}{E_3[r_1^{\,2}(b^2 D_{14} + r_2^{\,2} D_{15}) - a^2(b^2 D_{17} + r_2^{\,2} D_{16})]}, \tag{100}$$

where

$$D_{22} = D_2 E_3 + D_3 D_6 E_2 \ , \tag{101}$$

$$D_{23} = D_2 D_5 E_1 - D_1 D_4 E_2 \, , \tag{102}$$

$$D_{24} = D_2 E_1 - D_1 E_2 \, , \tag{103}$$

$$D_{25} = D_2 E_1 + D_1 D_4 E_2 \, . \tag{104}$$

In the next chapter, the yielding behavior of the single, two-layer and three-layer tubes will be presented.

CHAPTER 3

YIELDING OF COMPOSITE TUBES UNDER PRESSURE

3.1 General

So far, in order to investigate the yielding behavior of single, two-layer and three-layer tubes under the effect of internal or external pressure, the stress and deformation expressions have been derived. In this chapter, the elastic limit pressures and the locations of the yielding in the assemblies will be determined by using the two common yield criteria, Tresca's and von Mises yield criteria. In the next part, brief information about these two criteria is given. Then, the yielding behaviour of the tube assemblies is presented.

3.2 Tresca's Yield Criterion

This criterion takes its name from a French mechanical engineer Henri Édouard Tresca (1814-1885). It is also called the maximum shear stress yield criterion [16]. According to this criterion, the initial yielding occurs when the highest of the maximum shear stresses reaches to a critical value. In other words, yielding begins when the maximum shear stress at a point equals to the maximum shear stress at yield in uniaxial tension (or compression). Yielding under a multiaxial stress state can occur for any one of these conditions: $\sigma_2 - \sigma_3 = |Y|$, $\sigma_3 - \sigma_1 = |Y|$ or $\sigma_1 - \sigma_2 = |Y|$. Here $|Y|$ is the uniaxial yield stress. The yield surface for the maximum shear stress criterion is a regular hexagon in principal stress space. For a biaxial stress state ($\sigma_3 = 0$), the yield surface takes the form of an elongated hexagon

in the (σ_1 , σ_2) plane. The sketch in Fig 3.1 shows this hexagon plane and compares Tresca's and von Mises yield criteria.

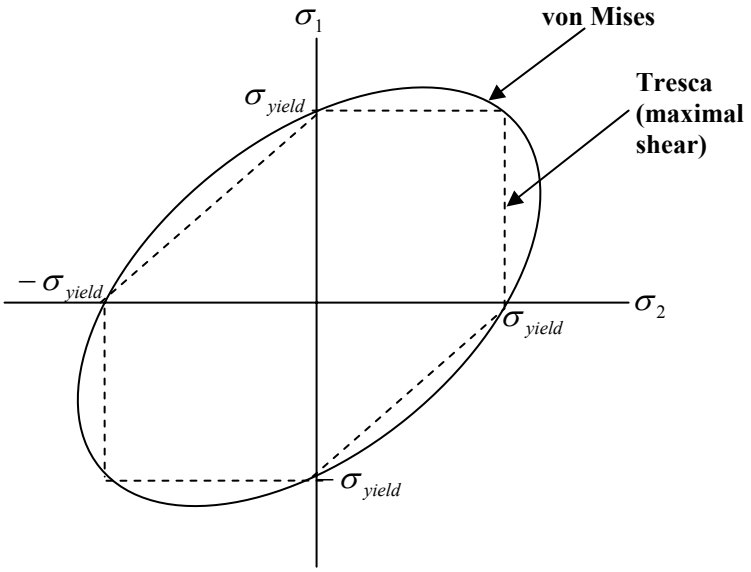

Figure 3.1 Comparison between Tresca's and von Mises yield criteria

For our problem, it is found that the maximum stress difference is between σ_r and σ_θ, therefore, for each layer of the tube, the yielding starts when $\sigma_\theta - \sigma_r = \sigma_0$ for the internal pressure case and it starts when $\sigma_r - \sigma_\theta = \sigma_0$ for the external pressure case. Introducing the dimensionless stress components $\overline{\sigma}_r = \sigma_r / \sigma_0$, $\overline{\sigma}_\theta = \sigma_\theta / \sigma_0$, and $\overline{\sigma}_z = \sigma_z / \sigma_0$, the dimensionless form of the criterion can be obtained as $\overline{\sigma}_\theta - \overline{\sigma}_r = 1$ for the internal pressure case and $\overline{\sigma}_r - \overline{\sigma}_\theta = 1$ for the external pressure case. Throughout this study, the dimensionless values of the stresses are used since the monitoring of the yielding at the tubes becomes easier. It should be noted that, for the internal pressure case, when $\overline{\sigma}_\theta - \overline{\sigma}_r < 1$ the tube is in elastic stress state. Similarly, for the external pressure case the tube is in elastic stress state for $\overline{\sigma}_r - \overline{\sigma}_\theta < 1$.

3.3 von Mises Yield Criterion

It is also called the distortional energy density criterion, and according to this criterion, yielding begins when the distortional strain energy density at a point equals the distortional strain energy density at yield in uniaxial tension (or compression) [16]. The distortional strain energy is the energy associated with a change in the shape of a body. The total strain energy density U_0 is divided into two parts: one part that causes volumetric change U_v and the one that causes distortion U_D. The distortional strain energy density is

$$U_D = \frac{(\sigma_1 - \sigma_2)^2 + (\sigma_2 - \sigma_3)^2 + (\sigma_3 - \sigma_1)^2}{12G}. \tag{105}$$

For a multiaxial stress state, the distortional energy density criterion states that yielding begins when $U_D = Y^2/6G$. Here, Y is the difference of the maximum stresses which is $\sqrt{\frac{1}{2}[(\sigma_1 - \sigma_2)^2 + (\sigma_2 - \sigma_3)^2 + (\sigma_3 - \sigma_1)^2]}$, and G is the shear modulus. Introducing the dimensionless stress variable

$$\phi = \sqrt{\frac{1}{2}[(\bar{\sigma}_r - \bar{\sigma}_\theta)^2 + (\bar{\sigma}_r - \bar{\sigma}_z)^2 + (\bar{\sigma}_\theta - \bar{\sigma}_z)^2]}, \tag{106}$$

the yielding behaviour of the tube assemblies can be monitored. For the values of $\phi < 1$ the assembly is in elastic stress state and for $\phi = 1$, the yielding begins. In von Mises criterion, different from Tresca's yield criterion, stress in z direction is included in the expressions for the considered problem.

3.4 Yielding of Single Tubes Under Internal Pressure

It is found that for the tubes under internal or external pressure yielding begins at the inner surface of the assembly. Using the stress expressions derived in the second

chapter, the elastic limit internal pressure according to Tresca's yield criterion ($\overline{\sigma}_\theta - \overline{\sigma}_r = 1$) is obtained as

$$\overline{P}_e = \frac{P}{\sigma_0} = \frac{1}{2}\left(1 - \frac{a^2}{b^2}\right). \tag{107}$$

On the other hand, by using von Mises yield criterion (Eq. (106)), one can find the elastic limit internal pressure for the single tubes as

$$\overline{P}_e = \sqrt{\frac{(b^2 - a^2)^2}{3b^4 + a^4(1-2\nu)^2}}\,, \tag{108}$$

for $\phi = 1$.

3.5 Yielding of Single Tubes Under External Pressure

Under external pressure, the yielding commences when $\overline{\sigma}_r - \overline{\sigma}_\theta = 1$ according to Tresca's yield criterion. By inserting the stress expressions obtained in the previous chapter, the elastic limit external pressure can be found as

$$\overline{P}_e = \frac{1}{2}\left(1 - \frac{a^2}{b^2}\right). \tag{109}$$

Similarly, using von Mises yield criterion, the elastic limit external pressure becomes

$$\overline{P}_e = \frac{a^2 - b^2}{2b^2}\sqrt{\frac{1}{\nu(\nu-1)+1}}\,. \tag{110}$$

3.6 Yielding of Two-Layer Tubes Under Internal Pressure

By considering the stress expressions for the two-layer tubes, which are derived in the second chapter, it is found that for both internal and external pressure cases,

yielding may begin at the inner surface of the assembly, at the interface or simultaneously at both locations. According to Tresca's criterion, for internal pressure case, yielding starts when $\sigma_{\theta 1} - \sigma_{r1} = \sigma_{01}$ at the inner surface of the assembly ($r = a$) and it starts at the interface ($r = r_1$) when $\sigma_{\theta 2} - \sigma_{r2} = \sigma_{02}$. Inserting the stress expressions into the first equation gives

$$\frac{-(2M_1 r_1^{\,2} P(b^2 M_7 + M_5 r_1^{\,2}))}{((-r_1^{\,2}(b^2 M_7 + M_5 r_1^{\,2}) + a^2(b^2 M_6 + M_8 r_1^{\,2}))(1+\nu_1)} = \sigma_{01}, \tag{111}$$

and the second equation becomes

$$\frac{4a^2 b^2 E_2 M_2 P(1-\nu_1^{\,2})}{r_1^{\,2}(b^2 M_7 + M_5 r_1^{\,2}) + a^2(b^2 M_6 + M_8 r_1^{\,2})(1+\nu_2)} = \sigma_{02}. \tag{112}$$

The elastic limit internal pressure that causes yielding starting from the inner surface ($r = a$) is found by the solution of Eq. (111) as

$$\overline{P_e} = \frac{(b^2 M_7 r_1^{\,2} + M_5 r_1^{\,4} - a^2(b^2 M_6 + M_8 r_1^{\,2}))(1+\nu_1)}{2M_1 r_1^{\,2}(b^2 M_7 + M_5 r_1^{\,2})} \tag{113}$$

where $\overline{P_e} = \dfrac{P}{\sigma_{01}}$.

Similarly, the elastic limit internal pressure that causes yielding at the interface ($r = r_1$) is found as

$$\overline{P_e} = \frac{r_1^{\,2}(b^2 M_7 + M_5 r_1^{\,2} - a^2(b^2 M_6 + M_8 r_1^{\,2}))(1+\nu_2)\sigma_{02}}{4a^2 b^2 E_2 M_2 (1-\nu_1^{\,2})\sigma_{01}}. \tag{114}$$

As mentioned above, for the two-layer tubes under internal pressure, the yielding may begin simultaneously at both locations (at $r = a$ and $r = r_1$). In order to find the

elastic limit internal pressure and the corresponding critical interface radius (r_{1cr}) that cause simultaneous yielding, Eqs. (111) and (112) should be solved at the same time for P and r_1. An example for this case will be given in the next chapter.

Similar to the case for Tresca's criterion, two equations that define the yielding at the above mentioned locations can also be written according to von Mises criterion (Eq. (106)). At the inner surface

$$\sqrt{\frac{M_1^{\,2}P^2(3r_1^{\,4}(b^2M_7+M_5r_1^{\,2})^2+a^4M_3^{\,2}(b^2M_6+M_8r_1^{\,2})^2)}{(b^2M_7r_1^{\,2}+M_5r_1^{\,4}-a^2(b^2M_6+M_8r_1^{\,2}))^2(1+\nu_1)^2}}=\sigma_{01}\ , \tag{115}$$

and at the interface ($r=r_1$)

$$\sqrt{\frac{4a^4E_2^{\,2}M_2^{\,2}P^2(3b^4+M_4^{\,2}r_1^{\,4})(1-\nu_1^{\,2})^2}{(b^2M_7r_1^{\,2}+M_5r_1^{\,4}-a^2(b^2M_6+M_8r_1^{\,2}))^2(1+\nu_2)^2}}=\sigma_{02}\,. \tag{116}$$

Similar to Tresca's criterion, the elastic limit internal pressure that causes yielding which starts from the inner surface ($r=a$) is found from the solution of Eq. (115), which is

$$\overline{P_e}=\frac{1}{M_1}\sqrt{\frac{(b^2M_7r_1^{\,2}+M_5r_1^{\,4}-a^2(b^2M_6+M_8r_1^{\,2}))^2(1+\nu_1)^2}{3r_1^{\,4}(b^2M_7+M_5r_1^{\,2})^2+a^4M_3(b^2M_6+M_8r_1^{\,2})^2}}\,. \tag{117}$$

On the other hand, the elastic limit internal pressure that causes yielding which commences at the interface ($r=r_1$) is found from Eq. (116) as

$$\overline{P_e}=\frac{\sigma_{02}}{2a^2E_2M_2\sigma_{01}}\sqrt{\frac{(b^2M_7r_1^{\,2}+M_5r_1^{\,4}-a^2(b^2M_6+M_8r_1^{\,2}))^2(1+\nu_2)^2}{(3b^4+M_4^{\,2}r_1^{\,4})(\nu_1^{\,2}-1)^2}}\,. \tag{118}$$

The simultaneous yielding behaviour which is explained for the Tresca's yield criterion is also observed for this condition of yielding. The details of this case will be given in the next chapter.

3.7 Yielding of Two-Layer Tubes Under External Pressure

According to Tresca's yield criterion, for the two-layer tubes under external pressure, the yielding begins when $\sigma_{r1} - \sigma_{\theta 1} = \sigma_{01}$ at the inner surface and when $\sigma_{r2} - \sigma_{\theta 2} = \sigma_{02}$ at the interface. Inserting the stress expressions into these equations, the following relations can be obtained for the external pressure case:

$$\frac{4b^2 E_1 M_1 r_1^{\,2} P(1-\nu_2^{\,2})}{r_1^{\,2}(b^2 M_7 + M_5 r_1^{\,2}) + a^2(b^2 M_6 + M_8 r_1^{\,2})(1+\nu_1)} = \sigma_{01}, \tag{119}$$

$$\frac{2b^2 M_2 P(a^2 M_8 - M_5 r_1^{\,2})}{r_1^{\,2}(b^2 M_7 + M_5 r_1^{\,2}) + a^2(b^2 M_6 + M_8 r_1^{\,2})(1+\nu_2)} = \sigma_{02}. \tag{120}$$

Using Eq. (119), the elastic limit external pressure that starts yielding at $r = a$ is found as

$$\overline{P_e} = \frac{(r_1^{\,2}(b^2 M_7 + M_5 r_1^{\,2}) + a^2(b^2 M_6 + M_8 r_1^{\,2}))(1+\nu_1)}{4b^2 E_1 M_1 r_1^{\,2}(1-\nu_2^{\,2})} \tag{121}$$

Using Eq. (120) the elastic limit external pressure that starts yielding at the interface becomes

$$\overline{P_e} = \frac{(b^2 M_7 r_1^{\,2} + M_5 r_1^{\,4} - a^2(b^2 M_6 + M_8 r_1^{\,2}))(1+\nu_2)\sigma_{02}}{2b^2 M_2(a^2 M_8 - M_5 r_1^{\,2})\sigma_{01}} \tag{122}$$

The simultaneous yielding behaviour observed for the internal pressure case is also found in external pressure case. The details will be given in the next chapter.

According to von Mises criterion, the yielding begins when $\phi = 1$. Considering the yield criterion given in Eq. (106) and inserting the stress expressions, which are obtained previously, into this equation, the condition for the yielding at the inner surface becomes

$$\sqrt{\frac{4b^4 E_1^{\,2} M_1^{\,2} (M_3^{\,2} + 3) P^2 r_1^{\,4} (1 - \nu_2^{\,2})^2}{(b^2 M_7 r_1^{\,2} + M_5 r_1^{\,4} - a^2 (b^2 M_6 + M_8 r_1^{\,2}))^2 (1 + \nu_1)^2}} = \sigma_{01}, \tag{123}$$

and at the interface ($r = r_1$), it becomes

$$\sqrt{\frac{b^4 M_2^{\,2} P^2 (a^4 (M_4^{\,2} M_6^{\,2} + 3M_8^{\,2}) - 2a^2 N_1 r_1^{\,2} + (3M_5^{\,2} + M_4^{\,2} M_7^{\,2}) r_1^{\,4})}{((b^2 M_7 r_1^{\,2} + M_5 r_1^{\,4} - a^2 (b^2 M_6 + M_8 r_1^{\,2}))^2 (1 + \nu_2)^2}} = \sigma_{02}. \tag{124}$$

Using Eq. (123), the elastic limit external pressure is obtained as

$$\overline{P_e} = \frac{1}{2b^2 E_1 M_1 r_1^{\,2}} \sqrt{\frac{(b^2 M_7 r_1^{\,2} + M_5 r_1^{\,4} - a^2 (b^2 M_6 + M_8 r_1^{\,2}))^2 (1 + \nu_1)^2}{(3 + M_3^{\,2})(1 - \nu_2^{\,2})^2}} \tag{125}$$

Similarly, the elastic limit external pressure that causes yielding at the interface is found as

$$\overline{P_e} = \frac{\sigma_{02}}{b^2 M_2 \sigma_{01}} \sqrt{\frac{(b^2 M_7 r_1^{\,2} + M_5 r_1^{\,4} - a^2 (b^2 M_6 + M_8 r_1^{\,2}))^2 (1 + \nu_2)^2}{a^4 (M_4^{\,2} M_6^{\,2} + 3M_8^{\,2}) - 2a^2 N_1 r_1^{\,2} + (3M_5^{\,2} + M_4^{\,2} M_7^{\,2}) r_1^{\,4}}} \tag{126}$$

where

$$N_1 = M_4^{\,2} M_6 M_7 + 3M_5 M_8. \tag{127}$$

Before coming to the three-layer tubes, the importance of the critical interface radius should be highlighted. For the two-layer tube assemblies under internal or external pressure;

a. For the yielding that starts at the inner surface ($r = a$), r_1 should be higher than the critical interface radius ($r_1 > r_{1cr}$).
b. For the yielding that starts at the interface ($r = r_1$), the interface radius should be lower than the critical interface radius ($r_1 < \bar{r}_{1cr}$).
c. For the simultaneous yielding at the inner surface and at the interface of the assembly $r_1 = r_{1cr}$.

These results show that the critical interface radius is an important factor that affects the yielding behaviour.

3.8 Yielding of Three-Layer Tubes Under Internal Pressure

It is found that, for the three-layer tubes under internal or external pressure, yielding may first begin at the inner surface of the assembly ($r = a$), at one of the interfaces of the assembly ($r = r_1$, $r = r_2$), at the two locations of the assembly at the same time ($r = a$ and $r = r_1$ or $r = a$ and $r = r_2$ or $r = r_1$ and $r = r_2$) or it may begin at the three layers at the same time. According to Tresca's criterion, the yield conditions for the internal pressure become $\sigma_{\theta 1} - \sigma_{r1} = \sigma_{01}$, $\sigma_{\theta 2} - \sigma_{r2} = \sigma_{02}$, $\sigma_{\theta 3} - \sigma_{r3} = \sigma_{03}$. The first equation is the criterion of yielding that starts at the inner surface ($r = a$) of the assembly, the second equation is the criterion of yielding that starts at the inner interface ($r = r_1$) of the assembly, and the last equation is the criterion of yielding that starts at the outer interface ($r = r_2$) of the assembly. Inserting the stress expressions, the first condition becomes

$$\frac{2D_1 r_1^{\,2} P(b^2 D_{14} + D_{15} r_2^{\,2})}{(r_1^{\,2}(b^2 D_{14} + D_{15} r_2^{\,2}) - a^2 (b^2 D_{17} + D_{16} r_2^{\,2}))(1+\nu_1)} = \sigma_{01} . \tag{128}$$

Similarly, the second and third conditions become

$$\frac{4a^2 D_2 E_2 r_2^{\,2} P(r_2^{\,2} D_{18} + D_{19} b^2)(1-\nu_1^{\,2})}{(r_1^{\,2}(b^2 D_{14} + D_{15} r_2^{\,2}) - a^2 (b^2 D_{17} + D_{16} r_2^{\,2}))(1+\nu_2)} = \sigma_{02} , \tag{129}$$

$$\frac{8a^2b^2D_3E_2E_3r_1^{\,2}P(1-\nu_1^{\,2})(1-\nu_2^{\,2})}{(r_1^{\,2}(b^2D_{14}+D_{15}r_2^{\,2})-a^2(b^2D_{17}+D_{16}r_2^{\,2}))(1+\nu_3)}=\sigma_{03}\,. \tag{130}$$

The elastic limit internal pressure causing the yielding at the inner surface ($r = a$) is obtained by using Eq. (128) as

$$\overline{P_e}=\frac{(r_1^{\,2}(b^2D_{14}+D_{15}r_2^{\,2})-a^2(b^2D_{17}+D_{16}r_2^{\,2}))(1+\nu_1)}{2D_1r_1^{\,2}(b^2D_{14}+D_{15}r_2^{\,2})}\,. \tag{131}$$

Similarly, the elastic limit internal pressure that starts yielding at the inner interface ($r = r_1$) is obtained by using Eq. (129) as

$$\overline{P_e}=\frac{(r_1^{\,2}(b^2D_{14}+D_{15}r_2^{\,2})-a^2(b^2D_{17}+D_{16}r_2^{\,2}))(1+\nu_2)\sigma_{02}}{4a^2D_2E_2r_2^{\,2}(b^2D_{19}+D_{18}r_2^{\,2})(1-\nu_1^{\,2})\sigma_{01}}\,. \tag{132}$$

Finally, the elastic limit internal pressure that causes yielding at the outer interface ($r = r_2$) is obtained by using Eq. (130) as

$$\overline{P_e}=\frac{(r_1^{\,2}(b^2D_{14}+D_{15}r_2^{\,2})-a^2(b^2D_{17}+D_{16}r_2^{\,2}))(1+\nu_3)\sigma_{03}}{8a^2b^2D_3E_2E_3r_1^{\,2}(1-\nu_1^{\,2})(1-\nu_2^{\,2})\sigma_{01}}\,. \tag{133}$$

As mentioned above, for the three layer tubes under internal or external pressure, yielding may begin simultaneously at more than one location. The elastic limit pressure and the corresponding interface coordinates at which the yielding begins simultaneously at the three locations can be found by solving Eqs. (128), (129), and (130) together. Investigations have revealed that simultaneous yielding only occurs under the restrictions of the properties of the materials. For the simultaneous yielding at the three locations mentioned above, the first layer's yield limit should be the highest, and the outer layer's yield limit should be the lowest.

Different from the case presented above, it is also possible that yielding may begin simultaneously at two different layers of the assembly. In order to find the elastic

limit pressure and the corresponding interface radius of the assembly, the corresponding two equations belonging to the yielding locations should be solved together. In addition, while solving the elastic limit pressure and critical interface radius, one of the interface radii at which the yielding has not yet begun and the inner surface radius *a* should be given. The given interface radius should be higher than the critical interface radius of the assembly for both internal and external pressure cases. All these cases will be clarified in the next chapter.

According to von Mises criterion, the yielding begins when $\phi = 1$ for each layer. Using this condition, the yielding equations at the inner surface ($r = a$), at the inner interface ($r = r_1$), and at the outer interface ($r = r_2$) are obtained as

$$\sqrt{\frac{D_1^{\,2} P^2 (3 r_1^{\,4} (b^2 D_{14} + D_{15} r_2^{\,2})^2 + a^4 D_4^{\,2} (b^2 D_{17} + D_{16} r_2^{\,2})^2)}{(r_1^{\,2} (b^2 D_{14} + D_{15} r_2^{\,2}) - a^2 (b^2 D_{17} + D_{16} r_2^{\,2}))^2 (1+\nu_1)^2}} = \sigma_{01}, \tag{134}$$

$$\sqrt{\frac{4a^4 D_2^{\,2} E_2^{\,2} P^2 (D_{21}^{\,2} D_5^{\,2} r_1^{\,4} r_2^{\,4} + 3 D_{18}^{\,2} r_2^{\,8} + 2 b^2 r_2^{\,2} N_2 + b^4 N_3)(1-\nu_1^{\,2})^2}{(r_1^{\,2} (b^2 D_{14} + D_{15} r_2^{\,2}) - a^2 (b^2 D_{17} + D_{16} r_2^{\,2}))^2 (1+\nu_2)^2}} = \sigma_{02}, \tag{135}$$

$$\sqrt{\frac{16a^4 D_3^{\,2} E_2^{\,2} E_3^{\,2} P^2 r_1^{\,4} (3b^4 + D_6^{\,2} r_2^{\,4})(1-\nu_1^{\,2})^2 (1-\nu_2^{\,2})^2}{(r_1^{\,2} (b^2 D_{14} + D_{15} r_2^{\,2}) - a^2 (b^2 D_{17} + D_{16} r_2^{\,2}))^2 (1+\nu_3)^2}} = \sigma_{03}, \tag{136}$$

where

$$N_2 = D_{20} D_{21} D_5^{\,2} r_1^{\,4} + 3 D_{18} D_{19} r_2^{\,4}, \tag{137}$$

$$N_3 = D_{20}^{\,2} D_5^{\,2} r_1^{\,4} + 3 D_{19}^{\,2} r_2^{\,4}. \tag{138}$$

Using Eq. (134), the elastic limit internal pressure causing the yielding start from $r = a$ is obtained as

$$\overline{P_e} = \frac{1}{D_1}\sqrt{\frac{(r_1^{\,2}(b^2 D_{14} + D_{15} r_2^{\,2}) \; - a^2 (b^2 D_{17} + D_{16} r_2^{\,2}))^2 (1+\nu_1^{\,2})}{3 r_1^{\,4} (b^2 D_{14} + D_{15} r_2^{\,2})^2 + a^4 D_4^{\,2} (b^2 D_{17} + D_{16} r_2^{\,2})^2}} \,. \tag{139}$$

For the yielding that starts at the inner interface ($r = r_1$), using Eq. (135), the corresponding elastic limit internal pressure is found as

$$\overline{P_e} = \frac{\sigma_{02}}{2a^2 D_2 E_2 \sigma_{01}}\sqrt{\frac{(r_1^{\,2}(b^2 D_{14} + D_{15} r_2^{\,2}) - a^2 (b^2 D_{17} + D_{16} r_2^{\,2}))^2 (1+\nu_2^{\,2})}{(D_{21}^{\,2} D_5^{\,2} r_1^{\,4} r_2^{\,4} + 3 D_{18}^{\,2} r_2^{\,8} + 2b^2 r_2^{\,2} N_2 + b^4 N_3)(-1+\nu_1^{\,2})^2}} \,. \tag{140}$$

Finally, using Eq. (136), the elastic limit internal pressure causing the yielding at the outer interface ($r = r_2$) is found as

$$\overline{P_e} = \frac{\sigma_{03}}{4a^2 D_3 E_2 E_3 r_1^{\,2} \sigma_{01}}\sqrt{\frac{(r_1^{\,2}(b^2 D_{14} + D_{15} r_2^{\,2}) - a^2 (b^2 D_{17} + D_{16} r_2^{\,2}))^2 (1+\nu_3)^2}{(3b^4 + D_6^{\,2} r_2^{\,4})(1-\nu_1^{\,2})^2 (1-\nu_2^{\,2})^2}} \,. \tag{141}$$

3.9 Yielding of Three-Layer Tubes Under External Pressure

Studies show that the yielding behaviour of the three-layer tubes under external pressure is similar to the case of internally pressurized three-layer tubes. The only difference is the yield condition. According to Tresca's criterion, the yield conditions for the three layers are: $\sigma_{r1} - \sigma_{\theta 1} = \sigma_{01}$, $\sigma_{r2} - \sigma_{\theta 2} = \sigma_{02}$ and $\sigma_{r3} - \sigma_{\theta 3} = \sigma_{03}$. The first equation is the criterion of yielding that starts at the inner surface ($r = a$) of the assembly, the second equation is the criterion of yielding that starts at the inner interface ($r = r_1$) of the assembly, and the last equation is the criterion of yielding that starts at the outer interface ($r = r_2$) of the assembly.

Using these expressions, the following yielding equations can be obtained:

$$\frac{8b^2 D_1 E_1 E_2 r_1^{\,2} r_2^{\,2} P (1-\nu_2^{\,2})(1-\nu_3^{\,2})}{(-r_1^{\,2}(b^2 D_{14} + D_{15} r_2^{\,2}) + a^2 (b^2 D_{17} + D_{16} r_2^{\,2}))(1+\nu_1)} = \sigma_{01} \,, \tag{142}$$

$$\frac{4b^2D_2E_2P(D_{22}a^2-D_{23}r_1^{\,2})r_2^{\,2}(1-\nu_3^{\,2})}{(-r_1^{\,2}(b^2D_{14}+D_{15}r_2^{\,2})+a^2(b^2D_{17}+D_{16}r_2^{\,2}))(1+\nu_2)}=\sigma_{02}\,, \tag{143}$$

$$\frac{2b^2D_3P(a^2D_{16}-D_{15}\ r_1^{\,2})}{(-r_1^{\,2}(b^2D_{14}+D_{15}r_2^{\,2})+a^2(b^2D_{17}+D_{16}r_2^{\,2}))(1+\nu_3)}=\sigma_{03}\,. \tag{144}$$

The elastic limit external pressure that causes yielding at the inner surface ($r = a$) is obtained by using Eq. (142) as

$$\overline{P_e}=\frac{(r_1^{\,2}(b^2D_{14}+D_{15}r_2^{\,2})-a^2(b^2D_{17}+D_{16}r_2^{\,2}))(1+\nu_1)}{8b^2D_1E_1E_2r_1^{\,2}r_2^{\,2}(1-\nu_2^{\,2})(1-\nu_3^{\,2})}\,. \tag{145}$$

Similarly, the elastic limit external pressure causing the yielding start at the inner interface ($r = r_1$) is obtained by using Eq. (143) as

$$\overline{P_e}=\frac{(-r_1^{\,2}(b^2D_{14}+D_{15}r_2^{\,2})+a^2(b^2D_{17}+D_{16}r_2^{\,2}))(1+\nu_2)\sigma_{02}}{4b^2D_2E_2(r_1^{\,2}D_{23}-D_{22}a^2)r_2^{\,2}(1-\nu_3^{\,2})\sigma_{01}}\,. \tag{146}$$

Finally, the elastic limit external pressure that causes yielding at the outer interface ($r = r_2$) is obtained by using Eq. (144) as

$$\overline{P_e}=\frac{(r_1^{\,2}(b^2D_{14}+D_{15}r_2^{\,2})-a^2(b^2D_{17}+D_{16}r_2^{\,2}))(1+\nu_3)\sigma_{03}}{2b^2D_3(a^2D_{16}-D_{15}r_1^{\,2})\sigma_{01}}\,. \tag{147}$$

Similar to the internal pressure case, for the three-layer tubes under external pressure, according to von Mises criterion, yielding begins as soon as $\phi = 1$. Using Eq. (106), the relations for the yielding that starts at the inner surface *(r=a)*, at the inner interface ($r = r_1$), and at the outer interface ($r = r_2$) can be obtained as

$$\sqrt{\frac{16b^4D_1^{\,2}(D_4^{\,2}+3)E_1^{\,2}E_2^{\,2}P^2r_1^{\,4}r_2^{\,4}(1-\nu_2^{\,2})^2(1-\nu_3^{\,2})^2}{(r_1^{\,2}(b^2D_{14}+D_{15}r_2^{\,2})-a^2(b^2D_{17}+D_{16}r_2^{\,2}))^2(1+\nu_1)^2}}=\sigma_{01}\,, \tag{148}$$

$$\sqrt{\frac{4b^4 D_2{}^2 E_2{}^2 P^2 (a^4 (3D_{22}{}^2 + D_{24}{}^2 D_5{}^2) - 2a^2 N_4 r_1{}^2 + N_5 r_1{}^4) r_2{}^4 (1-\nu_3{}^2)^2}{(r_1{}^2 (b^2 D_{14} + D_{15} r_2{}^2) - a^2 (b^2 D_{17} + D_{16} r_2{}^2))^2 (1+\nu_2)^2}} = \sigma_{02}, \quad (149)$$

$$\sqrt{\frac{b^4 D_3{}^2 P^2 (a^4 (3D_{16}{}^2 + D_{17}{}^2 D_6{}^2) - 2a^2 N_6 r_1{}^2 + (3D_{15}{}^2 + D_{14}{}^2 D_6{}^2) r_1{}^4)}{(r_1{}^2 (b^2 D_{14} + D_{15} r_2{}^2) - a^2 (b^2 D_{17} + D_{16} r_2{}^2))^2 (1+\nu_3)^2}} = \sigma_{03}, \quad (150)$$

where

$$N_4 = 3D_{22}\ D_{23}\ + D_{24} D_{25} D_5{}^2, \quad (151)$$

$$N_5 = 3D_{23}{}^2 + D_{25}{}^2 D_5{}^2\ , \quad (152)$$

$$N_6 = 3D_{15} D_{16} + D_{14} D_{17} D_6{}^2 . \quad (153)$$

Using Eq. (148), the elastic limit external pressure causing the yielding start from *(r = a)* is obtained as

$$\overline{P_e} = \frac{1}{4b^2 D_1 E_1 E_2 r_1{}^2 r_2{}^2} \sqrt{\frac{(r_1{}^2 (b^2 D_{14} + D_{15} r_2{}^2)\ - a^2 (b^2 D_{17} + D_{16} r_2{}^2))^2 (1+\nu_1{}^2)}{(D_4{}^2 + 3)(1-\nu_2{}^2)^2 (1-\nu_3{}^2)^2}} . \quad (154)$$

The elastic limit external pressure that causes yielding at the inner interface ($r = r_1$), is found by using Eq. (149) as

$$\overline{P_e} = \frac{N_7 \sigma_{02}}{\sigma_{01}} \sqrt{\frac{(r_1{}^2 (b^2 D_{14} + D_{15} r_2{}^2) - a^2 (b^2 D_{17} + D_{16} r_2{}^2))^2 (1+\nu_2{}^2)}{(a^4 (3D_{22}{}^2 + D_{24}{}^2 D_5{}^2) - 2a^2 N_4 r_1{}^2 + N_5 r_1{}^4)(1-\nu_3{}^2)^2}} , \quad (155)$$

where

$$N_7 = \frac{1}{2b^2 D_2 E_2 r_2{}^2}\ . \quad (156)$$

Finally, using Eq. (150), the elastic limit external pressure causing the yielding at the outer interface *(*$r = r_2$) is found as

$$\overline{P_e} = \frac{\sigma_{03}}{b^2 D_3 \sigma_{01}} \sqrt{\frac{(r_1^{\,2}(b^2 D_{14} + D_{15} r_2^{\,2}) - a^2 (b^2 D_{17} + D_{16} r_2^{\,2}))^2 (1+\nu_3)^2}{a^4 (3D_{16}^{\,2} + D_{17}^{\,2} D_6^{\,2}) - 2a^2 N_8 r_1^{\,2} + (3D_{15}^{\,2} + D_{14}^{\,2} D_6^{\,2}) r_1^{\,4}}}, \tag{157}$$

where

$$N_8 = 3D_{15}D_{16} + D_{14}D_{17}D_6^{\,2} \ . \tag{158}$$

Similar to the two-layer tubes, the critical radii that are obtained for the three-layer tubes are quite important in the determination of the yielding behaviour. If the yielding of only one layer is desired, there are some restrictions related to the critical interface radii of the considered three-layer tube. For instance, if we want the tube yield from the inner surface ($r = a$) first, then the corresponding interface radii should be chosen as follows: $r_1 > r_{1cr}$ and $r_2 > r_{2cr}$. Secondly, for the yielding that starts at the inner interface ($r = r_1$) first, the conditions should be $r_1 < r_{1cr}$ and $r_2 = r_{2cr}$. Thirdly, when $r_1 = r_{1cr}$ and $r_2 < r_{2cr}$, the yielding starts at the outer interface ($r = r_2$) first. In the next part, some numerical examples are handled to clarify the yielding behavior of the multi-layer tubes under pressure.

CHAPTER 4

NUMERICAL RESULTS

4.1 General

In Chapter Two, the derivations of the basic expressions of the composite tubes under internal and external pressure were presented. The stresses, displacements and integration constants for single, two and three-layer tubes were given in that chapter. In Chapter Three, the two yielding criteria, Tresca's yield criterion and von Mises yield criterion, were presented first. Then, the yielding behavior of one, two and three-layer composite tubes under internal and external pressure were analyzed according to the above mentioned yield criteria. The equations of the elastic limit pressures were also given in that chapter. In this chapter, some numerical results of the pressurized multi-layer tubes will be given. The yielding behavior of one layer tubes under pressure will be presented first; afterwards the behaviour of the two and three-layer composite tubes will be given. In addition, the results obtained by Tresca's criterion and von Mises criterion will be compared for the cases that are considered. Finally, an example problem given in the study of Hongjun et al. [17] will be handled.

In Table 4.1, the material properties that are used in this study are given. In the presentation of the numerical results the following dimensionless variables are used:

$$\bar{r} = \frac{r}{b}; \quad \bar{u} = \frac{uE_1}{\sigma_{01} b}; \quad \bar{\sigma}_i = \frac{\sigma_i}{\sigma_{01}}. \tag{159}$$

Table 4.1. Mechanical properties of the materials used in the numerical analyses

	E (GPa)	ν	σ_o (MPa)
Aluminum	70	0.35	100
Brass	105	0.35	410
Copper	120	0.365	265
Steel	200	0.30	430

4.2 Single Layer Tube Results

For a single layer tube, as it was mentioned in the previous chapter, yielding begins at the inner surface. According to Tresca's yield criterion, the stress and displacement distributions in a single layer steel tube under internal pressure are given in Fig 4.1. Here, the inner radius $\bar{a} = a/b$ =0.7 and the elastic limit internal pressure is obtained as $\overline{P}_e = 0.255$ using Eq. (107). By using Eqs. (13) and (14), the dimensionless integration constants are found as $\overline{C}_1 = C_1 / b^2$ =6.52925×10^{-4} and $\overline{C}_2 = C_2$ = 2.61170×10^{-4}. The stress variable according to Tresca's yielding criterion is given by $\phi = \overline{\sigma}_\theta$ - $\overline{\sigma}_r$. It can be observed from the figure that ϕ=1 at $r = a$ which shows the commencement of the yielding.

In Fig. 4.2, the distributions of stresses and displacement of an internally pressurized tube having the same dimensions is shown. The only difference from the previous graph is the consideration of von Mises criterion to monitor the yielding. The elastic limit internal pressure is found as $\overline{P}_e = 0.292581$ by using Eq. (108). The corresponding integration constants are found as $C_1 = 7.49150\times10^{-4}$ and $C_2 = 2.99660\times10^{-4}$ by the help of Eqs. (13) and (14).

Coming to the external pressure case, it is known that yielding begins at the inner surface of the tube as well. In Fig. 4.3, the stresses and displacement of a single layer steel tube with $\bar{a}$ =0.7 under external pressure is given for which the yielding begins

at $\overline{P}_e = 0.255$ according to Tresca's yield criterion. The elastic limit external pressure $\overline{P}_e$ is obtained by using Eq. (109). Using Eqs. (15) and (16), the integration constants are evaluated as $\overline{C}_1 = -6.52925 \times 10^{-4}$ and $\overline{C}_2 = -5.33000 \times 10^{-4}$.

The behaviour of a single layer steel tube ($\overline{a} = 0.7$ under the elastic limit external pressure considering the von Mises criterion is shown in Fig.4.4. Using Eq. (114), the elastic limit external pressure is calculated as $\overline{P}_e = 0.286897$. The corresponding integration constants are $C_1 = -7.34597 \times 10^{-4}$ and $C_2 = -5.99670 \times 10^{-4}$. It should be noted that $\phi = 1$ at the inner surface of the tube.

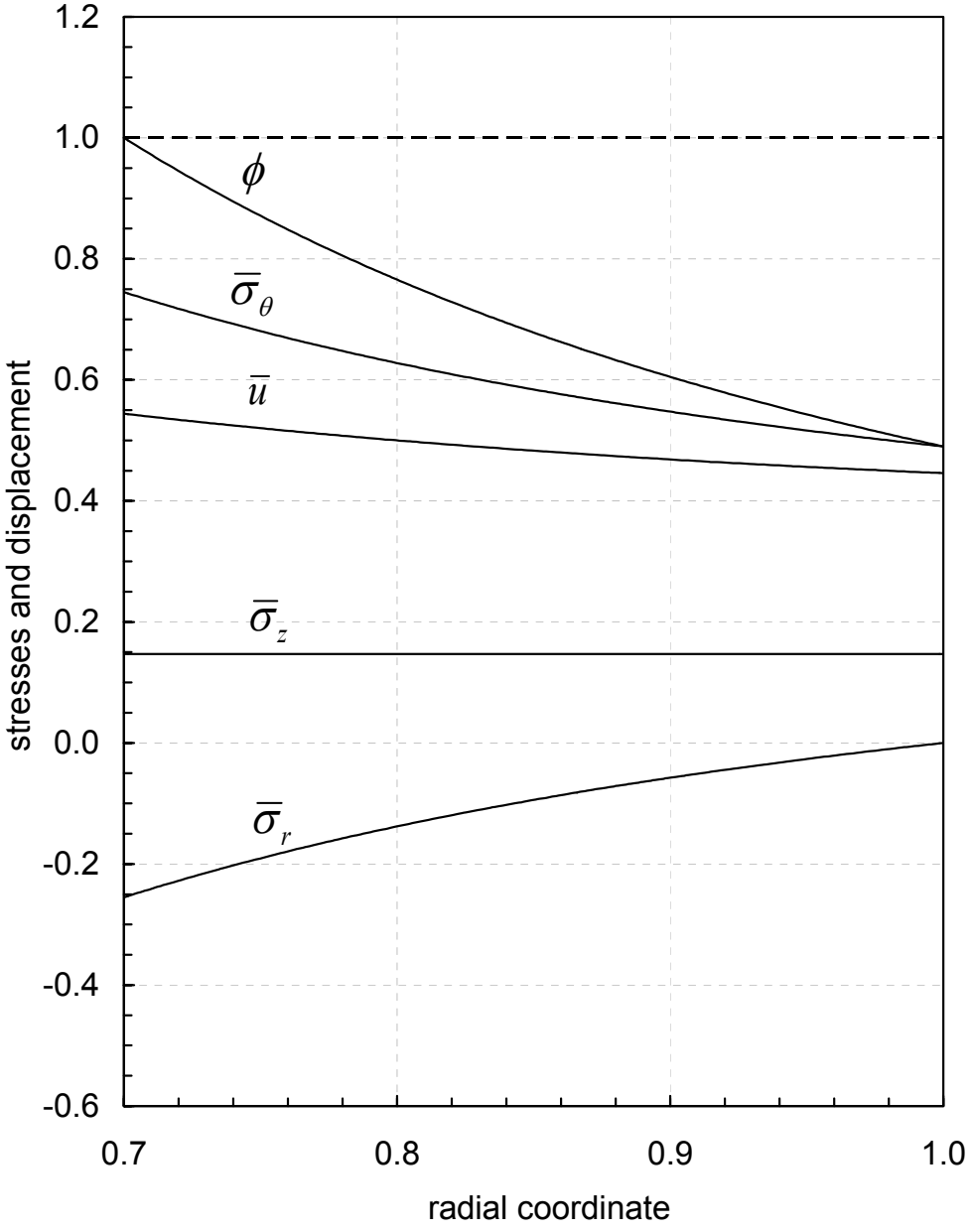

Figure 4.1 The distributions of stresses and displacement in a single layer steel tube ($\overline{a}$ =0.7) under elastic limit internal pressure $\overline{P}_e$=0.255

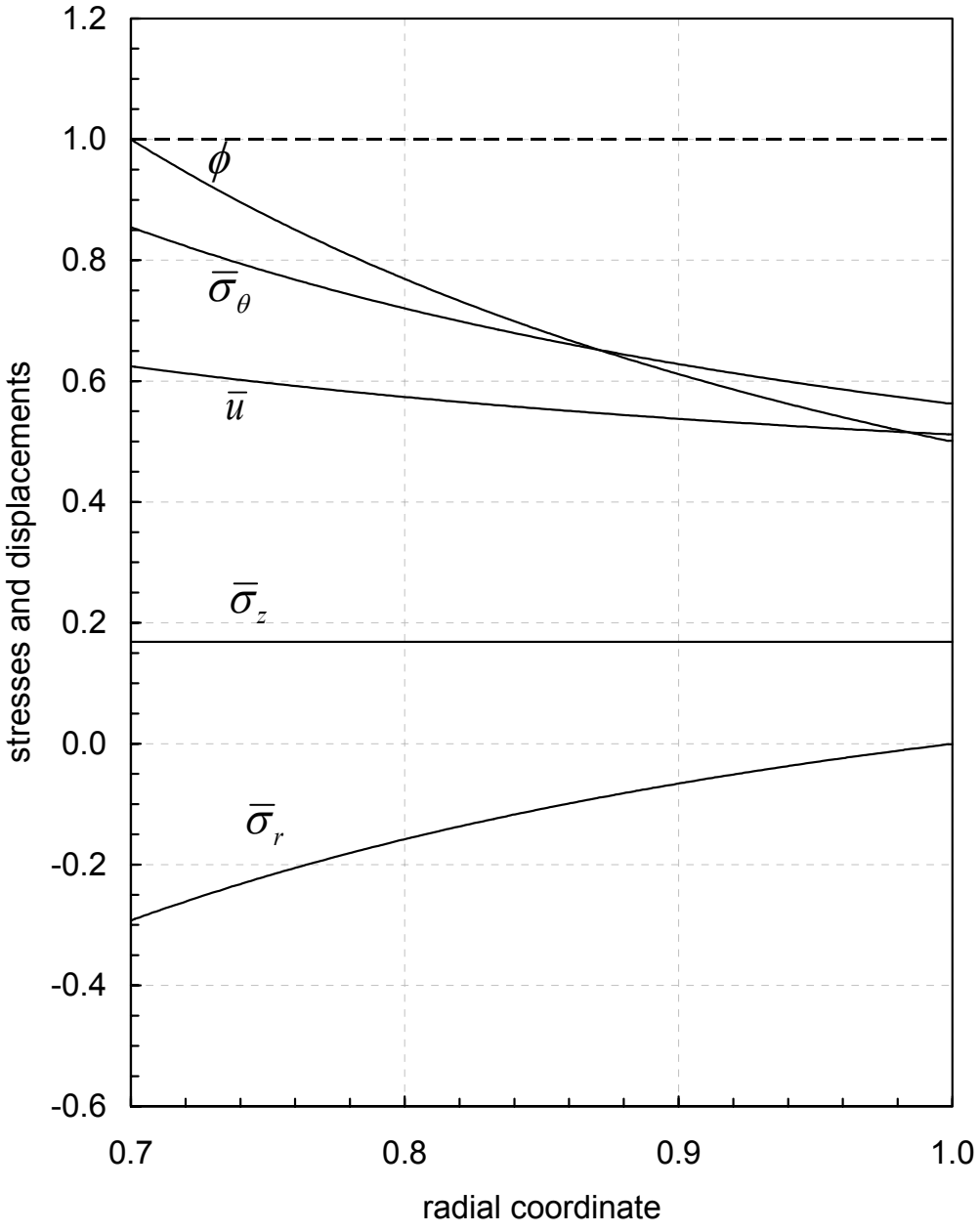

Figure 4.2 The distributions of stresses and displacement in a single layer steel tube ($\overline{a}$ =0.7) under elastic limit internal pressure $\overline{P}_e$=0.292581

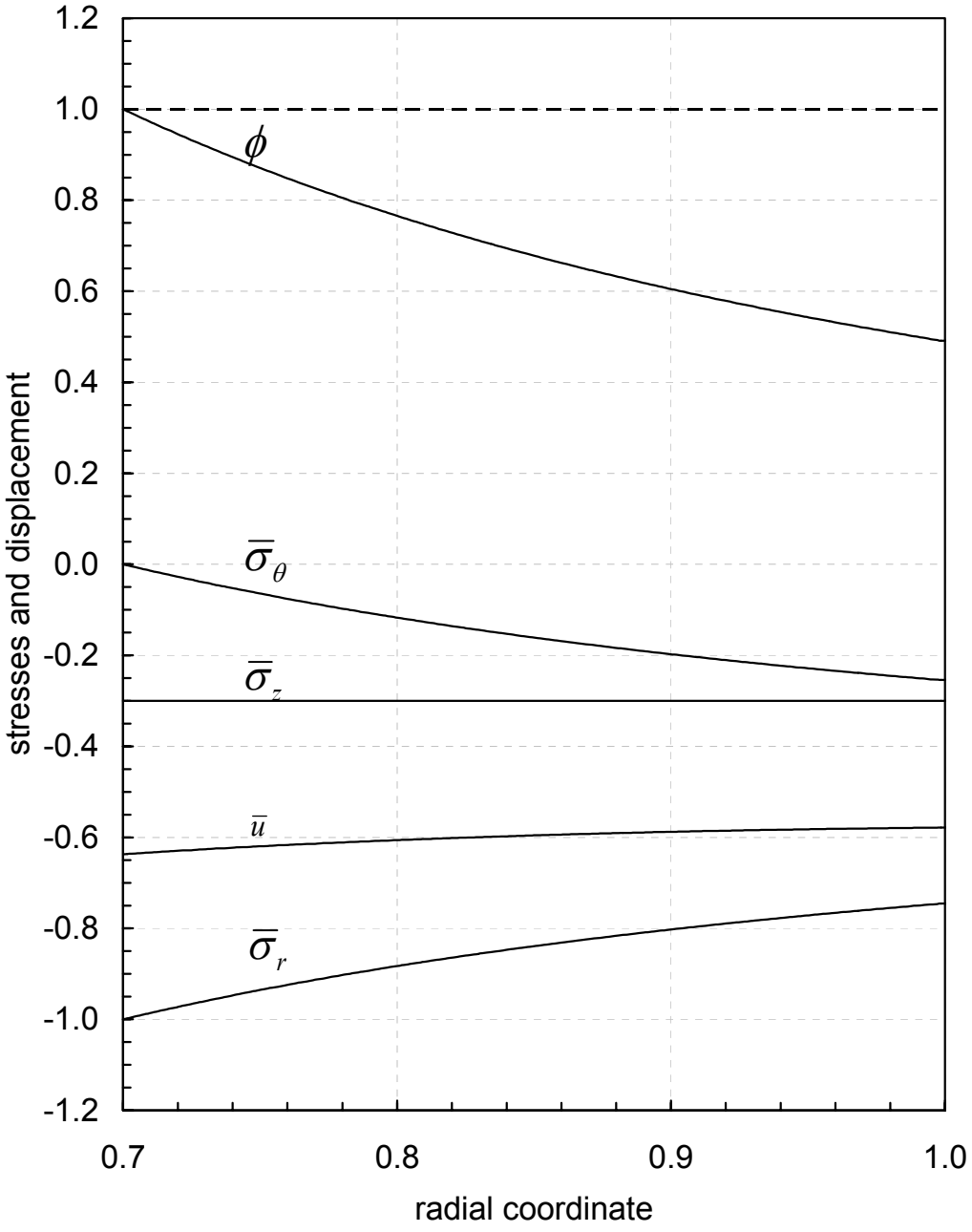

Figure 4.3 The distributions of stresses and displacement in a single layer steel tube ($\overline{a}$ =0.7) under elastic limit external pressure $\overline{P}_e$=0.255

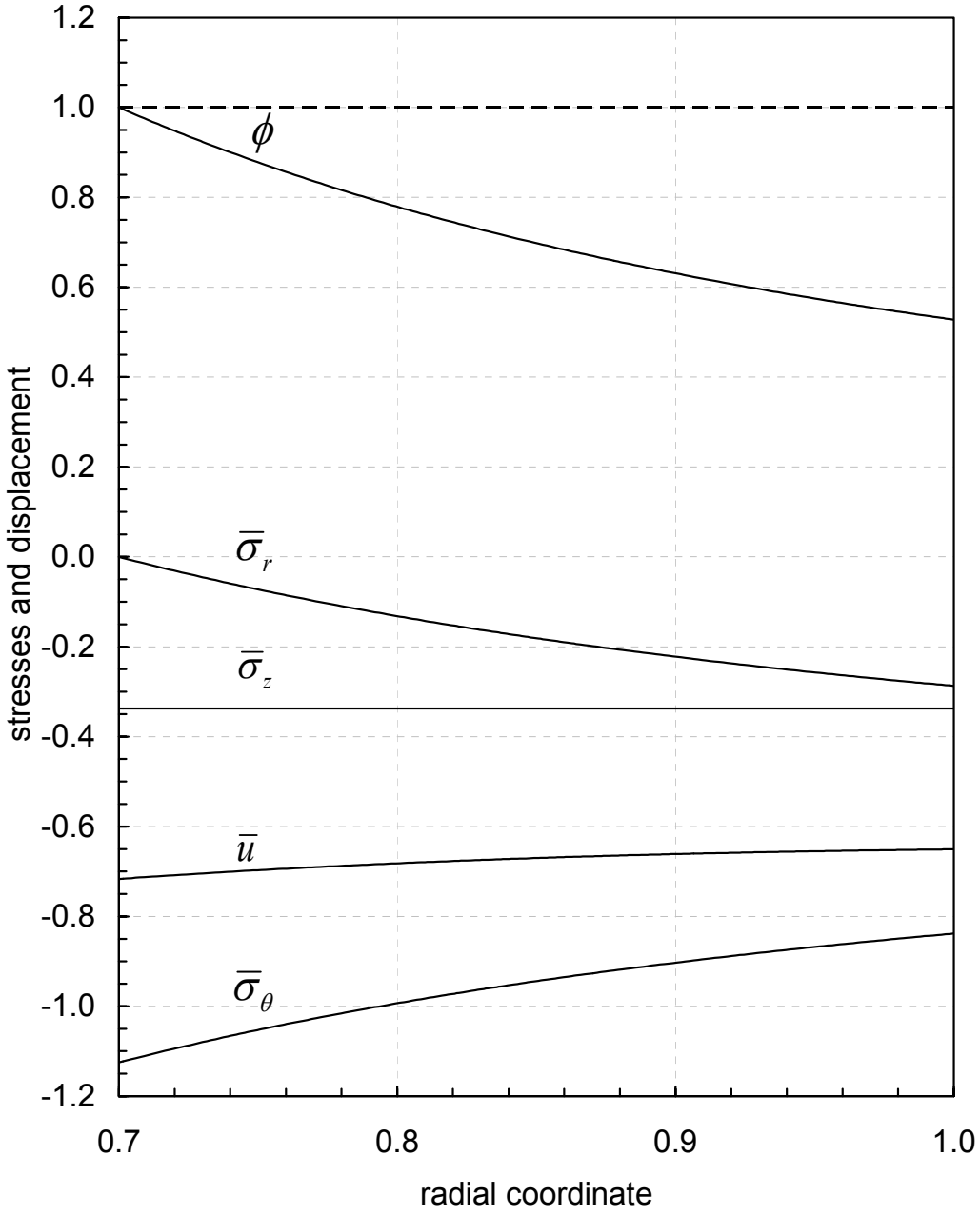

Figure 4.4 The distributions of stresses and displacement in a single layer steel tube ($\overline{a}$ =0.7) under elastic limit external pressure $\overline{P}_e$=0.286897

4.3 Two-Layer Tube Results

Before considering different material combinations, the verification of the expressions derived in the previous chapters is needed. For this purpose, a comparison between single layer tubes and two-layer tubes is made. A number of single layer tubes with different material properties are considered first. Using the expressions derived, the integration constants and elastic limit pressures are calculated for both internal and external pressure cases. On the other hand, these tubes are also modeled using two layer tubes (first tube: a to r_1 , second tube: r_1 to b). These two tubes are assumed to have the same material properties. The results show that for both pressure cases, the elastic limit pressures and the integration constants are identical for single and two-layer tubes. It can be concluded that the expressions derived for the two-layer tubes are correct.

Fig. 4.5 shows the simultaneous yielding of a two layer tube under internal pressure. The yielding criterion that is used is the Tresca's yield criterion and the inner layer of the tube is made of brass and the outer layer is made of copper. Here, $\overline{a}$ =0.6, elastic limit internal pressure and the corresponding critical interface radius is found as $\overline{P}_e$ =0.334061 and $\overline{r}_{1cr}$ =0.794711 by solving Eq. (111) and Eq. (112) together. Using Eqs. (31), (32), (33) and (34) the integration constants are obtained as $\overline{C}_1 = C_1 / b^2$ =9.48856×10^{-4}, $\overline{C}_2 = C_2$= 2.62420×10^{-4} , $\overline{C}_3 = C_3 / b^2$ =9.51190×10^{-4} and $\overline{C}_4 = C_4$=2.58723×10^{-4}. For this graph, it is worth underlying that the stress variable ϕ=1 at $r = a$ and at $r = r_1$ which shows the simultaneous yielding.

In order to present the yielding that starts at the inner surface ($r = a$), same two-layer tube assembly is considered. Taking $\overline{a}$ =0.6 and $\overline{r}_1$ =0.85, the elastic limit internal pressure is obtained as $\overline{P}_e$ =0.329630 using Eq.(113). Tresca's yield criterion is used to examine the behaviour. The corresponding integration constants are calculated as $\overline{C}_1 = 9.48857\times10^{-4}$, $\overline{C}_2 = 2.69428\times10^{-4}$, $\overline{C}_3 = 9.55704\times10^{-4}$ and $\overline{C}_4 =$ 2.59951×10^{-4}. Fig. 4.6 shows the consequent stresses and deformation. It should be noted that since the radius of the first layer is selected to be higher than the value of

the critical interface radius causing simultaneous yielding ($r_1 > r_{1cr}$), yielding begins from the inner layer of the tube.

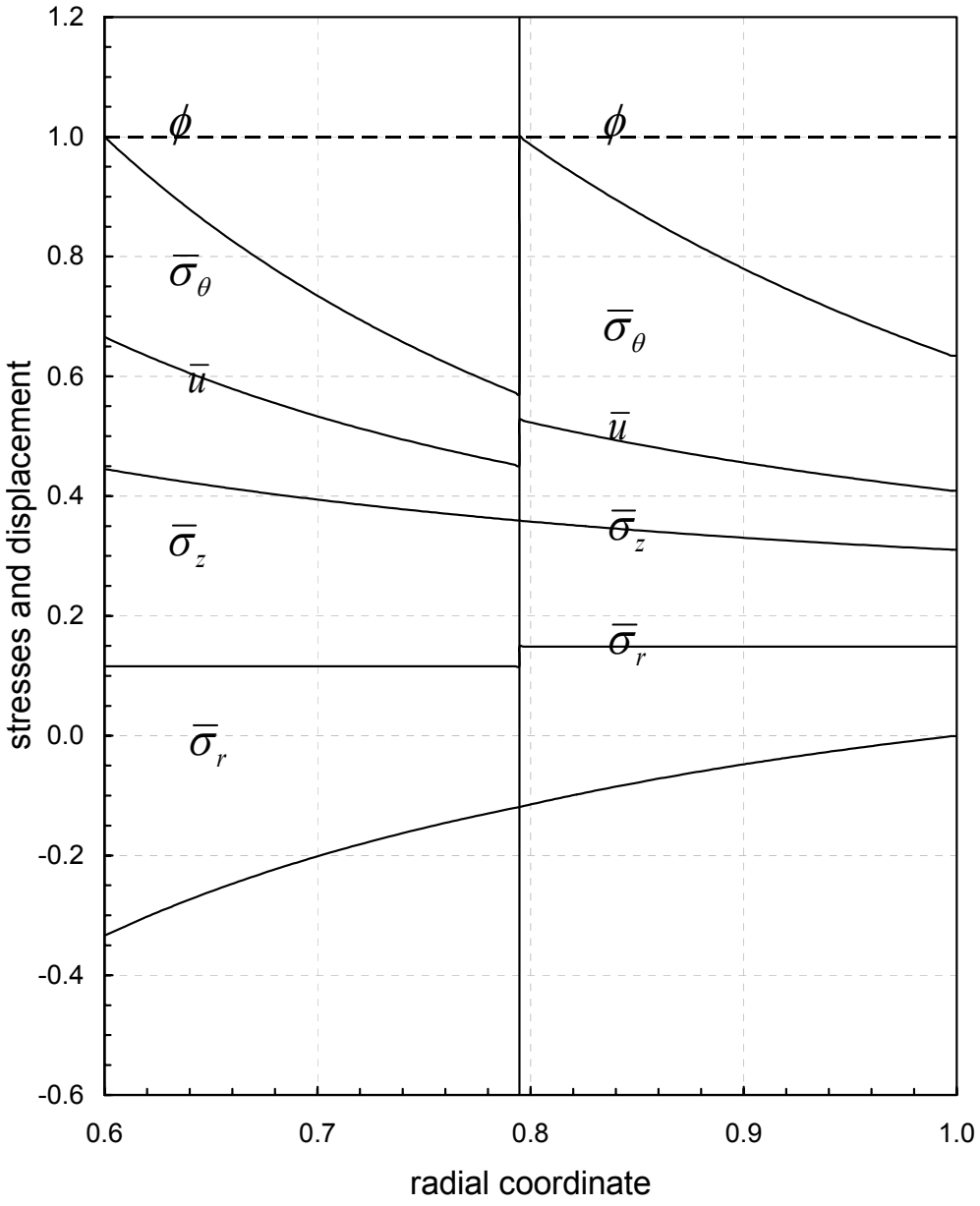

Figure 4.5 The distributions of stresses and displacement in a two layer brass-copper tube ($\bar{a}$ =0.6, $\bar{r}_1 = \bar{r}_{1cr}$ =0.794711) under elastic limit internal pressure $\bar{P}_e$ =0.334061

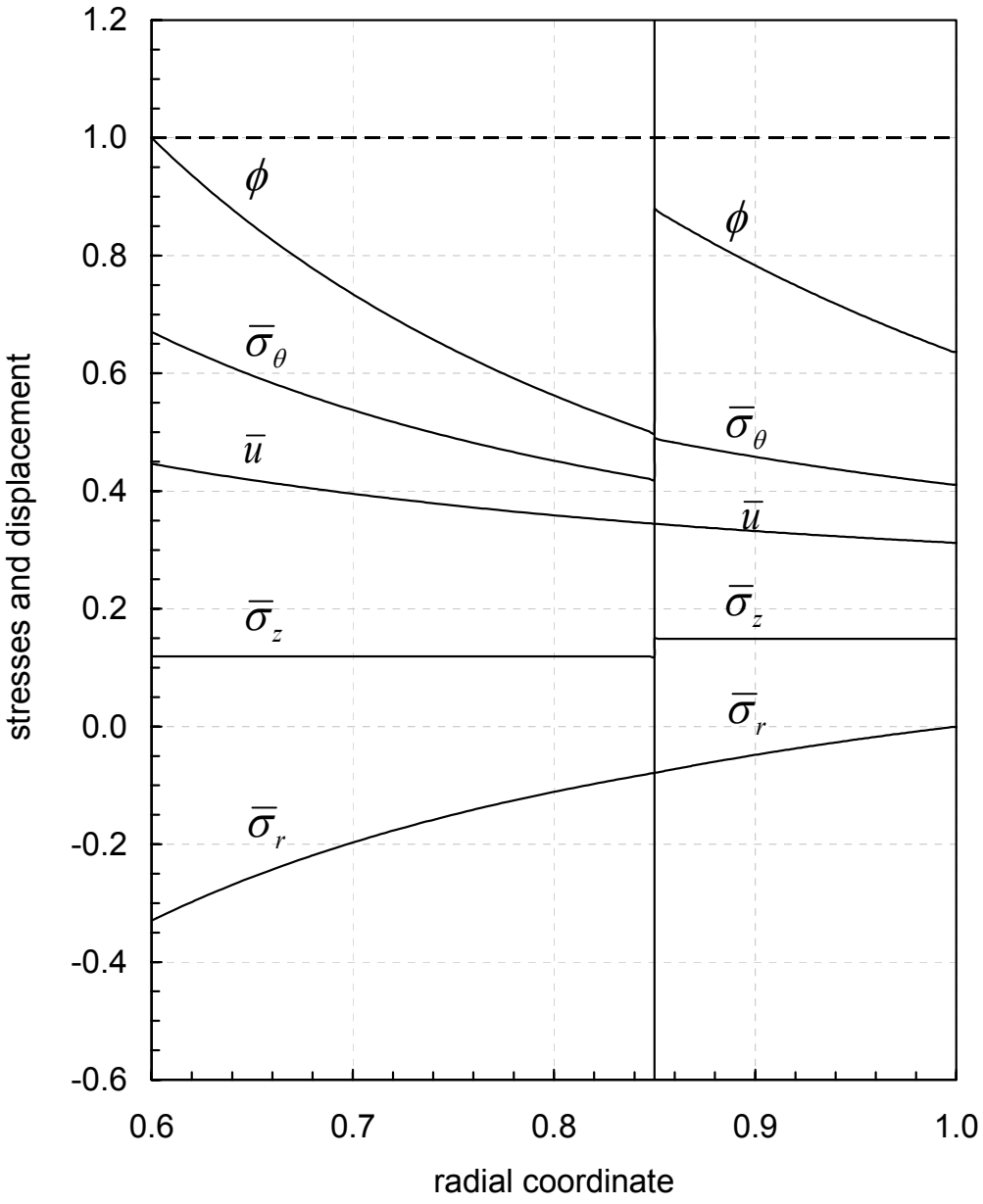

Figure 4.6 The distributions of stresses and displacement in a two layer brass-copper tube ($\bar{a}$ =0.6, $\bar{r}_1$ =0.85) under elastic limit internal pressure $\bar{P}_e$ =0.329630

Considering the same tube assembly, for $\bar{r}_1$=0.65 the yielding begins at the outer tube of the assembly according to Tresca's yield criterion as shown in Fig. 4.7. Here, the only difference from the previous case is the fact that the radius of the first layer is chosen to be smaller than the value of the critical interface radius ($r_1 < r_{1cr}$). The elastic limit internal pressure is computed as $\bar{P}_e$=0.236648 by using Eq. (114) and constants of integration are obtained as $\bar{C}_1 = 6.41648\times10^{-4}$, $\bar{C}_2 = 1.60465\times10^{-4}$, $\bar{C}_3 = 6.36319\times10^{-4}$ and $\bar{C}_4 = 1.73078\times10^{-4}$.

For the two layer tubes under internal pressure, von Mises yield criterion is also considered to monitor the yielding. Similar yielding behaviour in the tube assembly is observed when von Mises criterion is used. In order to compare these two criteria, Table 4.2 is prepared. For the three cases of yielding, the elastic limit pressures and the interface radii are shown in this table.

Table 4.2. Elastic limit pressures and interface radii for different yielding cases of the two-layer tubes under internal pressure ($\bar{a}$ =0.6)

Location(s) of yielding and yielding criterion	**Elastic limit internal pressure ($\bar{P}_e$)**	**Interface radius ($\bar{r}_1$)**
Simultaneous yielding at $r = a$ and at $r = r_1$ (Tresca's criterion)	0.334061	0.794711
Simultaneous yielding at $r = a$ and at $r = r_1$ (von Mises criterion)	0.384971	0.796058
Yielding at the inner surface $r = a$ (Tresca's criterion)	0.329630	0.85
Yielding at the inner surface $r = a$ (von Mises criterion)	0.379963	0.85
Yielding at the interface $r = r_1$ (Tresca's criterion)	0.236648	0.65
Yielding at the interface $r = r_1$ (von Mises criterion)	0.272659	0.65

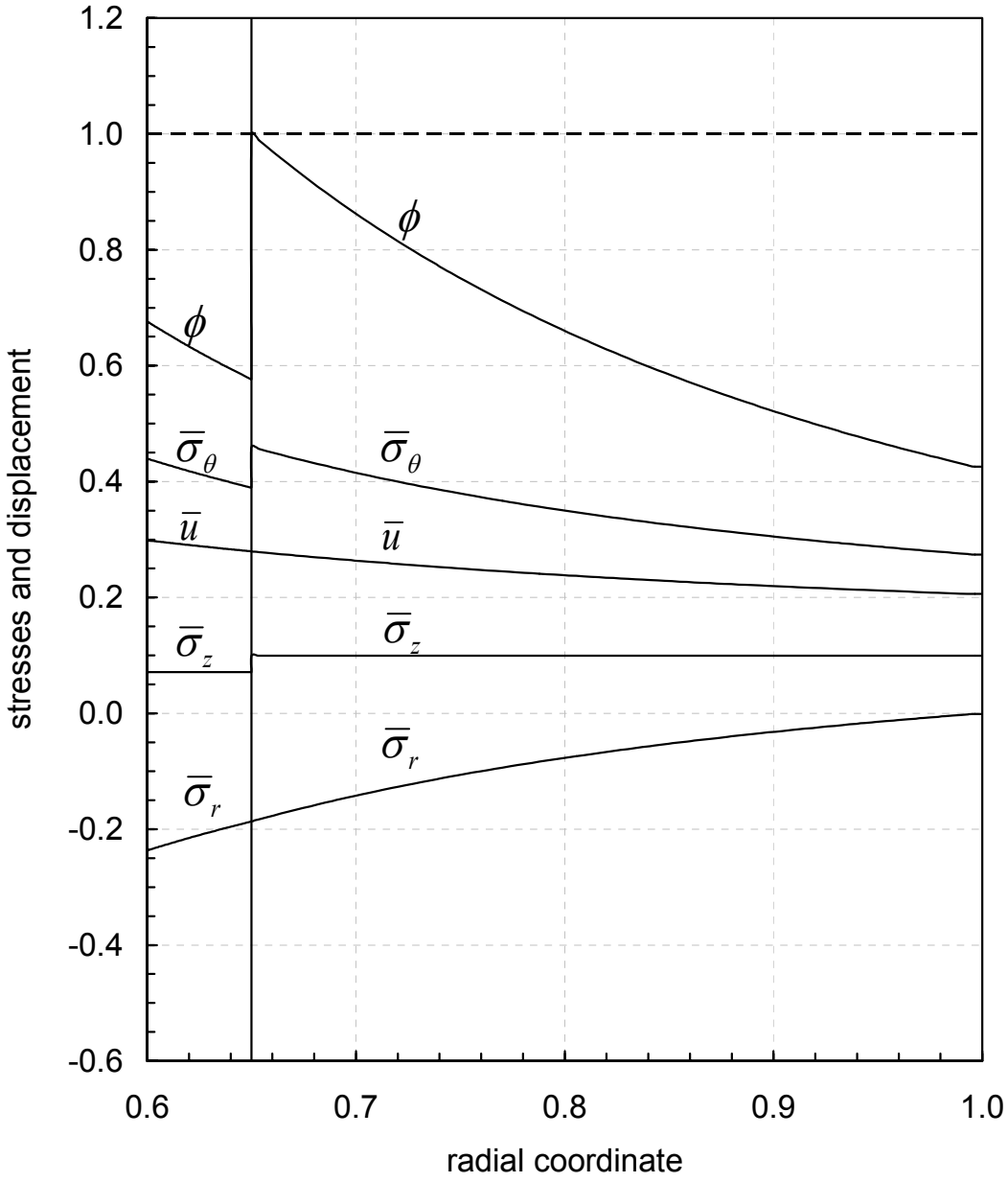

Figure 4.7 The distributions of stresses and displacement in a two layer brass-copper tube ($\bar{a}$ =0.6, $\bar{r}_1$ =0.65) under elastic limit internal pressure $\overline{P}_e$ =0.236648

The yielding behaviour of a two-layer tube under external pressure is also investigated. In Fig. 4.8, the stresses and displacement graph of a two-layer brass-copper tube under external pressure according to von Mises criterion is given. Here, $\bar{a}$ =0.5 and the elastic limit external pressure and the critical interface radius is found as $\bar{P}_e$=0.458597 and $\bar{r}_{1cr}$ =0.6898 by solving the Eqs. (123) and (124) together. The corresponding integration constants are calculated as $\bar{C}_1$ =-7.49702×10^{-4} , $\bar{C}_2$ =-8.99643×10^{-4} , $\bar{C}_3$ =-7.97900×10^{-4} and $\bar{C}_4$ = -7.98351×10^{-4} using Eqs.(43), (44), (45) and (46). As seen in this figure, yielding begins at $r=a$ and at $r=r_{1cr}$ simultaneously, as $\phi=1$ at these locations.

On the other hand, for the same tube assembly, taking $\bar{r}_1$=0.85, the yielding begins at the inner surface ($r=a$). The corresponding elastic limit external pressure is found as $\bar{P}_e$=0.440648 by using Eq. (125). The integration constants are obtained as $\bar{C}_1$ =-7.49702×10^{-4} , $\bar{C}_2$ =-8.99642×10^{-4} , $\bar{C}_3$ =-8.32520×10^{-4} and $\bar{C}_4$ =-7.85015×10^{-4}. The consequent stresses and deformation are given in Fig.4.9.

Finally, by choosing a radius lower than the critical interface radius of the two-layer brass-copper tube under external pressure ($\bar{r}_1$ = 0.65 < $\bar{r}_{1cr}$), the yielding begins at the interface (r = $\bar{r}_1$) as shown in Fig. 4.10. The elastic limit external pressure is obtained as $\bar{P}_e$=0.418738 by using Eq.(126). The corresponding integration constants are calculated as $\bar{C}_1$ =6.76437×10^{-4}, $\bar{C}_2$ =-8.11725×10^{-4}, $\bar{C}_3$ =-7.13172×10^{-4} and $\bar{C}_4$ =-7.24779×10^{-4}.

For the two layer tubes under external pressure, when Tresca's yield criterion is used, same yielding behavior but with different values of elastic limit pressures and critical interface radii is evaluated. In order to compare these two criteria, Table 4.3 is prepared. For the three cases of yielding, the elastic limit pressures and the interface radii are seen in this table. In the next part, the yielding of three layer-tubes under pressure will be presented.

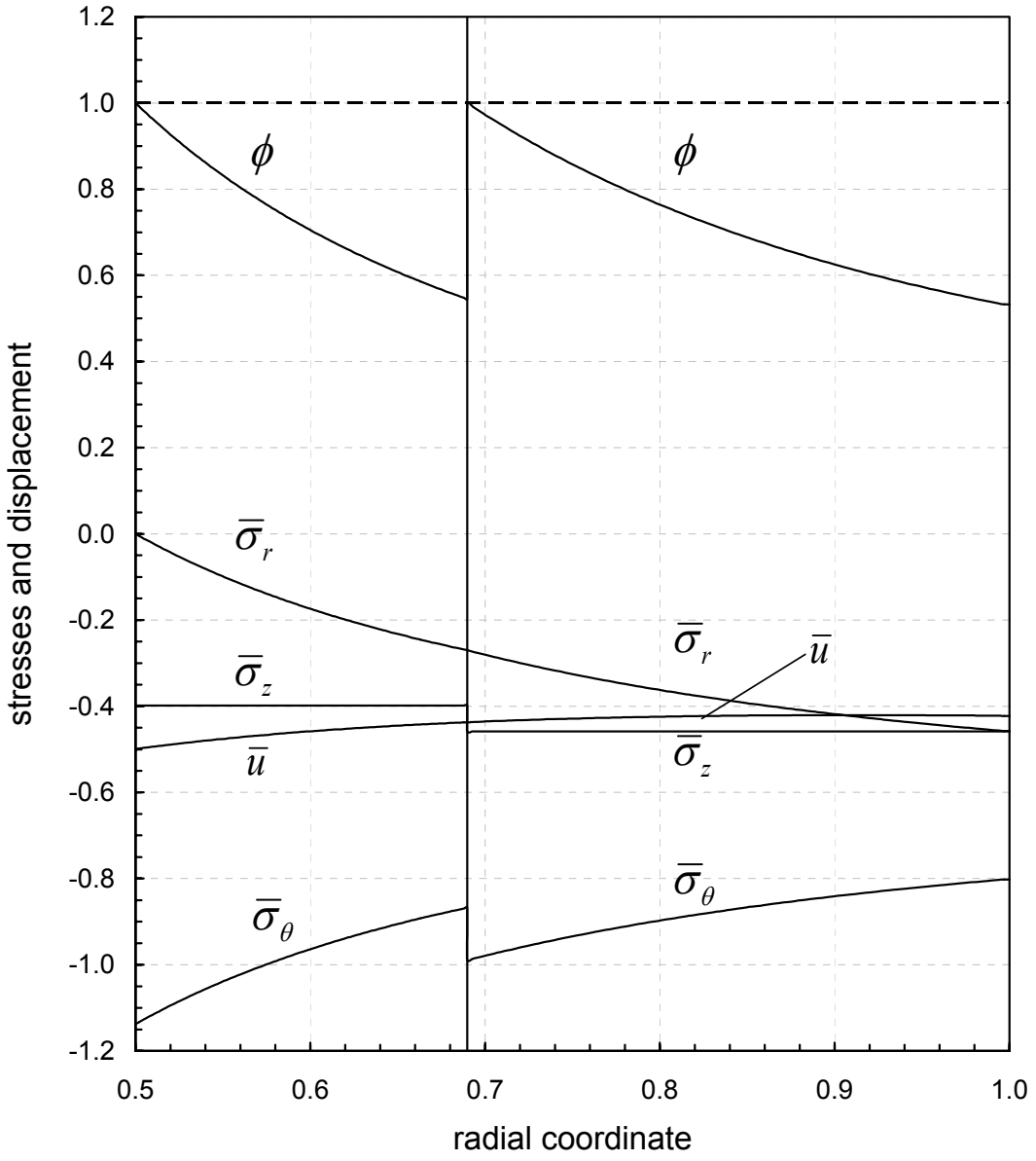

Figure 4.8 The distributions of stresses and displacement in a two-layer brass-copper tube ($\bar{a}$ =0.5, $\bar{r}_1 = \bar{r}_{1cr}$ =0.6898) under elastic limit external pressure $\bar{P}_e$ =0.458597

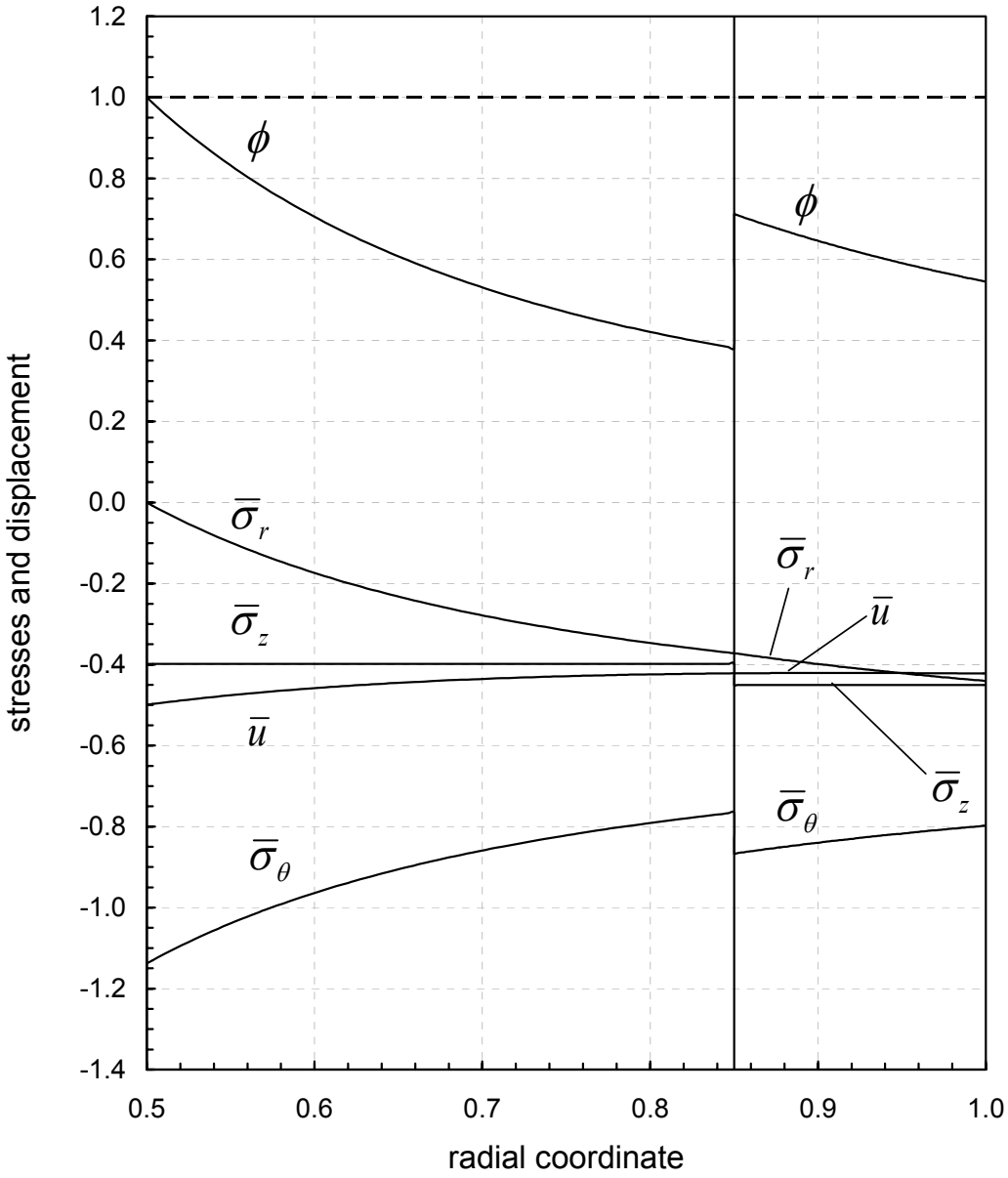

Figure 4.9 The distributions of stresses and displacement in a two-layer brass-copper tube ($\bar{a}$ =0.5, $\bar{r}_1$ =0.85) under elastic limit external pressure $\bar{P}_e$ =0.440648

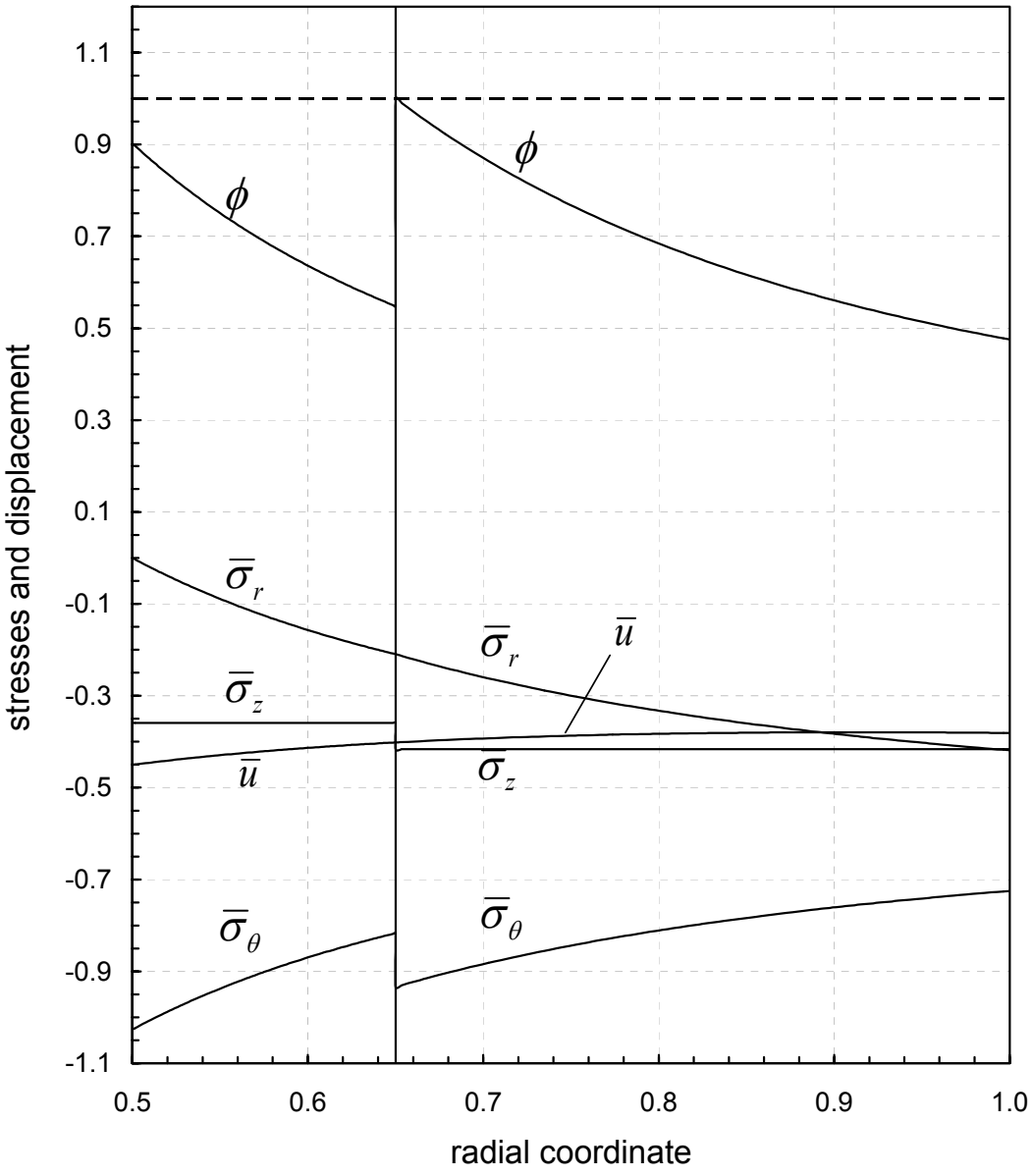

Figure 4.10 The distributions of stresses and displacement in a tw- layer brass-copper tube ($\bar{a}$ =0.5, $\bar{r}_1$ =0.65) under elastic limit internal pressure $\bar{P}_e$ =0.418738

Table 4.3 Elastic limit pressures and interface radii for different yielding cases of the two-layer tubes under external pressure ($\bar{a}$ =0.5)

Location(s) of yielding and yielding criterion	**Elastic limit external pressure ($\overline{P}_e$)**	**Interface radius ($\bar{r}_1$)**
Simultaneous yielding at $r = a$ and at $r = r_1$ (Tresca's criterion)	0.40401	0.681711
Simultaneous yielding at $r = a$ and at $r = r_1$ (von Mises criterion)	0.458597	0.689800
Yielding at the inner surface $r = a$ (Tresca's criterion)	0.387295	0.85
Yielding at the inner surface $r = a$ (von Mises criterion)	0.440648	0.85
Yielding at the interface $r = r_1$ (Tresca's criterion)	0.373615	0.65
Yielding at the interface $r = r_1$ (von Mises criterion)	0.418738	0.65

4.4 Three-Layer Tube Results

In order to check the derivations of the stress and displacement expressions of the three-layer tubes, a verification study is also performed as it was done for the two-layer tubes. Firstly, a single layer tube is taken, subsequently a second tube which is made of the same material and having the same dimension is considered. What makes the second tube different is the fact that it is composed of three layers, which have the same material properties as the single tube. The results show that the two assemblies are identically the same for both pressure cases.

In Fig. 4.11, the simultaneous yielding behavior of a three-layer tube under internal pressure according to the Tresca's criterion is shown. The first layer of the tube is made of brass, second layer is copper and the outer layer is aluminum. Since there are three different layers in the tube, two different critical interface radii should be

considered. For $\bar{a}$ =0.3, the elastic limit internal pressure and corresponding interface radii are calculated as $\bar{P}_e$=0.429459, $\bar{r}_{1cr}$=0.394202 and $\bar{r}_{2cr}$=0.507988 by the numerical solution of Eqs. (128), (129) and (130) together. The corresponding integration constants are computed as $\bar{C}_1 = C_1/b^2$=2.37214×10^{-4}, $\bar{C}_2 = C_2$= 1.11555×10^{-4}, $\bar{C}_3 = C_3/b^2$=2.34038×10^{-4}, $\bar{C}_4 = C_4$=1.31993×10^{-4}, $\bar{C}_5 = C_5/b^2$= 2.48835×10^{-4} and $\bar{C}_6 = C_6/b^2$=7.46506×10^{-4} by the help of Eqs. (68) to (73). It can be seen in this graph that $\phi = 1$ at $r = a$, $r = r_1$ and $r = r_2$ which shows the simultaneous yielding.

For the same material combination, the yielding begins at the inner surface ($r = a$) first when the interface radii are selected as $r_1 > r_{1cr}$ and $r_2 > r_{2cr}$. For $\bar{a}$ =0.3, $\bar{r}_1$=0.45 and $\bar{r}_2$=0.55, the elastic limit pressure is found as $\bar{P}_e$=0.432391 by using Esq. (131). The integration constants are calculated as $\bar{C}_1 = 2.37214\times10^{-4}$ $\bar{C}_2 = 1.06918\times10^{-4}$, $\bar{C}_3 = 2.34711\times10^{-4}$, $\bar{C}_4 = 1.19277\times10^{-4}$, $\bar{C}_5 = 2.48262\times10^{-4}$ and $\bar{C}_6 = 7.44788\times10^{-4}$. The consequent stresses and displacement are given in Fig. 4.12.

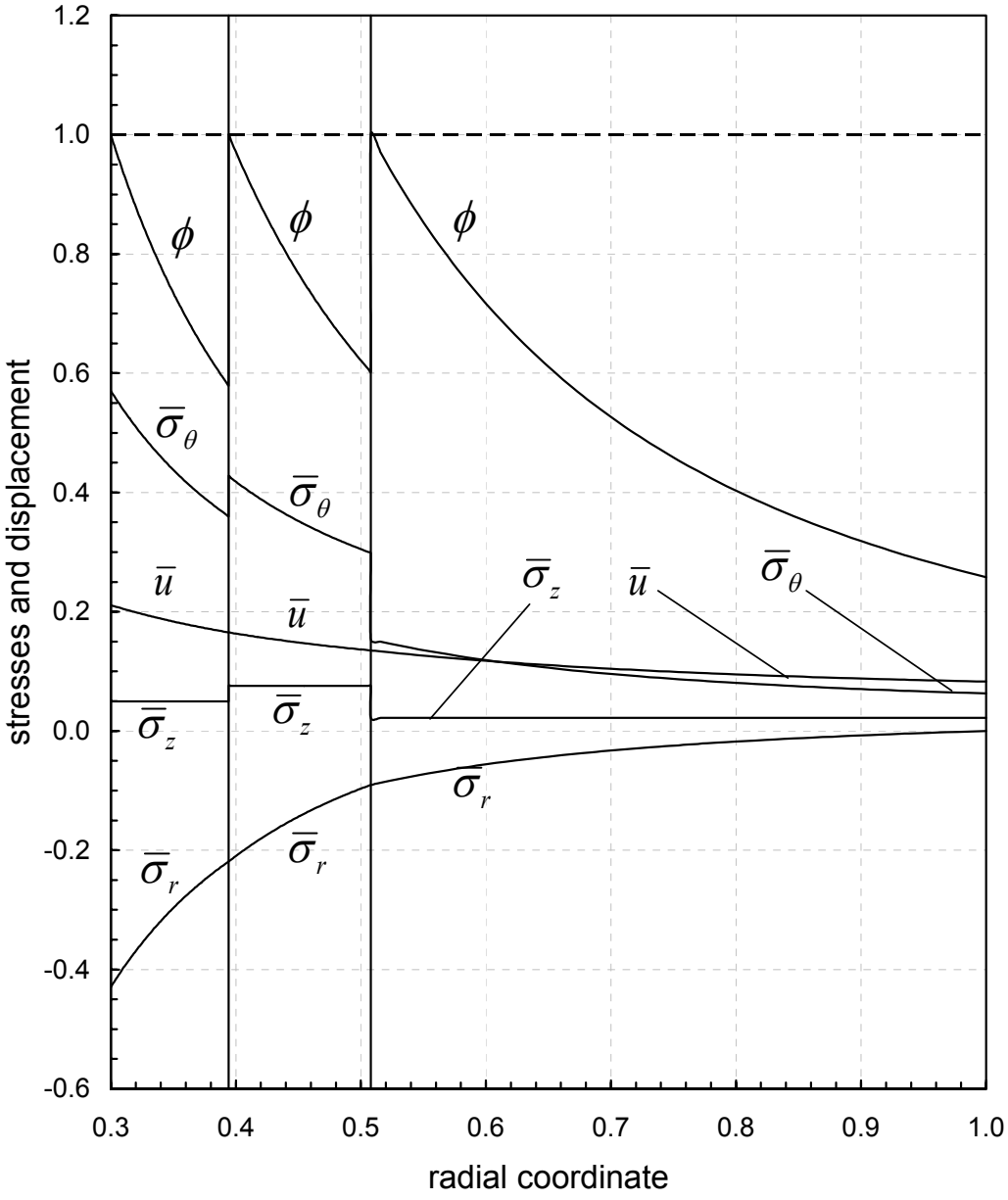

Figure 4.11 The distributions of stresses and displacement in a three-layer brass-copper-aluminum tube under elastic limit internal pressure $\bar{P}_e$=0.429459 ($\bar{a}$ =0.3, $\bar{r}_{1cr}$ =0.394202, $\bar{r}_{2cr}$ =0.507988)

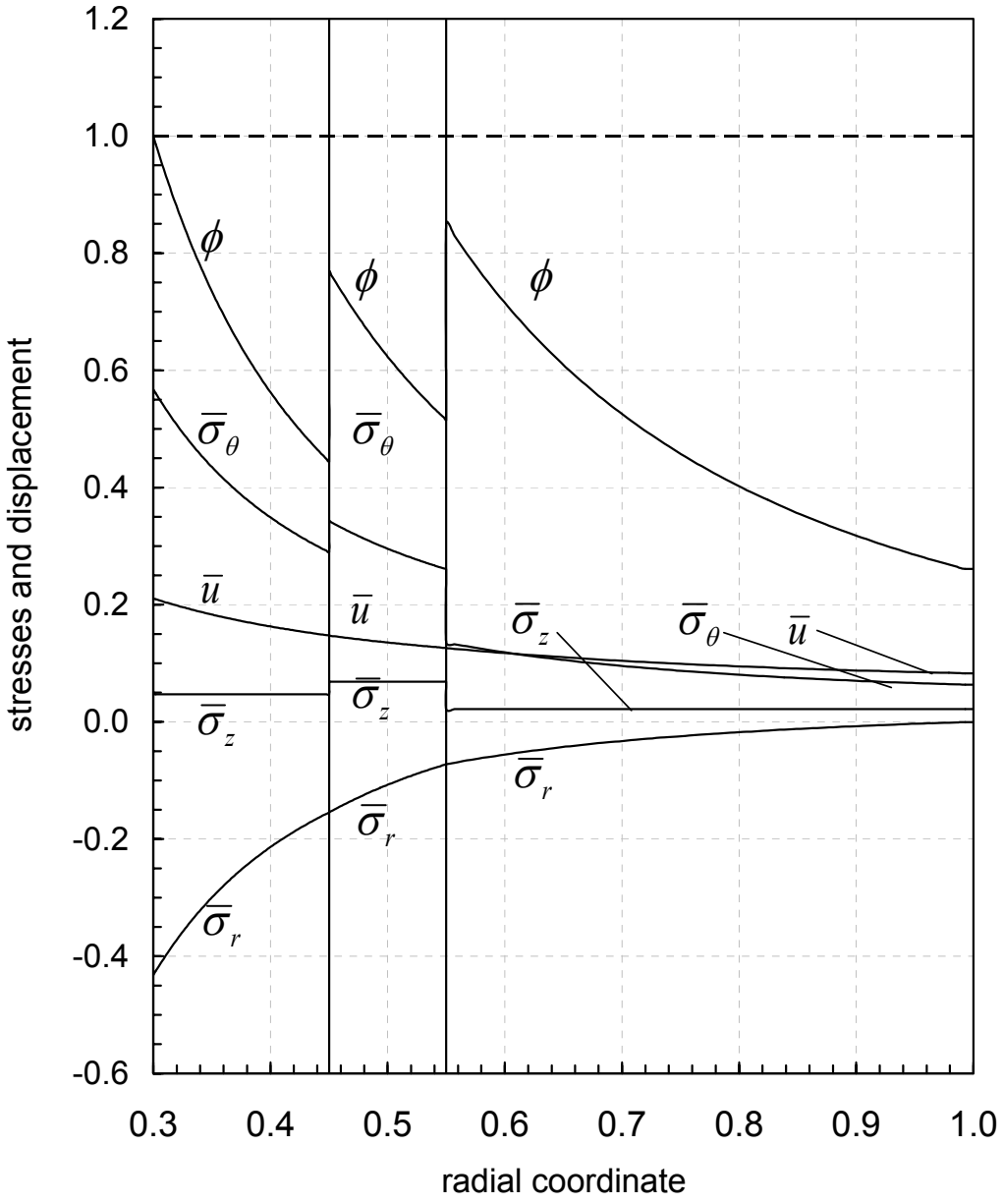

Figure 4.12 The distributions of stresses and displacement in a three layer brass-copper-aluminum tube under elastic limit internal pressure $\bar{P}_e$=0.432391 ($\bar{a}$ =0.3, $\bar{r}_1$=0.45, $\bar{r}_2$=0.55)

For a three-layer tube with the same material combination, yielding may begin at the inner interface ($r = r_1$) first. In order to have such yielding behaviour, the following criteria should be satisfied: $r_1 < r_{1cr}$ and $r_2 = r_{2cr}$. For $\bar{a}$=0.3, $\bar{r}_1$ = 0.35 and $\bar{r}_2$ = $\bar{r}_{2cr}$=0.507988, the corresponding elastic limit internal pressure is obtained as $\overline{P}_e$= 0.346022 by using Eq. (132). The integration constants are calculated as $\overline{C}_1 = 1.87650\times10^{-4}$, $\overline{C}_2 = 7.82928\times10^{-4}$, $\overline{C}_3 = 1.84495\times10^{-4}$, $\overline{C}_4 = 1.04051\times10^{-4}$, $\overline{C}_5 = 1.96160\times10^{-4}$ and $\overline{C}_6 = 5.88480\times10^{-4}$. Fig. 4.13 shows the corresponding stresses and displacement.

Similar to the case presented above, by changing the thickness of the layers, it is possible to have the yielding starting from the outer interface ($r = r_2$) first. For this purpose, $r_1 = r_{1cr}$ and $r_2 < r_{2cr}$ are the two criteria to be considered. For $\bar{a}$=0.3, $\bar{r}_1$ = $\bar{r}_{1cr}$=0.394202 and $\bar{r}_2$ = 0.45, the elastic limit pressure is obtained by using Eq. (133) as $\overline{P}_e$= 0.319417. The corresponding constants of integration are computed as follows: $\overline{C}_1 = 1.84381\times10^{-4}$, $\overline{C}_2 = 1.09470\times10^{-4}$, $\overline{C}_3 = 1.82464\times10^{-4}$, $\overline{C}_4$ = 1.21805 $\times10^{-4}$, $\overline{C}_5 = 1.95267\times10^{-4}$ and $\overline{C}_6 = 5.85803\times10^{-4}$. The stresses and displacement for this case is given in Fig.4.14.

Figure 4.15 is given in order to represent the behaviour of yielding at two different layers at the same time. For the same material combination, the interface radius, at which the yielding has not been started yet, should be selected to be higher than the critical interface radius belonging to the three-layer-simultaneous-yielding case. In the figure, yielding begins at the inner surface ($r = a$) and at the inner interface ($r = r_1$) at the same time. For the outer interface, the condition $r_2 > r_{2cr}$ is valid and, it is selected as $\bar{r}_2$=0.55. By solving Eqs. (128) and (129) together, the critical inner interface is calculated as $\bar{r}_{1cr}$ = 0.393877 and the corresponding elastic limit internal pressure is computed as $\overline{P}_e$= 0.439437. The integration constants are calculated as $\overline{C}_1 = 2.37214\times10^{-4}$, $\overline{C}_2 = 9.57768\times10^{-4}$, $\overline{C}_3 = 2.33652\times10^{-4}$, $\overline{C}_4 = 1.18748\times10^{-4}$, $\overline{C}_5 = 2.47142\times10^{-4}$ and $\overline{C}_6 = 7.41427\times10^{-4}$.

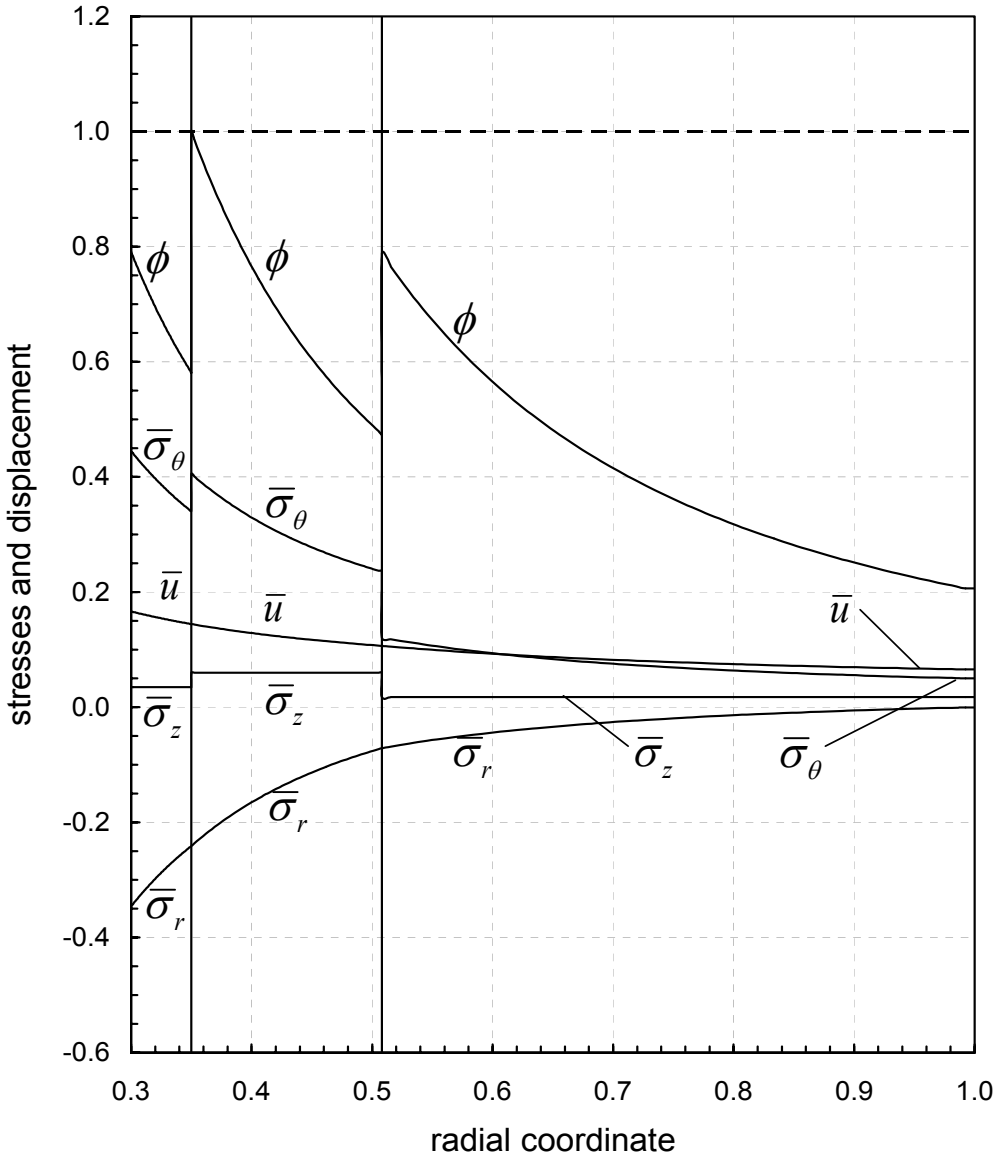

Figure 4.13 The distributions of stresses and displacement in a three-layer brass-copper-aluminum tube ($\bar{a}$ =0.3, $\bar{r}_1$=0.35, $\bar{r}_2=\bar{r}_{2cr}$ =0.507988) under elastic limit internal pressure $\bar{P}_e$=0.346022

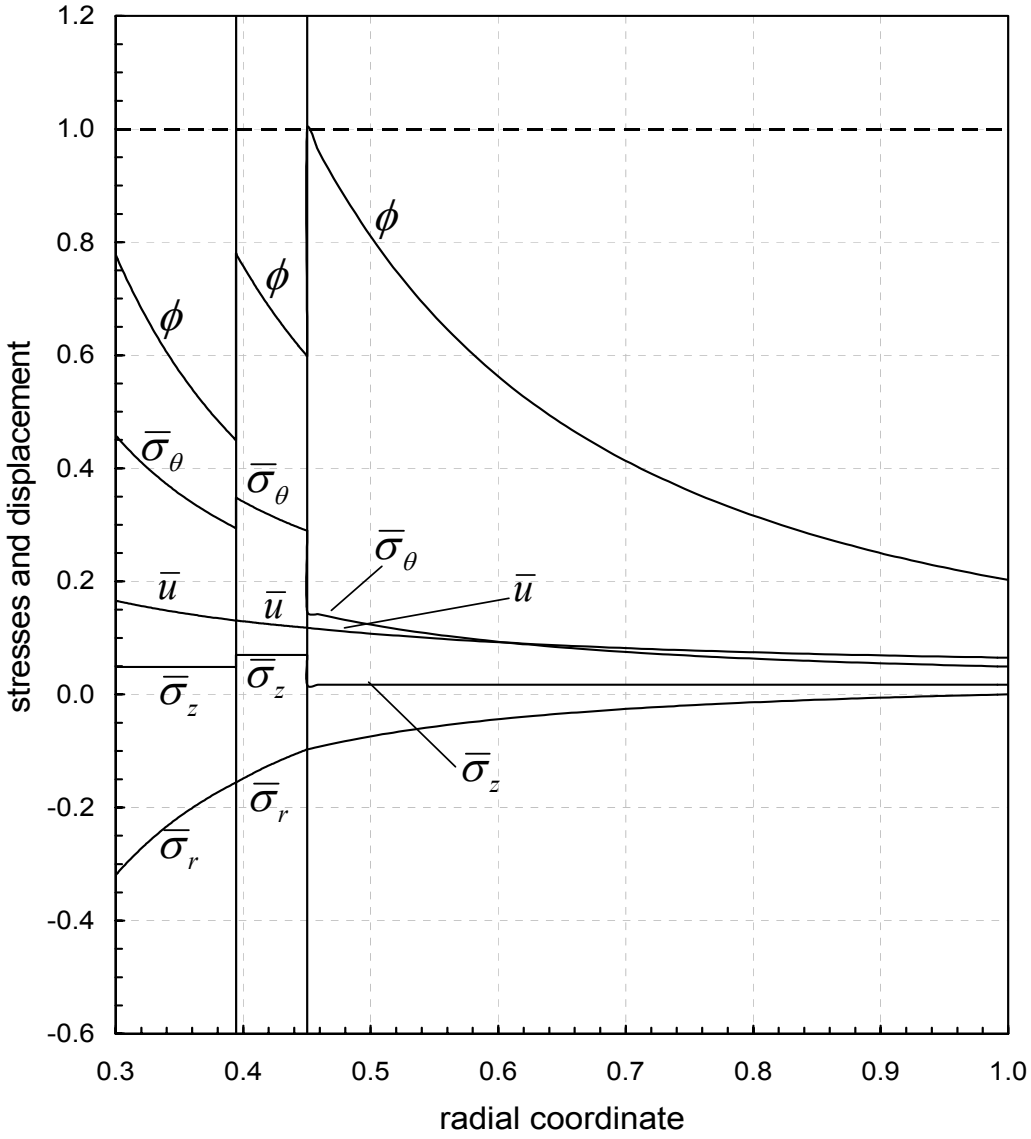

Figure 4.14 The distributions of stresses and displacement in a three layer brass-copper-aluminum tube ($\bar{a}$ =0.3, $\bar{r}_1$ = 0.394202, $\bar{r}_2$ = 0.45) under elastic limit internal pressure at $\bar{P}_e$=0.319417

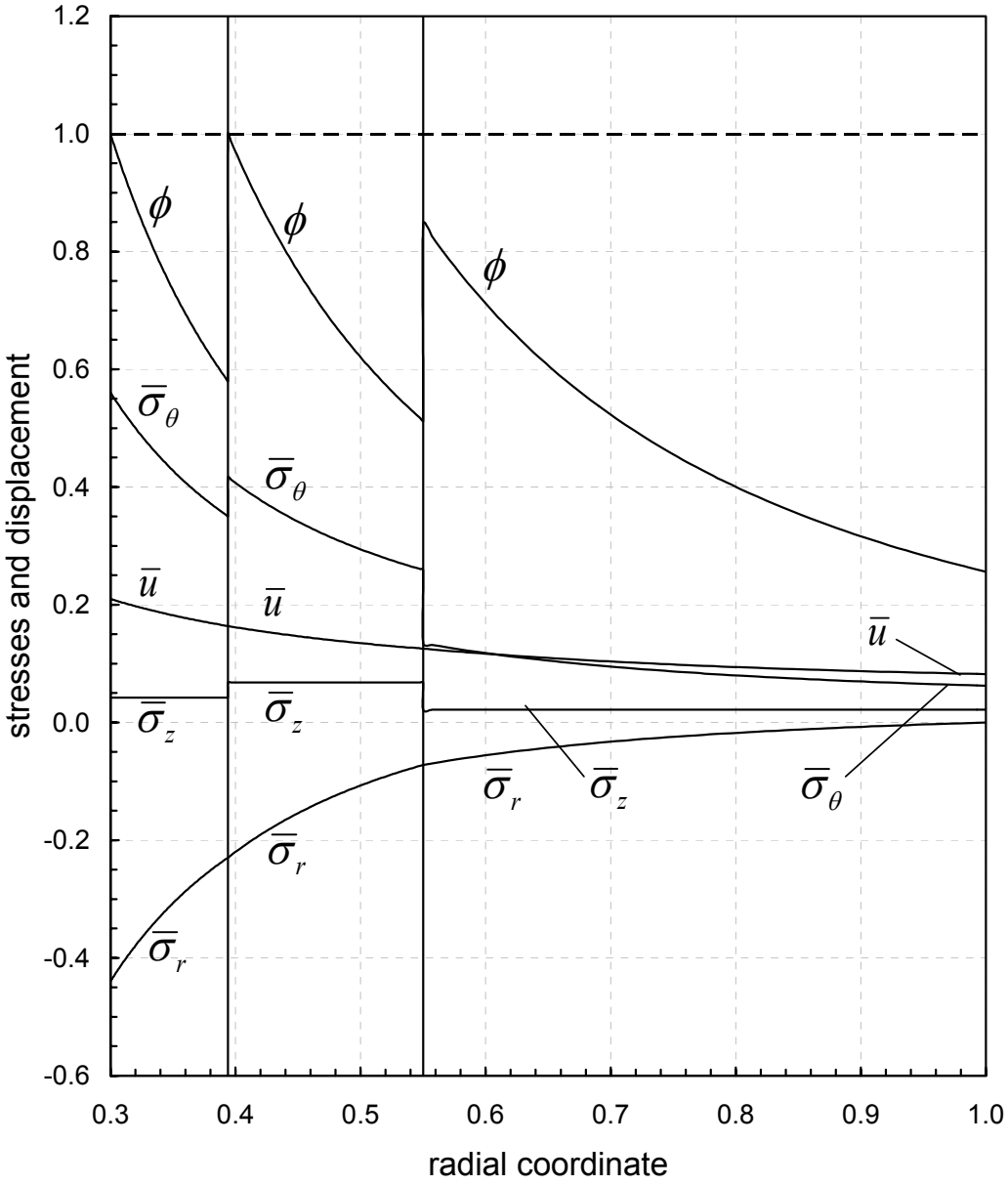

Figure 4.15 The distributions of stresses and displacement in a three-layer brass-copper-aluminum tube under elastic limit internal pressure $\bar{P}_e$=0.439437 ($\bar{a}$=0.3, $\bar{r}_{1cr}$ = 0.393877, $\bar{r}_2$=0.55)

The case where the inner and the outer layers start yielding simultaneously according to Tresca's yield criterion is shown in Fig. 4.16. For $\bar{a}$ =0.3 and $\bar{r}_1$ = 0.45, the elastic limit internal pressure and the critical outer interface radius is obtained by solving Eqs. (128) and (130) together as $\bar{P}_e$ =0.422694 and $\bar{r}_{2cr}$ =0.509206. The corresponding integration constants are calculated as $\bar{C}_1 = 2.37214\times10^{-4}$, $\bar{C}_2 = 1.22254\times10^{-4}$, $\bar{C}_3 = 2.35196\times10^{-4}$, $\bar{C}_4 = 1.32220\times10^{-4}$, $\bar{C}_5 = 2.50030\times10^{-4}$ and $\bar{C}_6 = 7.50091\times10^{-4}$.

Finally, in Fig. 4.17, the case in which the middle and the outer layers starts yielding at the same time according to Tresca's yield criterion is shown. For $\bar{a}$ =0.3 and assigning the elastic limit internal pressure $\bar{P}_e$ = 0.3, the critical inner and the outer interface radii are obtained by solving Eqs. (129) and (130) together as $\bar{r}_{1cr}$ = 0.334590 and $\bar{r}_{2cr}$ =0.432958, respectively. The corresponding integration constants are calculated as $\bar{C}_1 = 1.71171\times10^{-4}$, $\bar{C}_2 = 9.61421\times10^{-4}$, $\bar{C}_3 = 1.68607\times10^{-4}$, $\bar{C}_4 = 1.19045\times10^{-4}$, $\bar{C}_5 = 1.80757\times10^{-4}$ and $\bar{C}_6 = 5.42272\times10^{-4}$.

In order to make a comparison between Tresca's and von Mises yield criterion for the considered assemblies, Table 4.4 is prepared.

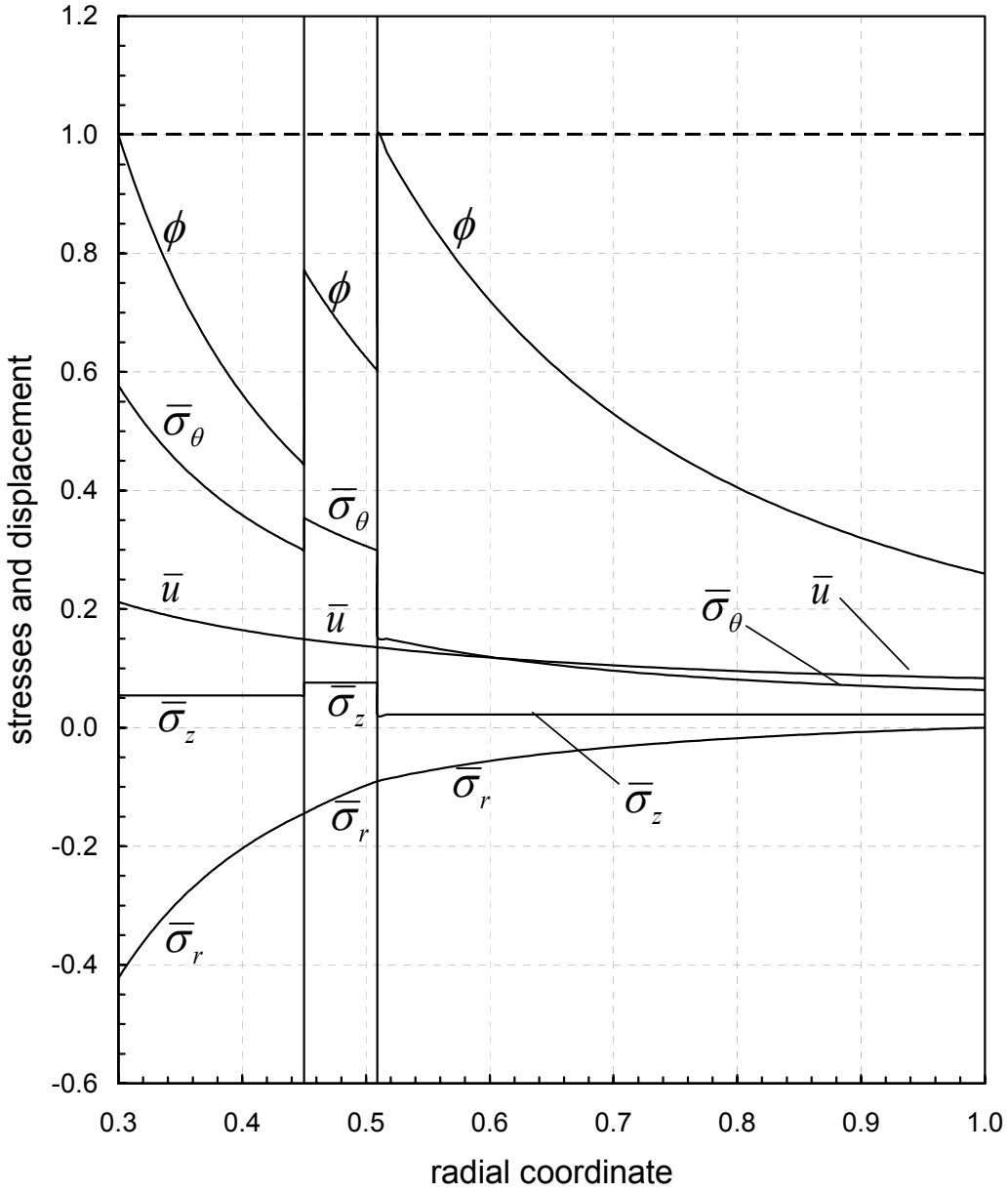

Figure 4.16 The distributions of stresses and displacement in a three-layer brass-copper-aluminum tube under elastic limit internal pressure $\bar{P}_e$=0.422694 ($\bar{a}$=0.3, $\bar{r}_1$ = 0.45, $\bar{r}_2 = \bar{r}_{2cr}$=0.509206)

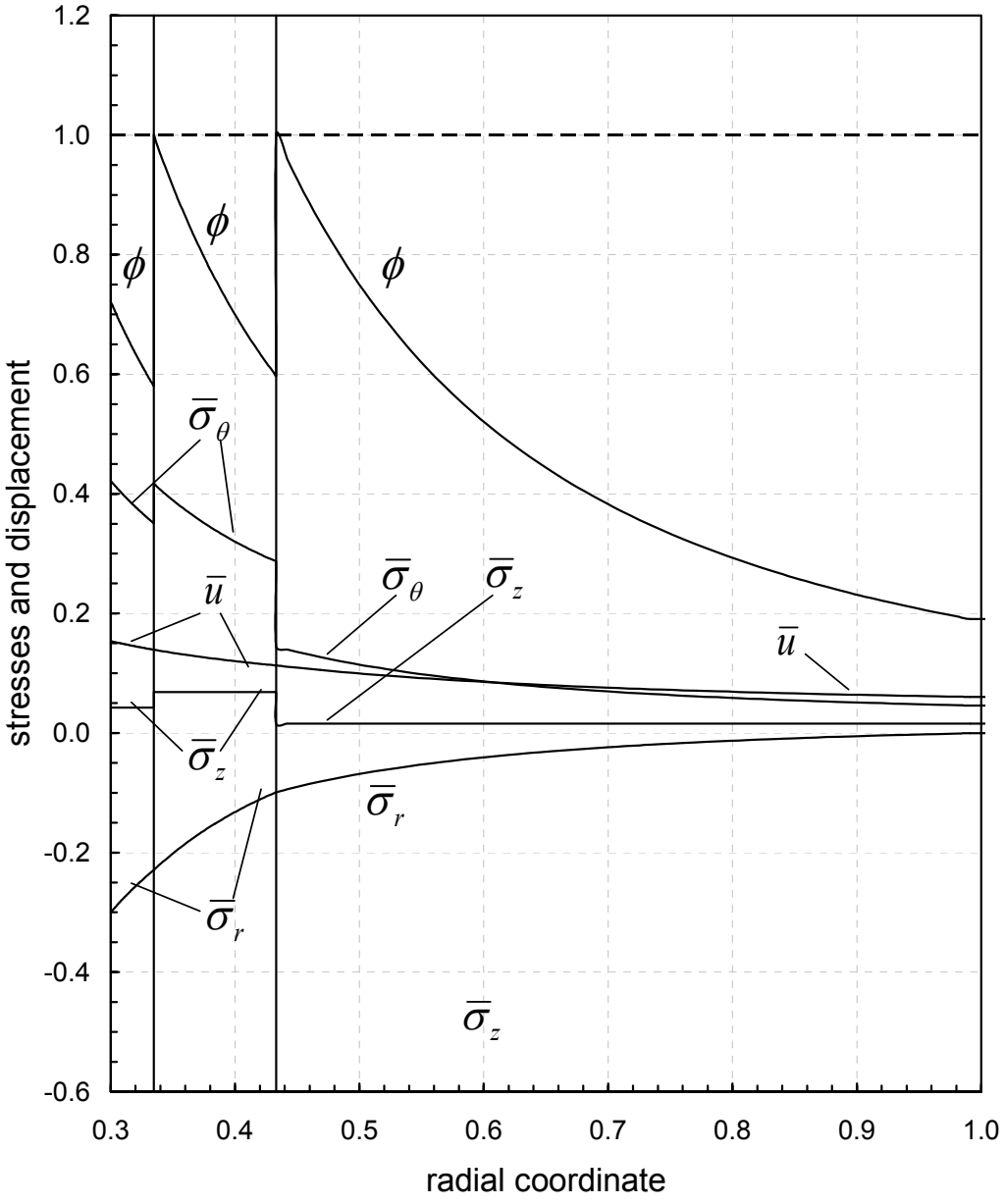

Figure 4.17 The distributions of stresses and displacement in a three-layer brass-copper-aluminum tube under elastic limit internal pressure $\bar{P}_e$=0.3

($\bar{a}$ =0.3, $\bar{r}_1 = \bar{r}_{1cr}$ = 0.334590, $\bar{r}_2 = \bar{r}_{2cr}$ =0.432958)

Table 4.4 Elastic limit pressures and interface radii for different yielding cases of the three-layer tubes under internal pressure ($\bar{a}$ =0.3)

Location(s) of yielding and yielding criterion	**Elastic limit external pressure ($\bar{P}_e$)**	**Interface radii ($\bar{r}_1$ and $\bar{r}_2$)**
Simultaneous yielding at $r = a$, $r = r_1$ and $r = r_2$ (Tresca's criterion)	0.429459	0.394202, 0.507988
Simultaneous yielding at $r = a$, $r = r_1$ and $r = r_2$ (von Mises criterion)	0.495768	0.394397, 0.508163
Yielding at the inner surface $r = a$ (Tresca's criterion)	0.432391	0.45 , 0.55
Yielding at the inner surface $r = a$ (von Mises criterion)	0.499146	0.45, 0.55
Yielding at the inner interface $r = r_1$ (Tresca's criterion)	0.346022	0.35, 0.507988
Yielding at the inner interface $r = r_1$ (von Mises criterion)	0.399279	0.35, 0.508163
Yielding at the outer interface $r = r_2$ (Tresca's criterion)	0.319417	0.394202, 0.45
Yielding at the outer interface $r = r_2$ (Tresca's criterion)	0.368570	0.394397, 0.45
Simultaneous yielding at $r = a$ and $r = r_1$ (Tresca's criterion)	0.439437	0.393877, 0.55
Simultaneous yielding at $r = a$ and $r = r_1$ (von Mises criterion)	0.507278	0.394040, 0.55
Simultaneous yielding at $r = a$ and $r = r_2$ (Tresca's criterion)	0.422694	0.45, 0.509206
Simultaneous yielding at $r = a$ and $r = r_2$ (von Mises criterion)	0.487959	0.45, 0.509365
Simultaneous yielding at $r = r_1$ and $r = r_2$ (Tresca's criterion)	0.3	0.334590, 0.432958
Simultaneous yielding at $r = r_1$ and $r = r_2$ (von Mises criterion)	0.3	0.357289, 0.461533

Coming to the external pressure case, using the same material combination (the inner layer is brass, the middle layer is copper and the outer layer is aluminum), a simultaneous yielding behaviour (at the three locations at the same time) is observed according to von Mises yield criterion. As shown in Fig. 4.18, the assembly may

yield at the three locations simultaneously when $\bar{a}$=0.3, $\bar{r}_{1cr}$=0.413880, $\bar{r}_{2cr}$=0.481949 at the elastic limit external pressure $\bar{P}_e$=0.451869. These values are calculated using Eqs. (148), (149) and (150). The corresponding integration constants are obtained as $\bar{C}_1$ = -2.69892×10^{-4}, $\bar{C}_2$ = -8.99642×10^{-4}, $\bar{C}_3$ = -2.87243×10^{-4}, $\bar{C}_4$ = -7.98350×10^{-4}, $\bar{C}_5$ = -2.09132×10^{-4} and $\bar{C}_6$ = -1.13463×10^{-4}. using Eqs. (95) to (100).

Similar to the internal pressure case, the assembly may also yield at the inner layer ($r = a$) first. This kind of behaviour is shown in Fig. 4.19. For $\bar{a}$=0.3, $\bar{r}_1$=0.45 and $\bar{r}_2$=0.55, by using Eq. (154), the elastic limit external pressure is found as $\bar{P}_e$=0.470063 and the corresponding integration constants are calculated as $\bar{C}_1$ = -2.69892×10^{-4}, $\bar{C}_2$ = -8.99642×10^{-4}, $\bar{C}_3$ = -2.91623×10^{-4}, $\bar{C}_4$ = -7.92332×10^{-4}, $\bar{C}_5$ = -1.77858×10^{-4} and $\bar{C}_6$ = -1.16841×10^{-4}. It should be noted that $\bar{r}_1$ = 0.45> $\bar{r}_{1cr}$ and $\bar{r}_2$ =0.55 > $\bar{r}_{2cr}$.

The yielding may also begin at the inner interface ($r = r_1$) first and this situation is shown in Fig. 4.20. For $\bar{a}$=0.3, $\bar{r}_1$=0.35 and $\bar{r}_2$ = $\bar{r}_{2cr}$ =0.481949, the elastic limit external pressure is obtained by the help of Eq. (155) is $\bar{P}_e$=0.346921, and the integration constants are calculated as $\bar{C}_1$ = -2.0086×10^{-4}, $\bar{C}_2$ = -6.6956×10^{-4}, $\bar{C}_3$ = -2.0868×10^{-4}, $\bar{C}_4$ = -6.0575×10^{-4}, $\bar{C}_5$ = -1.4792×10^{-4} and $\bar{C}_6$ = -8.6732×10^{-4}. It should be noted that $\bar{r}_1$ =0.35 < $\bar{r}_{1cr}$.

By changing the thickness of the layers, it is possible to have the yielding beginning from the outer interface ($r = r_2$) first. For this purpose, $r_1 = r_{1cr}$ and $r_2 < r_{2cr}$ are the two criteria to be considered. For $\bar{a}$=0.3, $\bar{r}_1$ = $\bar{r}_{1cr}$ = 0.413880 and $\bar{r}_2$ = 0.44, the elastic limit external pressure is obtained by using Eq. (157) as $\bar{P}_e$ = 0.358066 considering von Mises yield criterion. The constants of integration are computed as follows: $\bar{C}_1$ = -2.23439×10^{-4}, $\bar{C}_2$ = -7.44798×10^{-4}, $\bar{C}_3$ = -2.37804×10^{-4}, $\bar{C}_4$ =

-6.60940×10^{-4}, $\overline{C}_5 = -1.90270\times10^{-4}$ and $\overline{C}_6 = -9.06465\times10^{-4}$. The stresses and displacement for this case is given in Fig. 4.21.

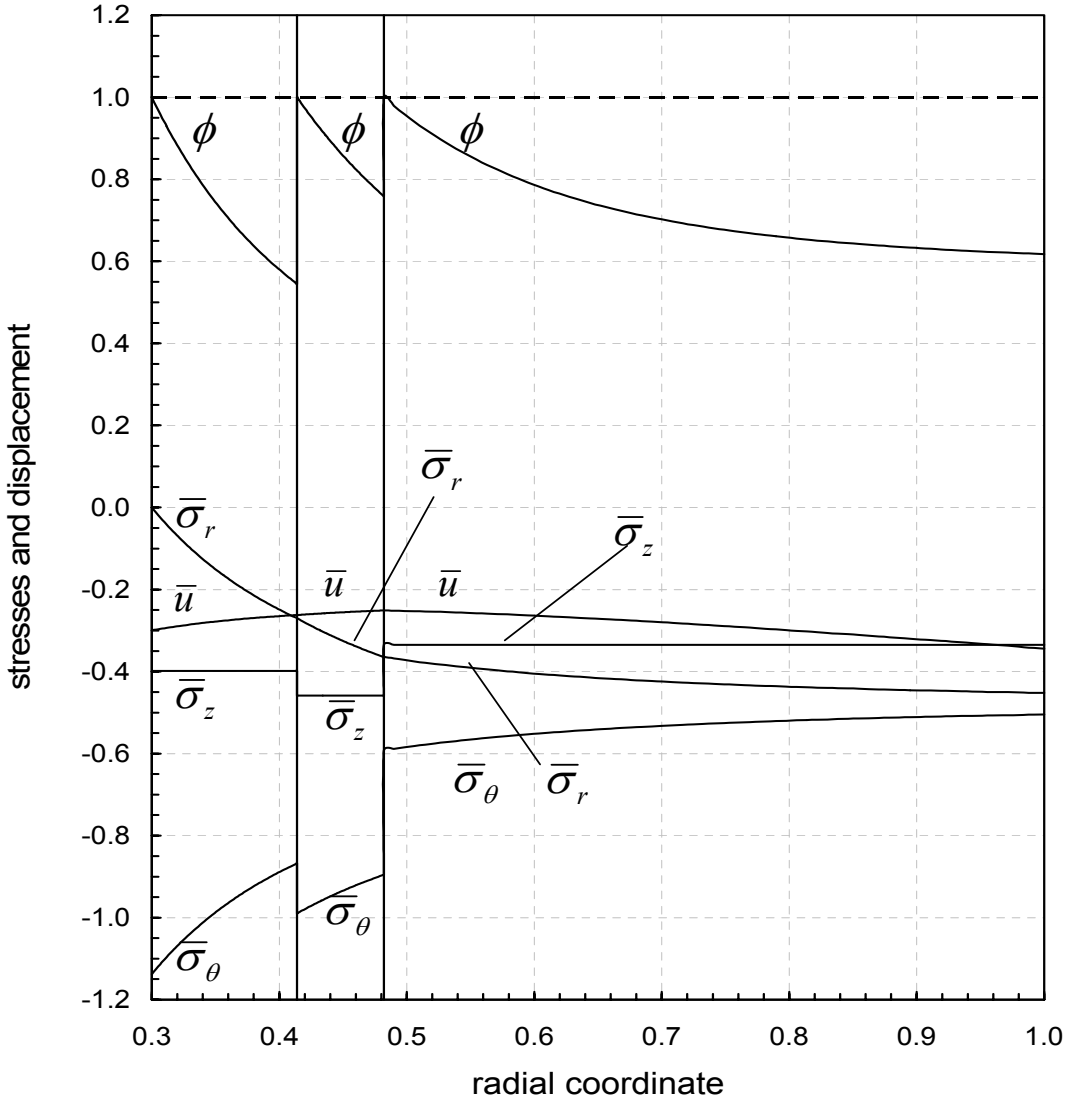

Figure 4.18 The distributions of stresses and displacement in a three-layer brass-copper-aluminum tube under elastic limit external pressure $\overline{P}_e$=0.451869 ($\overline{a}$ =0.3, $\overline{r}_{1cr}$ =0.413880, $\overline{r}_{2cr}$ =0.481949)

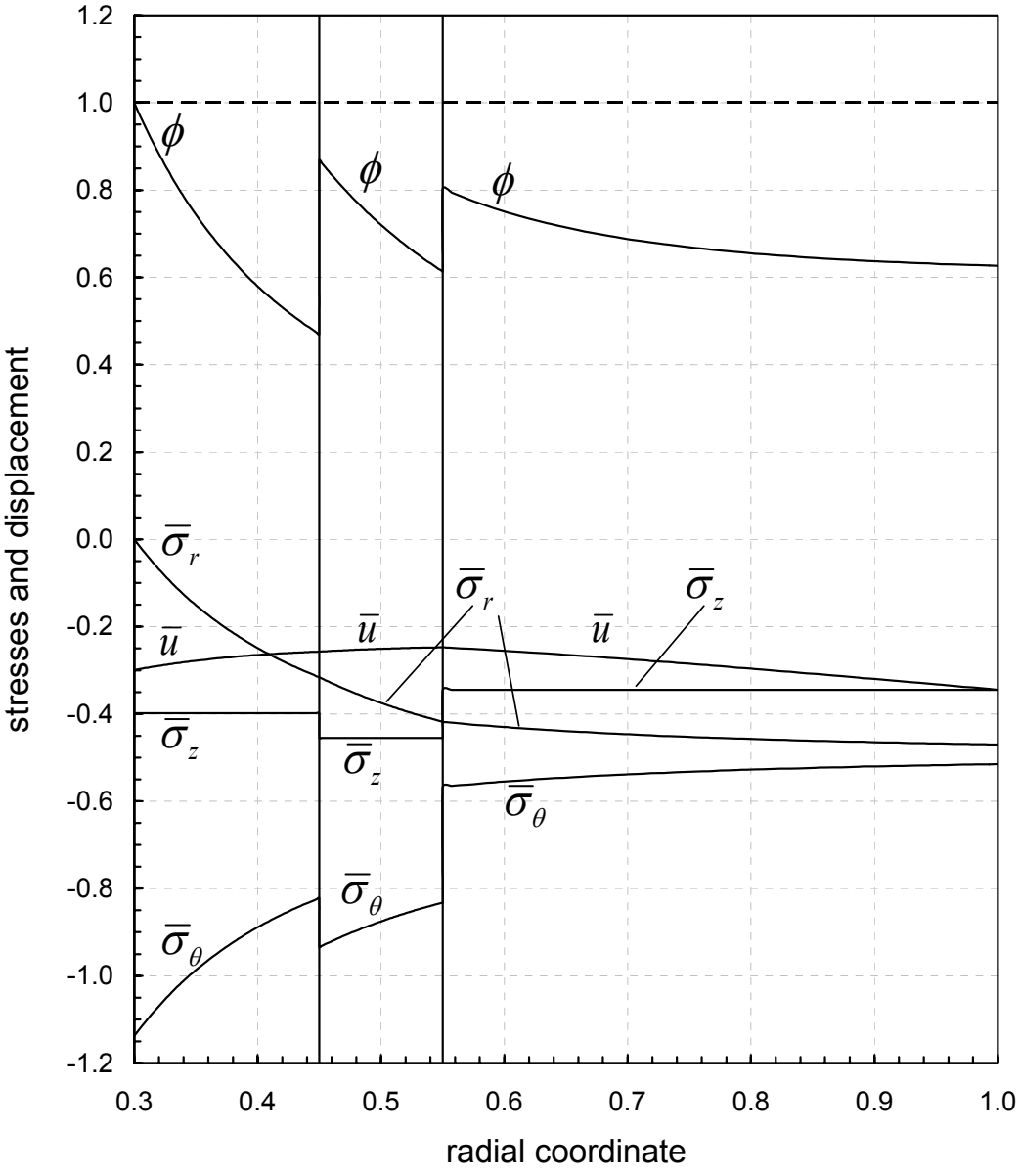

Figure 4.19 The distributions of stresses and displacement in a three-layer brass-copper-aluminum tube under elastic limit external pressure $\overline{P}_e$=0.470063 ($\bar{a}$ =0.3, $\bar{r}_1$ =0.45, $\bar{r}_2$ =0.55)

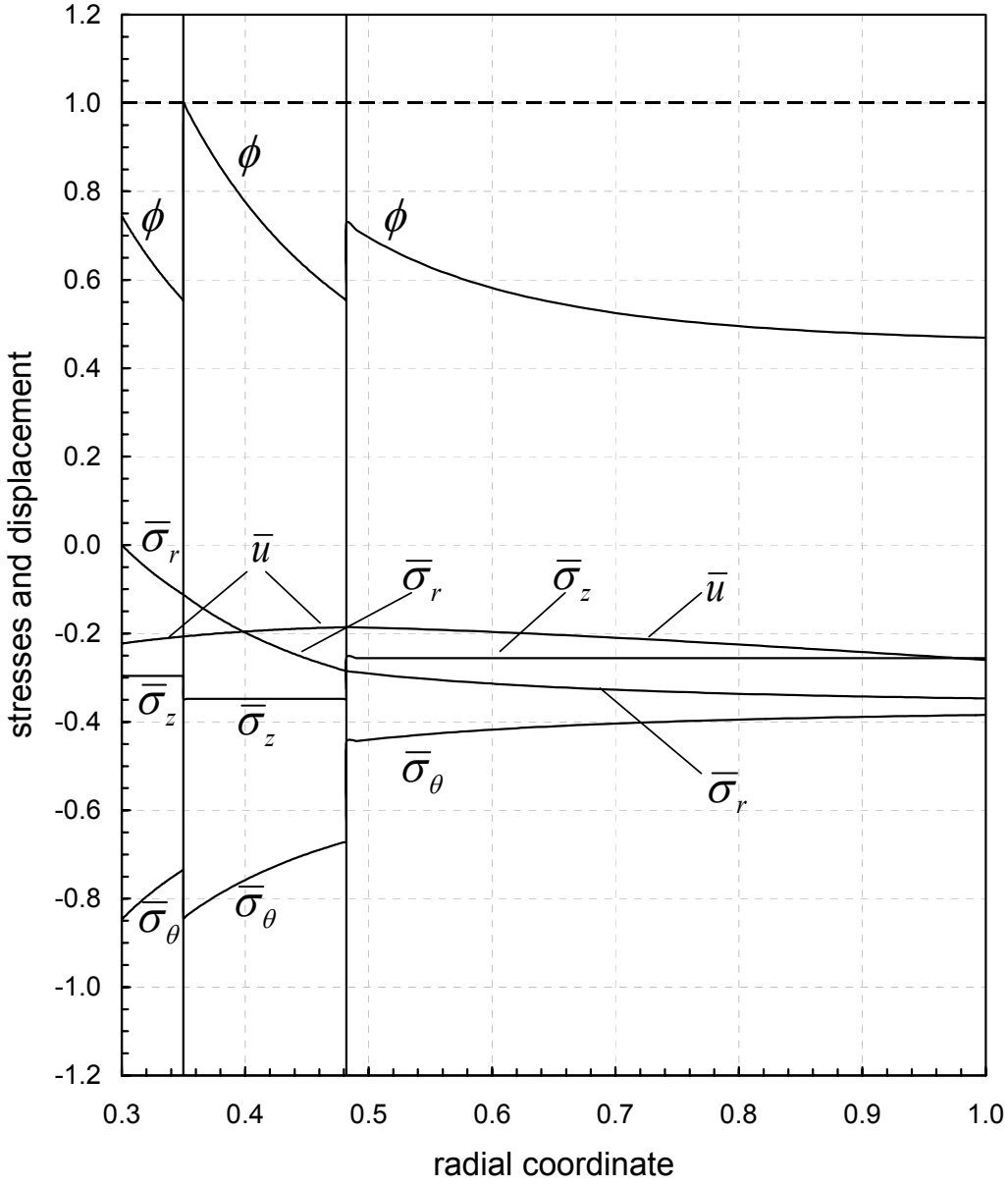

Figure 4.20 The distributions of stresses and displacement in a three-layer brass-copper-aluminum tube under elastic limit external pressure $\overline{P}_e$=0.346921 ($\bar{a}$=0.3, $\bar{r}_1$=0.35, $\bar{r}_2=\bar{r}_{2cr}$=0.481949)

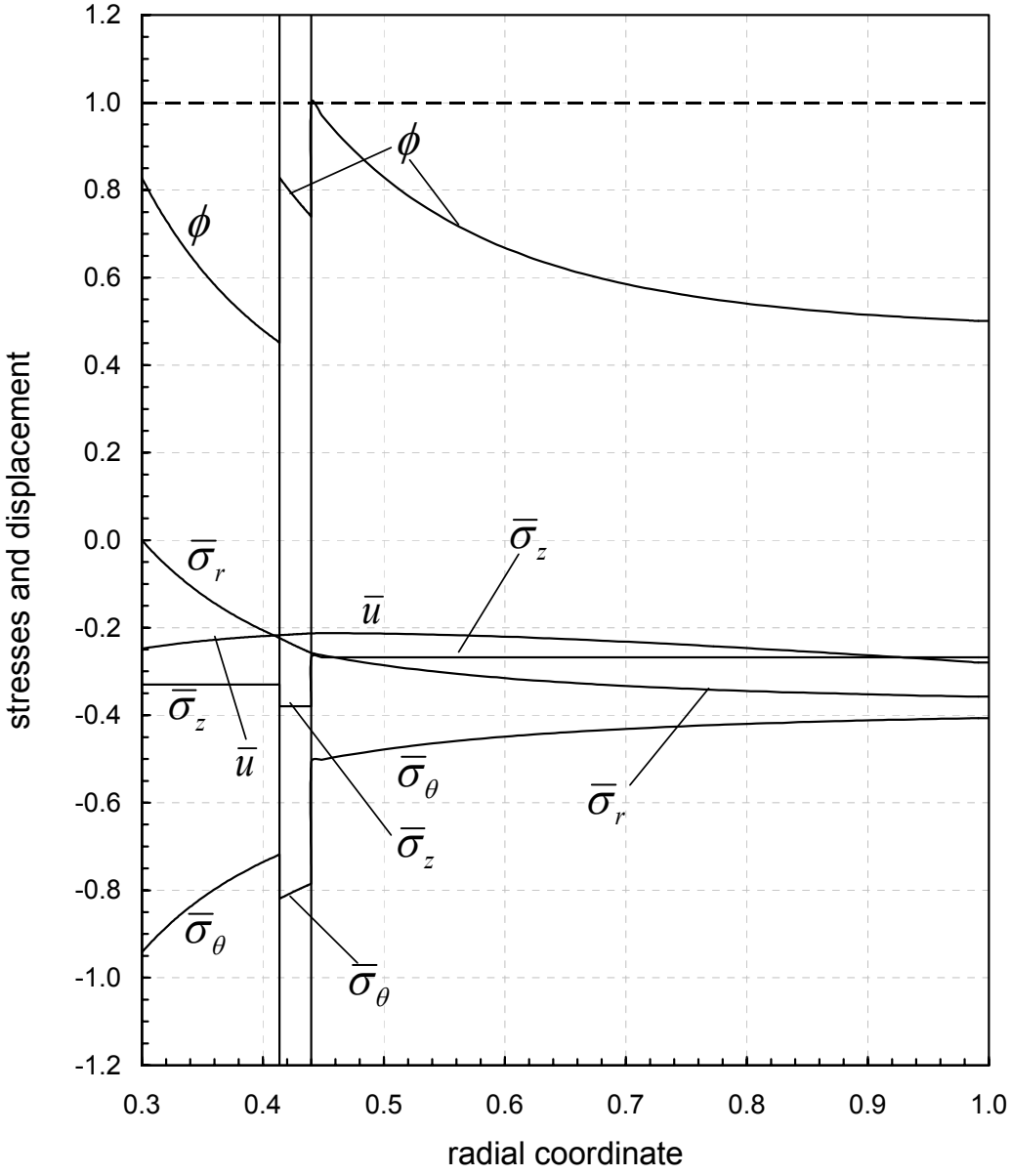

Figure 4.21 The distributions of stresses and displacement in a three layer brass-copper-aluminum tube under elastic limit external pressure $\bar{P}_e$=0.358066 ($\bar{a}$=0.3, $\bar{r}_1=\bar{r}_{1cr}$=0.413880, $\bar{r}_2$=0.44)

Having seen the situation where yielding under external pressure begins at a single layer first, different from the situations presented above, the yielding may start at two different layers at the same time according to von Mises yield criterion. In Fig. 4.22, the yielding begins at the inner surface ($r=a$) and at the inner interface ($r=r_1$) of the assembly for the same material combination. For $\bar{a}$=0.3 and $\bar{r}_2$=0.5, the elastic limit external pressure and the critical inner interface radius is calculated as $\overline{P}_e$=0.459011 and $\bar{r}_{1cr}$=0.413880 by solving Eqs. (148) and (149) together. The corresponding integration constants are obtained as $\overline{C}_1 = -2.69892\times10^{-4}$, $\overline{C}_2 = -8.99642\times10^{-4}$, $\overline{C}_3 = -2.87243\times10^{-4}$, $\overline{C}_4 = -7.98350\times10^{-4}$, $\overline{C}_5 = -1.99657\times10^{-4}$ and $\overline{C}_6 = -1.14873\times10^{-4}$.

In Fig 4.23 yielding starts at the inner layer ($r=a$) and the outer interface ($\bar{r}=\bar{r}_2$) of the composite tube at the same time. For $\bar{a}$=0.3, $\bar{r}_1$=0.45, the elastic limit external pressure and the critical outer interface are found as $\overline{P}_e$ =0.447096, and $\bar{r}_{2cr}$=0.485581 which is obtained by solving Eqs. (148) and (150) together. The integration constants are calculated as $\overline{C}_1 = -2.69892\times10^{-4}$, $\overline{C}_2 = -8.99642\times10^{-4}$, $\overline{C}_3 = -2.91623\times10^{-4}$, $\overline{C}_4 = -7.92331\times10^{-4}$, $\overline{C}_5 = -2.13296\times10^{-4}$ and $\overline{C}_6 = -1.12466\times10^{-4}$.

Finally, in Fig. 4.24, the case in which the middle and the outer layers starts yielding simultaneously according to von Mises's yield criterion is shown. For $\bar{a}$=0.3 and assigning the elastic limit external pressure $\overline{P}_e$ = 0.3, the inner and the outer interface radii are obtained by solving Eqs. (149), (150) together as $\bar{r}_{1cr}$=0.338355, $\bar{r}_{2cr}$=0.401616, respectively. The corresponding integration constants are calculated as $\overline{C}_1 = -1.88905\times10^{-4}$, $\overline{C}_2 = -6.29685\times10^{-4}$, $\overline{C}_3 = -1.95469\times10^{-4}$, $\overline{C}_4 = -5.72354\times10^{-4}$, $\overline{C}_5 = -1.65017\times10^{-4}$ and $\overline{C}_6 = -7.61148\times10^{-4}$.

In order to make a comparison between Tresca's and the von Mises yield criteria for the considered assemblies, Table 4.5 is prepared.

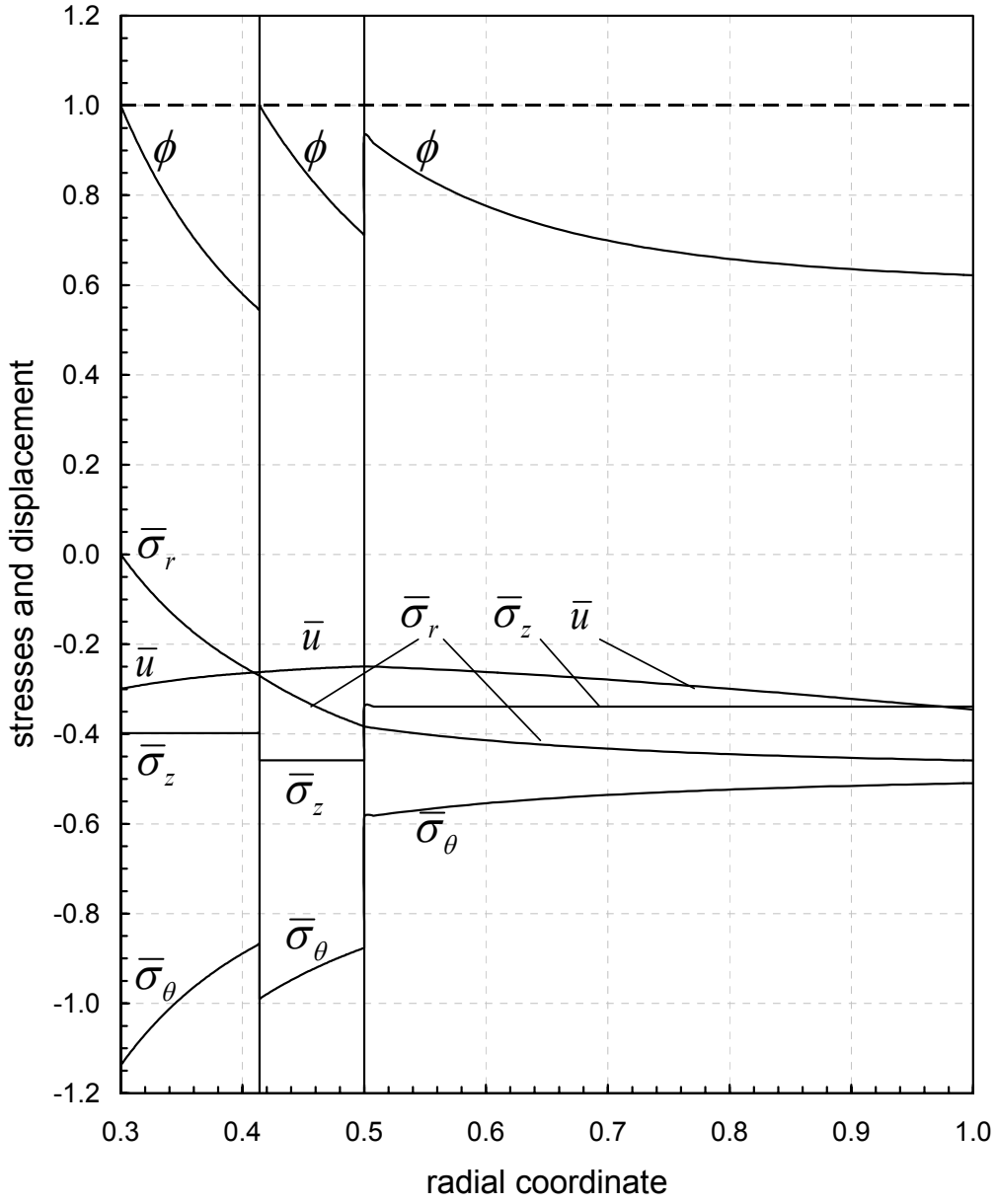

Figure 4.22 The distributions of stresses and displacement in a three-layer brass-copper-aluminum tube under elastic limit external pressure $\overline{P}_e$=0.459011 ($\bar{a}$=0.3, $\bar{r}_1=\bar{r}_{1cr}$=0.413880, $\bar{r}_2$=0.5)

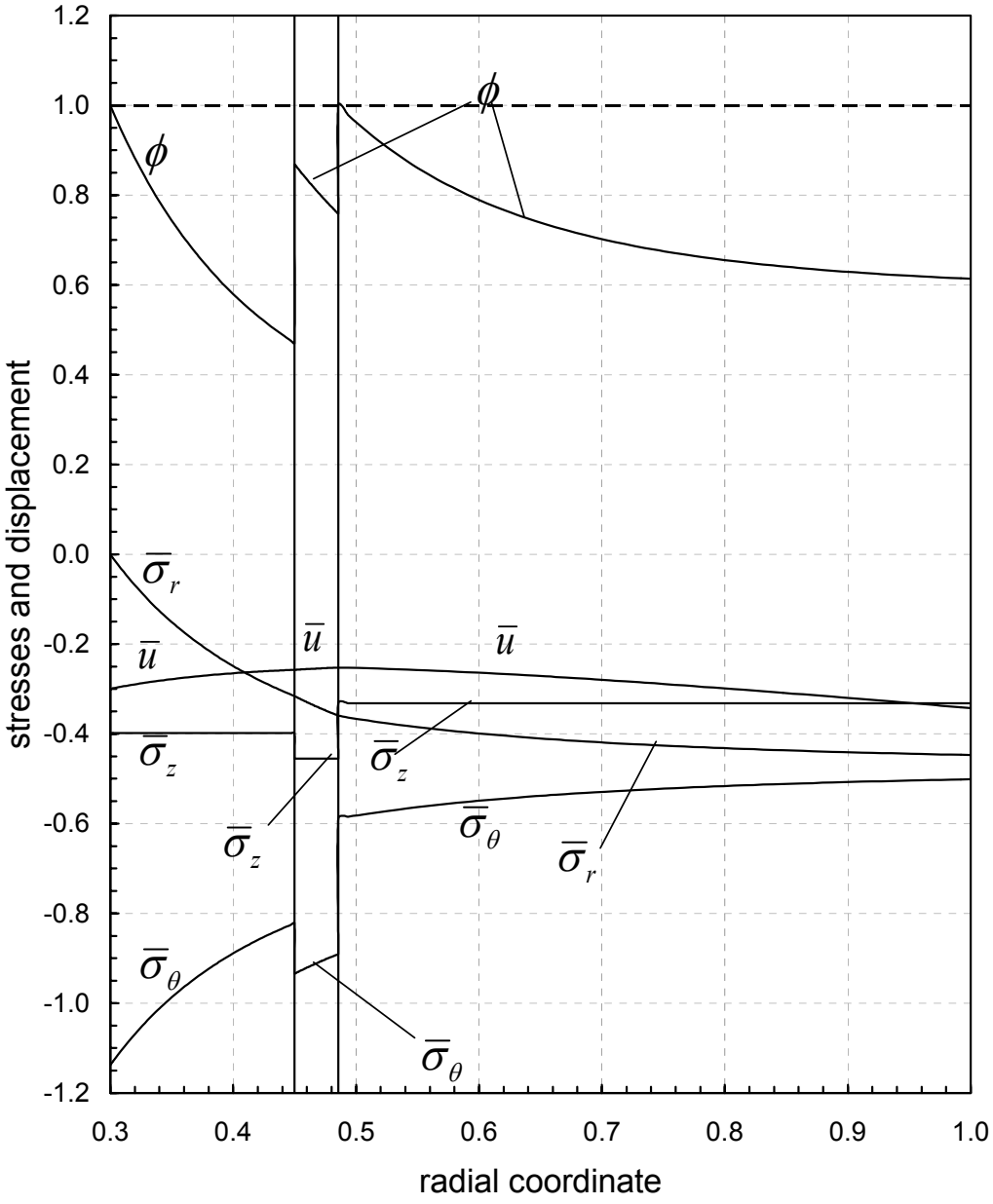

Figure 4.23 The distributions of stresses and displacement in a three-layer brass-copper-aluminum tube under elastic limit external pressure $\overline{P}_e$=0.447096 ($\bar{a}$=0.3, $\bar{r}_1$=0.45, $\bar{r}_{2cr}$=0.485581)

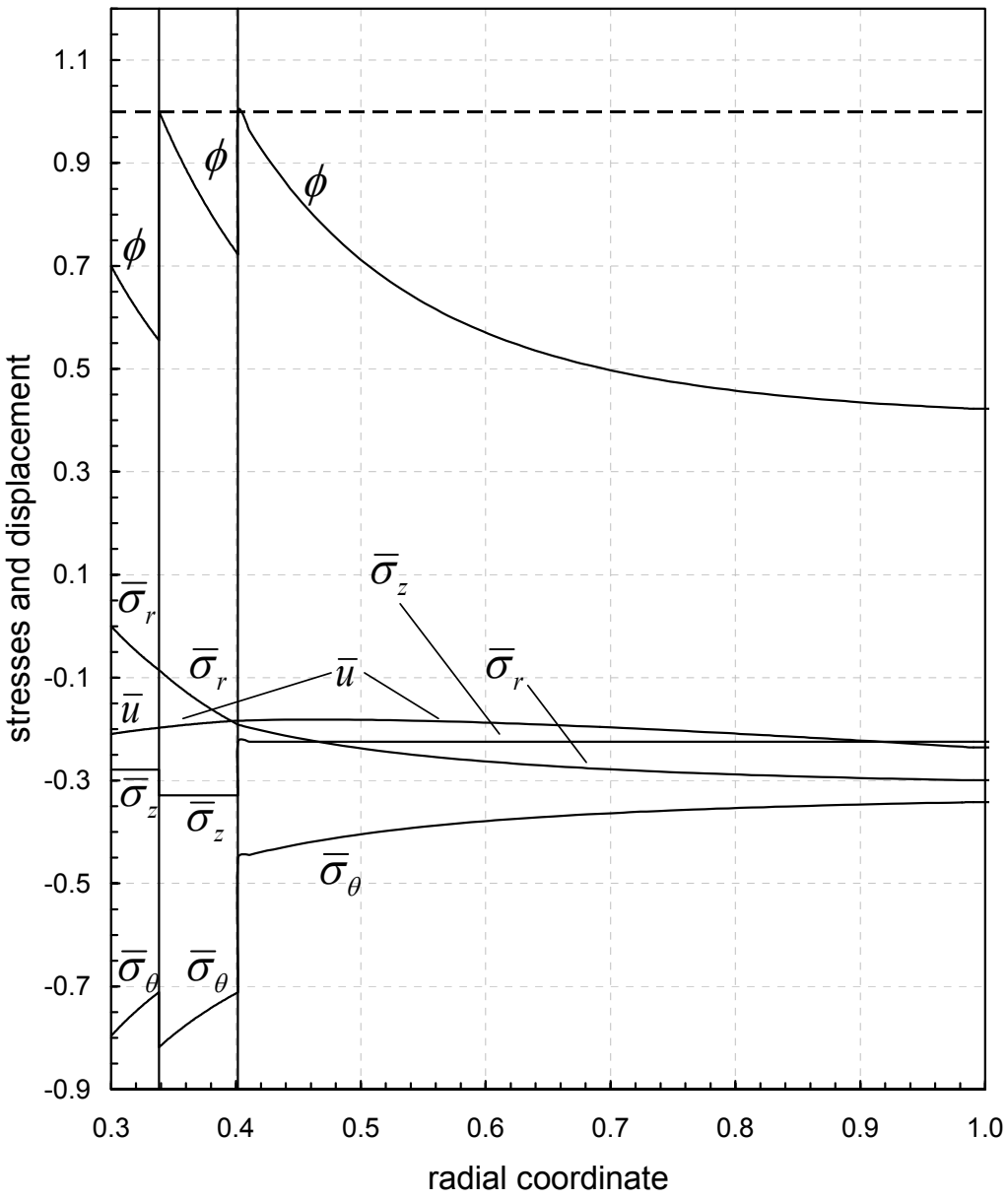

Figure 4.24 The distributions of stresses and displacement in a three-layer brass-copper-aluminum tube under elastic limit external pressure at $\bar{P}_e$=0.3

($\bar{a}$=0.3, $\bar{r}_1=\bar{r}_{1cr}$=0.338355, $\bar{r}_2=r_{2cr}$=0.401616)

Table 4.5 Elastic limit pressures and interface radii for different yielding cases of the three-layer tubes under external pressure ($\bar{a}$ =0.3)

Location(s) of yielding and yielding criterion	**Elastic limit external pressure ($\bar{P}_e$)**	**Interface radii ($\bar{r}_1$ and $\bar{r}_2$)**
Simultaneous yielding at $r = a$, $r = r_1$ and $r = r_2$ (Tresca's criterion)	0.385997	0.409026, 0.451441
Simultaneous yielding at $r = a$, $r = r_1$ and $r = r_2$ (von Mises criterion)	0.451869	0.413880, 0.481949
Yielding at the inner surface $r = a$ (Tresca's criterion)	0.413148	0.45, 0.55
Yielding at the inner surface $r = a$ (von Mises criterion)	0.470063	0.45, 0.55
Yielding at the inner interface $r = r_1$ (Tresca's criterion)	0.297893	0.35, 0.451441
Yielding at the inner interface $r = r_1$ (von Mises criterion)	0.346921	0.35, 0.481949
Yielding at the outer interface $r = r_2$ (Tresca's criterion)	0.353278	0.409026, 0.44
Yielding at the outer interface $r = r_2$ (Tresca's criterion)	0.358066	0.413880, 0.44
Simultaneous yielding at $r = a$ and $r = r_1$ (Tresca's criterion)	0.404234	0.409026, 0.50
Simultaneous yielding at $r = a$ and $r = r_1$ (von Mises criterion)	0.459011	0.413880, 0.50
Simultaneous yielding at $r = a$ and $r = r_2$ (Tresca's criterion)	0.385875	0.45, 0.455964
Simultaneous yielding at $r = a$ and $r = r_2$ (von Mises criterion)	0.447096	0.45, 0.485581
Simultaneous yielding at $r = r_1$ and $r = r_2$ (Tresca's criterion)	0.3	0.361651, 0.412416
Simultaneous yielding at $r = r_1$ and $r = r_2$ (von Mises criterion)	0.3	0.338355, 0.401616

4.5 An Example Problem

In order to check the validity of the derivations, an example problem, which was given by Hongjun et al. [17], is considered. According to their example problem, a three-layer hollow cylinder made of steel and concrete is taken into consideration and the inner and the outer layers of the tube assembly are made of steel and the middle layer is made of concrete. The radius of the inner and outer surfaces of the tubes is taken as 0.5 m. and 1.0 m, respectively. The thickness of the inner layer is 0.05 m and the thickness of the outer layer is 0.02 m. The middle layer is filled with concrete with 0.43 meters thickness. The modulus of elasticity for the steel layers is taken as 210 GPa and for the concrete layer it is taken as 23 GPa. The Poisson's ratio for the steel layers is taken as 0.28 and for the concrete layer it is taken as 0.18.

According to the study, the considered composite tube is faced with uniform pressure acting at the inner surface, which is $q = 100kN/m^2$ (0.1 MPa). The distributions of the stress components σ_r and σ_θ and the radial displacement u are given in that study and as it was expected, a large difference between the tangential stresses σ_θ is observed. The paper only considers the distribution of the stresses in the composite tube, where the dimensional variables are used.

As it was mentioned previously, the aim for examining this example problem is to validate the derivations of our study. For this purpose, the composite tube with the same uniform pressure, same dimensions and material properties are considered in our solution and the distributions of stresses σ_r and σ_θ and the displacement u are obtained. As seen in Figs. 4.23 to 4.25, same distributions of stresses and displacement are obtained which shows the correctness of our study. In these figures, the lines represent our results, while the thick dot points are the results of the study performed by Hongjun et al. [17].

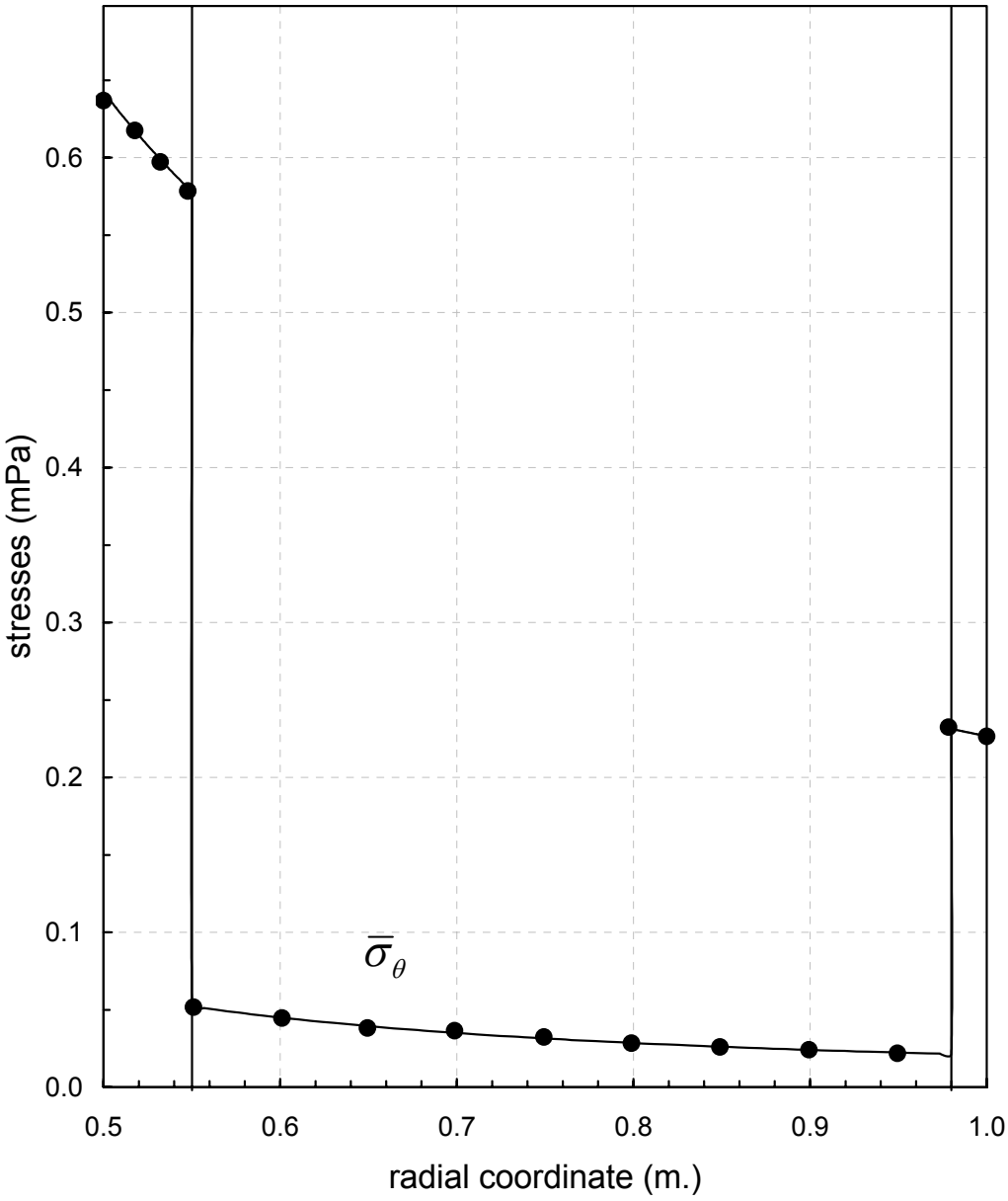

Figure 4.25 The distribution of the tangential stress (σ_θ) in a three-layer steel-concrete-steel tube under internal pressure (*r=0.5*, q=100kN/m² (0.1 MPa))

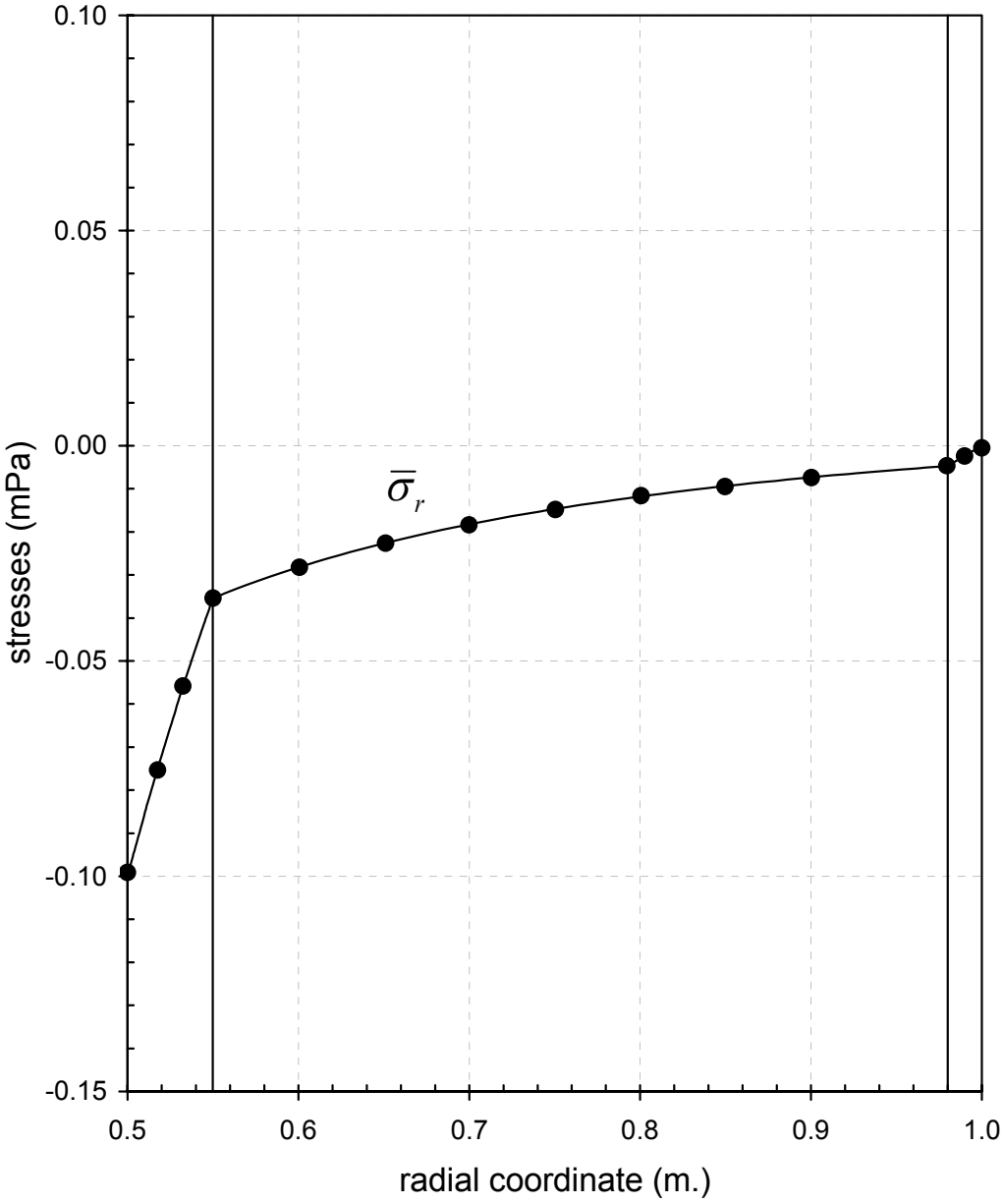

Figure 4.26 The distributions of the radial stress (σ_r) in a three-layer steel-concrete-steel tube under internal pressure (*r=0.5*, q=100kN/m² (0.1 MPa))

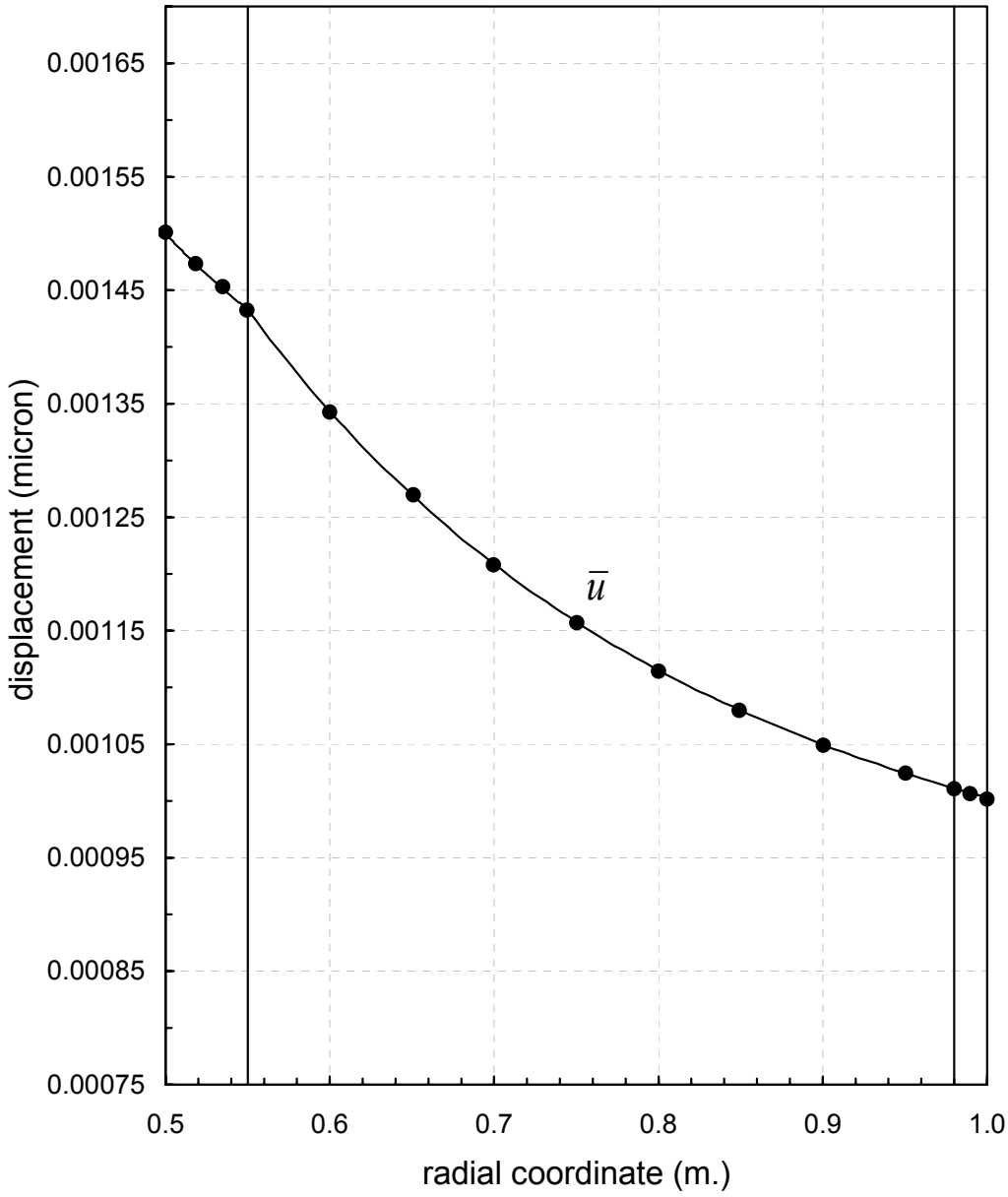

Figure 4.27 The distributions of the displacement in a three-layer steel-concrete-steel tube under internal pressure (*r=0.5*, q=100kN/m² (0.1 MPa))

CHAPTER 5

SUMMARY AND CONCLUSION

In this study, the deformation behavior of the single, two and three-layer tubes under internal and external pressure is presented. Firstly, the expressions of the stresses and displacement for the single layer tubes are derived considering the plane strain assumption. Afterwards, studies are carried on with finding the expressions of the stresses and displacements of two and three-layer tubes under pressure loading. By using the stress expressions, the yielding behaviour of the tubes is studied in details. For a set of combination of materials, Tresca's and von Mises yield criteria are used to monitor the commencement of the plastic flow at the tubes. Finally, the elastic limit pressures and critical interface radii that are obtained by these two criteria are compared. It should be noted that the material properties of the tube layers are quite important in determining the yielding behavior of the assemblies.

It is found in the studies that, for a single layer tube, the yielding begins at the inner surface of the assembly ($r = a$) under both internal and external pressure case. On the other hand, for the two-layer tubes under external or internal pressure, yielding may start;

1. At the inner surface ($r = a$) first,
2. At the interface of the two-layer tubes ($r = r_1$) first.
3. Simultaneously at the inner layer ($r = a$) and at the interface ($r = r_1$) of the assembly.

For the three-layer tubes, monitoring the yielding behaviour is more difficult. Studies show that for both internal and external pressure cases, the plastic flow may start;

1. At the inner surface of the assembly ($r = a$) first.

2. At the inner interface ($r = r_1$) first.

3. At the outer interface ($r = r_2$) first.

4. Simultaneously at the inner surface ($r = a$) and at the inner interface ($r = r_1$) first.

5. Simultaneously at the inner surface ($r = a$) and at the outer interface ($r = r_2$) first.

6. Simultaneously at the inner interface ($r = r_1$) and at the outer interface ($r = r_2$) first.

7. Simultaneously at the inner surface (r = a), at the inner interface ($r = r_1$), and at the outer interface ($r = r_2$) of the assembly.

For single layer tubes, the yielding starts at the inner layer $r = a$, however, different case of plastic flow can be observed for two and three-layer tubes as listed above. Moreover, for these tubes, yielding does not only begin at only one location, it is also possible that it may start at several locations at the same time. Apart from the simultaneous yielding of all layers for two and three-layer tube assemblies, it is beneficial to refresh the conditions for different yielding cases:

1. For the two-layer tubes, yielding may begin from the inner surface or at the interface first under internal or external pressure. It is found that if the thickness of the inner tube material is selected to be higher than the critical radius ($r_1 > r_{1cr}$), yielding begins at the inner surface ($r = a$) first. On the other hand, if the thickness of the inner tube is smaller than the critical radius ($r_1 < r_{1cr}$), yielding starts at the interface (r = r_1), which is the surface of the outer layer.

2. For the three-layer tubes, comparing to single and two-layer tubes, the yielding behaviour is quite different. After using a number of material combinations, the simultaneous yielding case at the three locations ($r = a$, $r = r_1$ and $r = r_2$) can be observed. It is found that, the yield limit (σ_0) of the

materials affect the condition of the yielding significantly. If the yield limit of the material of the inner tube is higher than the yield limit of the middle tube, and the yield limit of the material of the middle tube is higher than the yield limit of the outer tube ($\sigma_{01} > \sigma_{02} > \sigma_{03}$), the assembly may yield simultaneously at the three locations stated above. Similar to the two-layer tubes, if the inner interface r_1 is selected to be higher than the critical inner radius r_{1cr} and the outer interface r_2 is selected to be higher than the outer critical radius r_{2cr}, the yielding begins at the inner surface of the tube ($r = a$) first. For yielding that starts at the inner interface r_1, the outer interface radius should be equal to r_{2cr} and the thickness of the inner tube should be smaller than the critical inner radius $r_{1\,cr}$. For the yielding which starts from the outer interface r_2, r_1 should be equal to $r_{1\,cr}$, and $r_2 < r_{2cr}$.

3. Coming to the simultaneous yielding at the two locations of the assembly, it is known that by solving two of the three equations together, it is possible to find the elastic limit pressure and the corresponding critical interface radius; however, the value of the other interface radius should be in some limits. For the yielding from the inner surface *a* and from the inner interface r_1, the value of the outer interface r_2 should be higher than the critical outer interface radius r_{2cr}, which is obtained by the numerical solution of the three equations given in the previous chapter. The assembly may also yield from the inner and the outer interfaces (r_1 and r_2) simultaneously. For this purpose, the inner radius, r_1, should be higher than the critical inner radius $r_{1\,cr}$, which is obtained by the numerical solution of the corresponding equations.

Another aim of this study was to compare Tresca's yield criterion with von Mises yield criterion. According to the results obtained after the analyses, the following findings can be listed:

1. For the single layer tubes under internal or external pressure, the elastic limit pressure according to von Mises criterion is higher than the one which is

found by Tresca's criterion. This means that Tresca's criterion is safer than von Mises criterion. It should be noted that von Mises criterion makes more sense since the stress component in ''z'' direction (axial stress) is also considered while calculating the elastic limit pressures.

2. For the simultaneous yielding of the two-layer tubes under internal pressure, similar to single layer tubes, the elastic limit pressure calculated by using von Mises criterion is approximately 15 percent higher than the one which is found by Tresca's criterion. On the other hand, the corresponding critical interface radii are nearly the same for both criteria. Coming to the external pressure case, similar to the internal pressure case, the elastic limit pressure according to von Mises criterion is approximately 13 percent higher than the one which is found by Tresca's criterion. Same as the internal pressure case, the critical interface radii calculated by the two criteria are nearly the same.

3. Focusing on the simultaneous yielding behaviour of the three-layer tubes under internal pressure, it is seen that there is a small difference between the critical interface radii, whereas the elastic limit pressures calculated using von Mises criterion is approximately 15 percent higher than the one obtained by Tresca's criterion. These results show that Tresca's criterion is safer than von Mises's criterion, but von Mises's outcomes are closer to the reality because of the fact that was mentioned above. For the external pressure case, the elastic limit pressures according to von Mises criterion are approximately 17 percent higher than the ones obtained by Tresca's criterion.

4. For the yielding cases of the three-layer tubes, in which the yielding starts from two different locations at the same time, it is observed that the differences between the pressure values obtained by using Tresca's and von Mises criteria are not significant. For internal pressure case, it can be stated that Tresca's criterion is safer, whereas it is far away from the findings calculated by the values calculated by von Mises's criterion. On the other hand, it is difficult to make a comment on the external pressure case since the

elastic limit pressures calculated by using von Mises criterion is higher than that is obtained by using Tresca's criterion whereas in some cases the thickness of the corresponding tube layers obtained by using von Mises criterion is higher than that are obtained by Tresca's criterion.

In general, for the internal pressure cases of the single, two and three-layer tubes, if the assembly is to be designed by using Tresca's criterion, it would be safer since lower elastic limit pressures can be obtained while compared with von Mises criterion. For the external pressure case, a result like internal pressure case can not be stated as the yielding behaviour of the multi-layer tubes under external pressure is quite complex.

For the future studies, this study may be a step to develop analytical solutions for the pressurized tubes under different loading and boundary conditions. Moreover, experimental studies based on multi-layer pressurized tubes can be performed. Lastly, the elastic-plastic analysis of multi-layer tubes can be studied in the future.

REFERENCES

[1] Akış T., Eraslan A.N., Deformation analysis of elastic-plastic two-layer tubes subject to pressure: an analytical approach, Turkish J. Eng. Env. Sci. 28 (2004) , 261- 268.

[2] Akis T., Eraslan A.N., Yielding of two-layer shrink-fitted composite tubes subject to radial pressure, Forschung Ingenieurwes 69, (2005): 187–196.

[3] You L.H., Zhang J.J., You X.Y., Elastic analysis of internally pressurized thick-walled spherical pressure vessels of functionally graded materials, International Journal of Pressure Vessels and Piping, 82 (2005) 347–354.

[4] Liew K.M., Kitipornchai S., Zhang X.Z., Lim C.W., Analysis of the thermal stress behaviour of functionally graded hollow circular cylinders, International Journal of Solids and Structures, 40 (2003) 2355–2380.

[5] Shao Z.S., Mechanical and thermal stresses of a functionally graded circular hollow cylinder with finite length, International Journal of Pressure Vessels and Piping, 82 (2005) 155–163.

[6] Tarn J.Q., Exact solutions for functionally graded anisotropic cylinders subjected to thermal and mechanical loads, International Journal of Solids and Structures, 38 (2001) 8189-8206.

[7] Eslami M.R., Babaei M.H., Poultangari R., Thermal and mechanical stresses in a functionally graded thick sphere, International Journal of Pressure Vessels and Piping, 82 (2005) 522–527.

[8] Eraslan A.N., Apatay T., Analytical solution of nonlinear strain hardening preheated pressure tube, Turkish J. Eng. Env. Sci., 32 (2008), 41-50.

[9] Dai H.L., Fu Y.M., Dong Z.M., Exact solutions for functionally graded pressure vessels in a uniform magnetic field, International Journal of Solids and Structures, 43 (2006) 5570–5580.

[10] Zhifei S., Taotao Z., Hongjun X., Exact solutions of heterogeneous elastic hollow cylinders, Composite Structures, 79 (2007) 140–147.

[11] Timoshenko, S.P., Goodier J.N., Theory of elasticity. 3rd ed. New York: McGraw-Hill Book Company; 1970.

[12] Akis T., Elastoplastic analysis of functionally graded spherical pressure vessels, Computational Materials Science, 46 (2009) 545–554.

[13] Akis T., Eraslan A.N., Plane strain analytical solutions for a functionally graded elastic–plastic pressurized tube, International Journal of Pressure Vessels and Piping, 83 (2006) 635–644.

[14] Güven U., Baykara C., On stress distributions in functionally graded isotropic spheres subjected to internal pressure, Mechanics Research Communications, 28 (2001), 277-281.

[15] Tutuncu N., Ozturk M., Exact solutions for stresses in functionally graded pressure vessels, Composites Part B 32 (2001), 683-686.

[16] Boresi A.P., Schmidt, R.J., Sidebottom, O.M., Advanced Mechanics of Materials. 5th ed., John Wiley and Sons, 1993.

[17] Hongjun X., Zhifei S., Taotao Z., Elastic analyses of heterogeneous hollow cylinders, Mechanics Research Communications 33(2006), 681-691.